

Aus der Klinik für Hals- Nasen- und Ohrenheilkunde
der Heinrich-Heine-Universität Düsseldorf

Direktor: Univ.-Prof. Dr. Jörg Schipper

**Adoptive T-cell-Therapy via Chimeric Antigen
Receptors (CARs) against Leukemia in
Combination with a human Suicide Gene**

Dissertation

zur Erlangung des Grades eines Doktors der Medizin der
Medizinischen Fakultät der Heinrich-Heine-Universität
Düsseldorf

vorgelegt von

Tabea Constanze Ibach

2020

Als Inauguraldissertation gedruckt mit der Genehmigung der
Medizinischen Fakultät der Heinrich-Heine-Universität
Düsseldorf

gez.:

Dekan: Prof. Dr. med. Nikolaj Klöcker

Erstgutachter: Prof. Dr. med. Helmut Hanenberg

Zweitgutachter: Prof. Dr. med. Norbert Gattermann

Teile dieser Arbeit wurden veröffentlicht:

EUROPEAN PATENT APPLICATION: European Patent Office, Nr. EP3293199; Authors: Hanenberg, Helmut; Röllecke, Katharina; Wiek, Constanze; Ibach, Tabea; Rössig, Claudia; Date of publication: 14.03.2018 Bulletin 2018/11, Application number: 16187740.2; Date of filing: 08.09.2016

Summary

Autologous T-cells equipped with a chimeric antigen receptor (CAR) represent a novel and highly successful approach in the fight against B-cell lineage leukemia and lymphoma. However, using CARs for the treatment of myeloid and T-cell lineage malignancies and especially solid cancers has proven to be much more difficult and will require several modifications for increased specificity and safety.

One obstacle in the search for an ideal CAR construct is the design of an optimal region that connects the single chain fragment with the transmembrane region of the CAR, the so-called hinge region or spacer. Therefore, a major focus of this thesis was to develop a new universal hinge region of human origin that can replace the commonly used CH₂CH₃ fragment of human IgG and ideally contains epitopes recognized by monoclonal antibodies that facilitate the detection and selection of CAR-expressing T-cells under GMP-compliant conditions. To this end, different hinges derived from the human surface molecules CD34 or CD271 were introduced into a standard CD19 CAR construct and expressed in primary human T-cells using lentiviral vectors. The results demonstrated that two hinge regions (#C3 and #C6) from human CD34 allowed to detect and also enrich CAR-expressing human T-cells via the MACS microbeads system and did not affect the cytotoxic activities of the genetically modified T-cells against CD19+ leukemic cells.

The inclusion of a safety switch that facilitates *in vivo* control of the engineered T-cells is also important to control potentially life-threatening adverse events in the patient. Therefore, the cDNA of a novel human suicide gene system, a human modified CYP4B1 enzyme which has been developed by our laboratory to activate the prodrug 4-*Ipomeanol*, was introduced into the CD19 CAR constructs. The new hinges enabled selection of highly CAR expressing human T-cells that were efficiently eliminated after killing their CD19+ target cells by incubation with 4-*Ipomeanol*. I also verified that a naturally occurring similar prodrug, *Perilla ketone*, could be used to kill the selected CD19 CAR positive T-cells that coexpressed the suicide gene. Finally, I tested whether the two prodrugs, 4-*Ipomeanol* and *Perilla ketone*, can also be activated by the most important cytochromes in human hepatocytes. To this end, I stably expressed the human cytochromes 1A2, 3A4, 3A5 and 2E1 in the human liver cell line HepG2 and demonstrated that only 1A2 expression led to cellular toxicity at high concentrations.

In summary, I successfully established a new hinge region derived from human CD34 that can be used in standard CAR constructs in combination with a suicide gene for improved safety of human CAR T-cells.

Zusammenfassung

Autologe T-Zellen, die chimäre Antigenrezeptoren (CARs) exprimieren, stellen einen vielversprechenden Ansatz im Kampf gegen B-Zell Leukämien und Lymphome dar. Die Verwendung von CARs gegen myeloische und T-Zell Erkrankungen und insbesondere gegen solide Tumoren hat sich jedoch als sehr viel komplizierter herausgestellt und diverse Anpassungen zum Erreichen einer erhöhten Spezifität und Sicherheit sind erforderlich.

Eine Hürde in der Entwicklung eines idealen CAR Konstruktes ist der Aufbau einer optimalen Gelenkregion, welche das *single chain fragment* mit der Transmembran-Domäne des CARs verbindet und als "*hinge*"-Region oder "*spacer*" bezeichnet wird. Ein Hauptziel dieser Dissertation war daher die Entwicklung einer neuen, universellen *hinge*-Region für CARs, welche das bisher häufig benutzte CH₂CH₃ Fragment aus dem humanen IgG ersetzt und idealerweise Epitope von monoklonalen Antikörpern enthält, wodurch man die CAR+ T-Zellen unter Einhaltung von GMP-Standards markieren und selektionieren kann.

Hierzu wurden verschiedenen *hinge*-Regionen aus CD34 oder CD271 in einen CD19 CAR integriert und durch lentivirale Vektoren in primären humanen T-Zellen exprimiert. Es konnte gezeigt werden, dass zwei *hinge*-Regionen (#C3 und #C6) aus dem humanen CD34 die Identifizierung und Anreicherung mit dem MACS microbeads System ermöglichten und dabei die Zytotoxizität der genetisch modifizierten T-Zellen gegen CD19+ Leukämiezellen nicht beeinflussten.

Desweiteren ist ein Sicherheitsschalter, der eine Kontrolle der genetisch veränderten T-Zellen *in vivo* ermöglicht, nötig, um die Therapie bei potentiell lebensgefährlichen Nebenwirkungen stoppen zu können. Daher wurde die cDNA eines neuen, in unserem Labor entwickelten Suizidgens, welches aus einer modifizierten Version des humanen Enzyms CYP4B1 besteht und das Pro-Pharmakon 4-Ipomeanol aktiviert, zusätzlich in die CD19 CAR Konstrukte integriert. Die neuen *hinge*-Regionen ermöglichten die Selektion von T-Zellen, welche den CAR stark exprimierten und nach dem Töten der CD19+ Zielzellen effizient durch die Inkubation mit 4-Ipomeanol eliminiert werden konnten. Es wurde zudem gezeigt, dass ein natürlich vorkommendes zweites Pro-Pharmakon, Perilla ketone, ebenfalls benutzt werden konnte um die selektionierten CD19+ CAR T-Zellen, welche das Suizidgen exprimierten, zu töten. Zuletzt wurde getestet, ob die beiden Pro-Pharmaka, 4-Ipomeanol und Perilla ketone, zusätzlich von den wichtigsten Leberzytochromen aktiviert werden können. Zu diesem Zweck wurden die humanen Zytochrome 1A2, 3A4, 3A5 and 2E1 stabil in der humanen Leberzelllinie HepG2 exprimiert. So konnte gezeigt werden, dass nur 1A2 in hohen Konzentrationen zu Zelltoxizität führte.

Zusammenfassend etablierte ich erfolgreich eine neue *hinge*-Region, welche aus dem humanen CD34 stammt und in CAR Konstrukten in Kombination mit einem Suizidgen für verbesserte Sicherheit der CAR T-Zellen verwendet werden kann.

TABLE OF CONTENTS

1	INTRODUCTION	1
1.1	Experimental therapies	1
1.1.1	Chimeric antigen receptors	2
1.1.2	Clinical use of adoptive T-cell therapy with CARs	5
1.1.3	CAR targets for hematologic malignancies	6
1.1.4	Obstacles in clinical trials	8
1.2	The Suicide Gene System	11
1.2.1	Development of Suicide Gene Systems	11
1.2.2	CYP4B1-System	12
1.3	Objective of this thesis	15
2	MATERIAL AND METHODS	16
2.1	Material	16
2.1.1	Commercial Kits and enzymes	16
2.1.2	Length and size standards	16
2.1.3	Oligonucleotides	16
2.1.4	Plasmids	17
2.1.5	Expression vectors	18
2.1.6	Bacteria	19
2.1.7	Cell lines	19
2.1.8	Primary cells	19
2.1.9	Antibodies	20
2.1.10	Buffer and solutions	20
2.2	Molecular biological methods	22
2.2.1	Primer annealing	22
2.2.2	PCR amplification of plasmid fragments	22
2.2.3	Gel electrophoresis	22
2.2.4	Restriction digestion of plasmid DNA	22
2.2.5	Dephosphorylation of plasmid DNA	23
2.2.6	Ligation	23
2.2.7	Transformation of plasmid-DNA in <i>E. coli</i>	23
2.2.8	Isolation of plasmid DNA from bacteria	24
2.2.9	DNA sequencing	24
2.3	Cell cultivation methods	24
2.3.1	Cultivation of cell lines	24

2.3.2	Cryoconservation of eukaryotic cell lines	25
2.3.3	Isolation of primary T-cells	25
2.3.4	Vector production and transduction	25
2.3.5	FACS analysis	27
2.3.6	Cell separation via MACS	28
2.3.7	Cytotoxicity assays	28
2.3.8	Cell proliferation assays	29
2.4	Protein Biochemical Methods	31
2.4.1	Mild lysis of eukaryotic cells	31
2.4.2	Western Blot	31
3	RESULTS	33
3.1	Defining a new linker for CARs	33
3.1.1	Requirements for a new hinge region	33
3.1.2	Functional tests in Jurkat cells	37
3.1.2.1	Expression of CARs in Jurkat cells	37
3.1.2.2	MACS selection of transduced Jurkat cells	38
3.1.3	Functional tests in primary human T-cells	41
3.1.3.1	Expression of CARs in primary human T-cells	41
3.1.3.2	MACS selection of primary human T-cells	41
3.1.3.3	Cytotoxicity assay with leukemic B-cells	42
3.1.3.4	Toxassays with 4-Ipomeanol and Perilla ketone	45
3.2	Hepatotoxicity assays with different cytochromes	47
3.2.1	Hepatotoxicity assays with 4-Ipomeanol and Perilla ketone	49
3.2.2	Western Blot and MFI	52
4	DISCUSSION	54
4.1	Establishing a new detection sequence as part of a CAR	55
4.2	Metabolisation of 4-IPO and PK by different liver enzymes	59
4.3	Cytotoxicity and subsequent elimination of modified CAR T-cells	63
4.4	Future directions of CAR therapy	64
5	BIBLIOGRAPHY	69
6	APPENDIX	85
6.1	List of figures	85
6.2	List of tables	86
6.3	List of abbreviations	86

1 INTRODUCTION

1.1 Experimental therapies

In 2000, Hanahan et Weinberg defined six „hallmarks of cancer“ as biological prerequisites for the development of human tumors as a framework to understand the complex biology of cancer. These hallmarks were evading growth suppressors, sustaining proliferative signaling, resisting cell death, enabling replicative immortality, inducing angiogenesis and activating invasion and metastasis [1]. About ten years later, “evading immune destruction” was recognized as an additional hallmark of cancer [2]. Cancer immune surveillance is nowadays considered to be a paramount host protection process as tumors can only manifest if the autologous immune system fails. Studies with immunodeficient mice indicated that both, the innate and adaptive arm of the immune system are capable of “immune-editing”, i.e. of enhancing immune surveillance and tumor eradication [3]. In general, it is well established that highly immunogenic cancer cells are eliminated in immunocompetent individuals, however they can thrive in immunodeficient hosts [4].

Tumor cells develop different mechanisms to escape the host immune responses. Malignant cells often downregulate key immune regulatory molecules like major histocompatibility complex (MHC) class I molecules on their surface which are essential for T-cells to detect and kill the malignant cells [5]. In addition, all tumor cells originate from healthy human cells and therefore express primarily “self-antigens”. During T-cell development, natural thymic selection processes eliminate lymphocytes that express T-cell receptors with high affinity and activity towards autologous antigens. Therefore, the surviving T-cells are immunologically tolerant against antigens on the tumor cell surface [6, 7]. Some tumors even produce factors that are deleterious for T-cell survival [8, 9] or recruit cells that are actively immunosuppressive, like regulatory T-cells [10]. To address these two principle survival strategies of malignant cells, the lack of “immune-editing” in cancer patients and the ability of tumors to evade the immune system, researchers have tried to modify the human immune system to enhance its natural ability to fight malignancies [11].

The detection of tumor-associated antigens (TAAs) in the 1990s strongly suggested that the immune system was able to distinguish tumor cells from healthy tissue and resulted in an increased specificity of cancer therapies [12]. TAAs can be divided into three groups [13]. The first group contains antigens that are overexpressed in tumors but are also present on

healthy tissue. This includes lineage-specific antigens that are characteristic for a cell line and can also be expressed in tumors emerging from that cell lineage. The second group is formed by cancer germline antigens which are normally expressed only on germline cells. The 3rd group comprises neo-antigens that develop via somatic mutations during tumor development and therefore are tumor specific antigens. These different types of tumor-associated antigens require distinct targeting approaches [13].

The introduction of the monoclonal antibodies Muromonab® against CD3 on T-lymphocytes and Rituximab® against the B-cell specific lineage marker CD20 were considered major breakthroughs, since treatment with both lead to apoptosis of the target cells after binding [14, 15]. Another approach to increase the activity of the immune system against malignant cells is the use of inflammatory cytokines like IFN- γ . This will upregulate the MHC class I expression on malignant cells and induce intensified natural killer (NK) and cytotoxic T-cell activities as well as production of other cytokines and chemokines [16]. IFN- γ against Chronic Myeloid Leukemia (CML) was recommended as first line treatment until the introduction of the tyrosine kinase inhibitor Imatinib [17]. Nowadays both are often used in combination [18]. However, in many malignancies, the immune response mediated by “artificial” or recombinant antibodies or cytokines is either not strong enough to induce complete remission or leads to too many adverse events [19, 20].

Adoptive cellular therapies (ACTs) are often complex biological therapies involving the *ex vivo* processing of immune effector cells and represent promising yet challenging approaches in the treatment of hematological malignancies. In contrast to protein or small-molecule therapeutics, ACT strengthens the ability of the patient’s immune system to recognize and kill tumor cells by transferring immune effector cells such as T-cells or NK cells to the patient. These immune cells can be donor-derived cells from another individuals or patients’ autologous cells. Specific therapeutic regimes that modify immune cells have been available for more than 20 years, but it has proven to be very challenging to develop ACT to the point at which they can be used as standard of care [21, 22].

1.1.1 Chimeric antigen receptors

In order to enhance the anti-tumor response of the patient’s immune system, research initially tried to increase the amount of tumor-specific T-cells in the patient’s blood stream and within the malignant tissue. To this end, tumor-infiltrating lymphocytes (TILs) were identified in cancer samples and isolated, *in vitro* expanded and then transfused back into the

patient [23, 24]. This approach was very expensive and time-consuming and, most importantly, only showed limited clinical efficacy.

Further development of ACT led to T-cells that were equipped via transfer vectors with a T-cell receptor (TCR) specific against an overexpressed antigen on the tumor cell surface [25]. This increased the affinity of the TCR-modified T-cells towards the tumor [26]. *In vivo* studies showed that the modified receptors do not necessarily mediate autoimmune tissue infiltration or damage when expressed in T-cells [27]. Nevertheless, heterodimerization of endogenous and transgenic TCR chains on the cell surface led to new and unwanted receptor specificities against autologous MHC-peptide complexes and mediated autoimmune reactions [28, 29]. Another major disadvantage of these modified TCRs is that their activation is still restricted to parallel recognition of the target antigen on MHC molecules on the tumor cell surface [30-32].

Most of these problems can be addressed by the more recently developed chimeric antigen receptors (CARs), that combine the ability of a monoclonal antibody to detect a surface antigen with specific antigen-recognition and activation pathways of T-cells in a single molecule [33-36]. In contrast to the native TCR, CARs directly recognize target antigens that are expressed on the tumor cell surface, instead of antigens that are processed and presented by MHC molecules. Therefore, after recognition of the surface antigen, the CAR T-cells are activated in a MHC-independent manner and subsequently kill the malignant cell.

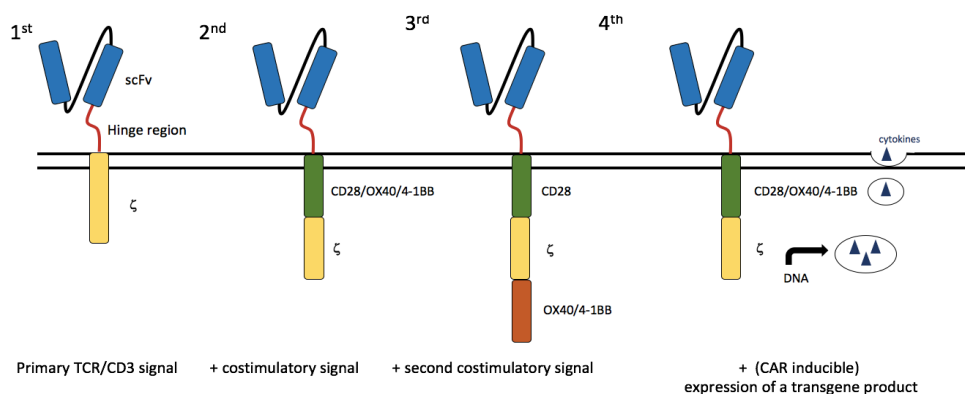


Figure 1. Evolution of CAR-models with growing signaling capacities. 1st generation CARs with a CD3 ζ domain have an ITAM signaling molecule incorporated; 2nd generation CARs contain an additional intracellular costimulatory domain; 3rd generation CARs are equipped with a second costimulatory domain; 4th generation CARs utilize a CAR-inducible promoter for enhanced cytokine production. Modified after TRUCKS: the fourth generation of CARs, Chmielewski et al., 2015 [37]

A typical CAR consists of an ectodomain which comprises a binding section, an extracellular hinge and spacer region, a transmembrane domain and the signaling endodomain. The binding section is a **single-chain variable fragment (scFv)** derived from a monoclonal antibody and can be chosen to detect the epitope of a specific tumor-associated antigen. The

scFv comprises the variable heavy and light chains of a monoclonal antibody joined by a flexible linker region. Possible detection sites for CARs include epitopes from various cancer- and leukemia- associated antigens, such as carcinoembryonic antigen (CEA), CD30 or CD19 as well as viral antigens on virus-infected cells like HIV [30, 38, 39]. Current studies also use proteins or carbohydrates as targets, this enlarges the spectrum of diseases that are potentially treatable with CAR therapy [40, 41]. The affinity of the scFv is decisive for CAR efficacy [42, 43]. For example, CARs containing high-affinity scFvs for ROR1, a tumor-associated molecule, led to greater effector function in T-cells than low-affinity scFvs [42]. However, there is a certain threshold above which a further increase in affinity does no longer enhance the anti-tumor effect [44].

Similar to the standard TCR interaction with tumor cells, the recognition of cells by the CAR is determined by the structure of the antigen on the target cell and the location and accessibility of the epitope that is recognized. Therefore, the **hinge region** between the T-cell membrane and the scFv has to provide flexibility and a certain length, depending on the structure of the target molecule [45, 46]. Shorter hinge sequences were derived from e.g. CD8 α [33, 47]; other groups used sequences of different lengths derived from the IgG1 or IgG4 hinge region [48-50]. A longer sequence is thought to be required for effective tumor recognition *in vivo* if the target epitope is located very proximal to the tumor-cell membrane [45, 46].

The **transmembrane domain** connects the extra- and intracellular parts of a CAR and anchors the CAR in the cell membrane, thereby creating a structural link between the ecto- and endodomain [22]. Initially, transmembrane domains were mainly derived from CD3 ζ , but CARs with domains from CD28 proved to persist longer *in vivo* [22, 48].

Intracellular T-cell activation depends on the phosphorylation of immunoreceptor tyrosine-based activation motifs (ITAMs), which are present in the cytoplasmic CD3 ζ domain of the original T-cell receptor complex. In addition to TCR signals, T-cells need costimulatory signals for strong activation. Therefore, the **endodomain** of CARs contains the CD3 ζ domain as well as one or more costimulatory domains like CD28 or 4-1BB, that enhance the proliferation and persistence of T-cells [51]. The ideal intracellular chain is still an issue of controversy. Haynes *et al.* compared the most promising types, the TCR CD3 ζ and the Fc γ receptor for IgE and demonstrated the superior signaling capacities of CD3 ζ [52]. *In vivo*, CARs with only CD3 ζ did not trigger the production of optimal amounts of cytokines and only led to transient cell division that did not induce a prolonged anti-tumor response [53, 54]. These CARs were retrospectively called 1st generation CARs. Further development led to 2nd generation CARs which contain an additional costimulatory domain, mostly derived from CD28. These CARs

showed prolonged proliferation of the modified T-cells as well as enhanced intracellular signaling [55-58]. Other costimulatory domains that were already used are CD137 (4-1BB), CD244 (2B4) or CD134 (OX40)[48, 51, 59-61]. It remains to be defined, which of these alternative domains leads to the ideal amount of cytokine release and proliferation of CAR T-cells, since experiments with different domains have shown promising results. More recently developed constructs to treat malignancies are the 3rd generation CARs (Figure 1), which contain the CD3 ζ and the CD28-domain plus the intracellular part of a second costimulatory molecule, for example OX40 [62, 63]. Those tripartite signaling CARs have not yet been tested as extensively in research and clinical studies as the 2nd generation CARs, and concerns that the lower signaling threshold might lead to activation of modified T-cells without prior antigen detection have to be further investigated. Recently, a 4th generation of CARs has been developed specifically to target solid tumors (Figure 1). These so-called "TRUCKs" (T-cells redirected for universal cytokine-mediated killing) try to overcome the therapeutic limits of CARs when targeting solid tumors with large phenotypic heterogeneity by the inducible release of transgenic immune modifiers like IL-12 [37]. This leads to a more local production of cytokines within the tumor microenvironment and therefore improves the conditions for T-cell persistence in solid tumors [64].

1.1.2 Clinical use of adoptive T-cell therapy with CARs

Currently, clinical studies with CARs against hematologic malignancies focus on patients that have already been intensively pretreated, often with unsuccessful stem cell transplantation. Prior to adoptive T-cell therapy, lymphodepletion via chemotherapy is considered important to create a receptive environment for T-cell engraftment. Lymphodepletion might favor homeostatic expansion of the infused cells via enhanced cytokine production and decrease the number of immunosuppressive cells like regulatory T-cells which normally secrete inhibitory cytokines [65-67]. The toxicity of myeloablative chemotherapy can be a major problem, however the latest non-myeloablative chemotherapeutic regimes use lower doses of e.g. cyclophosphamide that do not destroy the bone marrow completely [68, 69].

For clinical applications with CAR T-cells, autologous T-cells are isolated from the patient's blood before chemotherapy and equipped with a CAR *in vitro*. Current clinical trials primarily use lentiviral vectors to insert the CAR genome into the T-cell DNA via viral gene transfer, since lentiviral vectors mediate a predictable efficiency of stable transgene insertion with a predefined copy number [33, 34, 47, 70, 71]. *In vitro* expansion is mediated by either activation via TCR triggering and/or by preconditioning with stimulatory cytokines like IL-2 [72, 73]. After chemotherapy and parallel expansion of the T-cells to therapeutic numbers, T-

cells equipped with CARs are reinfused into the patient's peripheral veins. *In vivo*, the cells are stimulated by the CAR-mediated interaction with target-antigen expressing cells. Upon binding of the CAR, activation signals are transmitted into the nucleus of the T-cell, triggering cytotoxic effector functions of the T-cell against its target cell, like the secretion of perforin and granzymes. Perforin penetrates the tumor cell surface so that granzymes can enter the cell and induce apoptosis [74]. The T-cell also expresses the Fas Ligand (FasL) and the tumor necrosis factor related apoptosis inducing ligand (TRAIL) which induce apoptosis signals within the tumor cell. Pro-inflammatory cytokines like IL2, IFN γ and TNF α are released and activate various immune cells. The detection of a matching antigen also initiates proliferation of the CAR T-cells and therefore further enhances the immune response [75].

While most clinical trials in the field of CAR therapy are conducted with autologous T-cell transplantation, donor-derived CAR T-cells are emerging as an alternative opportunity. Recent studies inserted CD19 CARs in donor-derived lymphocytes to enhance their graft-versus-malignancy activity [50, 76]. The T-cells for genetic modification are cells that circulate in the patient's blood after allogeneic hematopoietic stem cell transplantation (HSCT), and were therefore originally donor cells from the HSCT donor but have already undergone thymic selection in the patients' immune system. The results were mixed, e.g. in a trial that treated ten patients with persisting B-cell malignancies despite prior allogeneic HSCT with a single infusion of CD19 CAR T-cells, three of them experienced complete remission [77]. The remission was likely due to CD19-specific immune responses rather than general donor-versus-host response against allogeneic antigens [76, 77].

1.1.3 CAR targets for hematologic malignancies

Research in CAR target design intends to identify extracellular domains that recognize and bind to malignant cells without serious toxicity to normal tissues. An obstacle in the treatment of B-cell malignancies is that the majority of B-cell lymphoma and leukemia target antigens suitable for CAR recognition are primarily expressed in healthy B-cells. CAR T-cells can be used to target a highly and consistently expressed B-cell lineage-specific antigen like CD19, CD20 or CD22, resulting in elimination of malignant and also normal B-cells. As shown in Figure 2, the expression of CD20 starts in PreB-cells, while CD19 and CD22 are already expressed in ProB-cells. The three expression patterns for CD19, CD20 and CD22 are maintained until the B-cells mature to plasma cells.

Based on the expression pattern, CD20 has been used to target B-cell leukemias and lymphomas, which has been done in few studies with 1st generation CARs [49, 78].

Specifically, patients with diffuse large B-cell lymphoma (DLBCL), follicular or mantle cell lymphomas received CD20-specific modified T-cells. In one study, the patients with mantle cell lymphoma also received IL-2 injections and the clones persisted for up to nine weeks and induced remission [78]. However, the DLBCL patients showed no clinical response and the transferred genetically modified T-cells vanished rapidly [49]. CD19 and CD22 can also be used to treat preB-ALL as well as B-cell leukemias and lymphomas. Haso *et al.* developed a CAR that binds a membrane-proximal epitope of CD22 and *in vitro* experiments targeting preB-cell acute lymphatic leukemia (ALL) showed promising results [79]. A protein consisting of an exotoxin of *Pseudomonas* that is covalently bound to the scFv of CD22 has been successfully used to target lymphomas in clinical trials [80, 81].

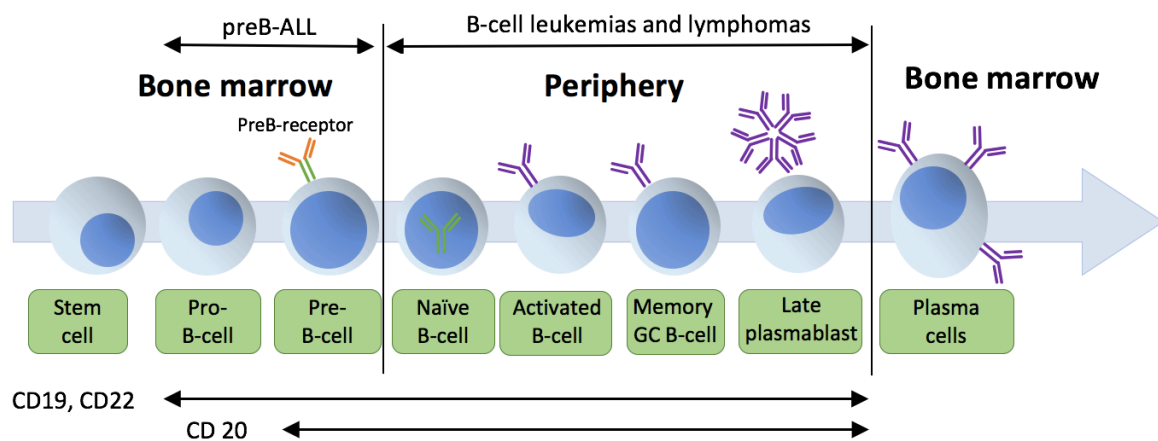


Figure 2. Antigen representation on B-lineages and associated B-cell malignancies. CD19 and CD22 are expressed from Pro-B-cell until maturation into plasma cells. CD20 expression starts in Pre-B-cells and lasts until maturation into plasma cells. Modified after Blanc *et al.*, 2011 [82]

CD19, a 95-kDa transmembrane glycoprotein, is an attractive marker for B-cell malignancies because it is expressed on all stages of the B-cell lineage except plasma cells and is often maintained on cells that have undergone neoplastic transformation [83, 84]. Correspondingly, treatment with CD19 specific CARs leads to permanent depletion of all CD19+ B-cells as long as CD19-targeted CAR T-cells are present in the patient. Most success against hematologic malignancies has been achieved with CARs targeting CD19. In March 2019, over 150 active CAR-related trials were listed on the online database of clinical studies by the U.S. National Library of Medicine [85]. In 2003, Brentjens *et al.* showed that expanding peripheral blood T-cells that were genetically engineered to target CD19 persisted in immunodeficient tumor-bearing mice and eradicated CD19+ cell lines and primary ALL cells [86]. Almost nine years later, a successful case study of a patient with chronic lymphatic leukemia (CLL) treated with autologous T-cells equipped with a 2nd generation CD19 CAR was published [33]. The patient remained in complete remission for over 10 months. Other

clinical trials with CD19-targeted CARs followed, often with patients suffering from chemorefractory diseases or relapses after non-successful allogeneic stem cell transplantation [87, 88]. These studies used either 4-1BB or CD28 as costimulatory domains and also differed in the use of retroviral and lentiviral gene transfer. While earlier studies were directed against indolent Non-Hodgkin-lymphoma (NHL) and CLL, more recent trials showed that CD19 CAR T-cells can also efficiently treat more aggressive acute lymphatic leukemias (ALL) [34, 87, 89]. Some trials had to be stopped due to severe side effects and toxicities, most notably a trial by Juno therapeutics that led to five cases of fatal cerebral edema after admission of CD19 CARs [90, 91]. In summary, a review in August 2017 stated that from 234 registered patients that were treated with CD19 CARs, more than 60% showed an objective anti-tumor response while only 20% did not respond at all [92].

1.1.4 Obstacles in clinical trials

While recent clinical CAR trials like the CLL- and ALL-studies by June *et al.* were successful in their overall outcome, serious adverse events have been reported as well [33, 87]. CAR-induced toxicity can be divided into *off-target* and *on-target* toxicity. *Off-target* toxicity occurs, if the CAR cross-reacts with an epitope that is not located on the tumor cell and is activated without connection to the tumor. The intended interaction between CAR and antigen on the tumor cell can lead to *on-target* toxicity. Another form of *on-target* toxicity may occur if the targeted epitope is detected by the CAR somewhere else than on tumor cells, i.e. "*on-target, off-tumor*".

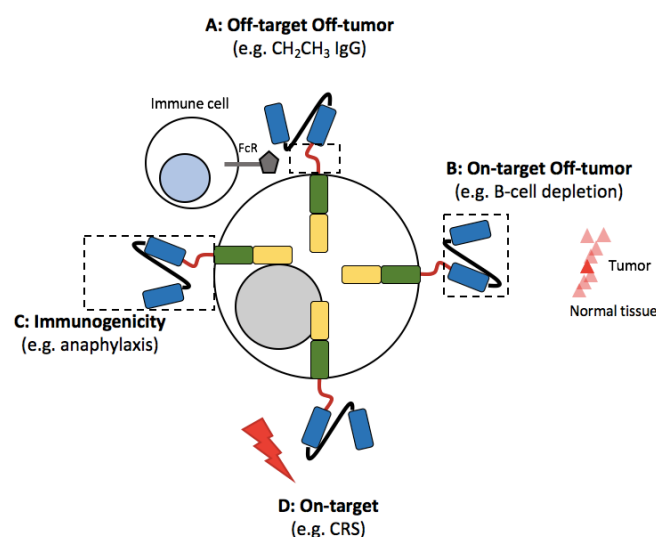


Figure 3. Toxicities associated with CARs. **A. Off-target, Off-tumor toxicities.** CARs with extracellular IgG CH₂CH₃ spacer might interact with innate immune cells, leading to antigen independent activation of the immune system as well as of CAR T-cells. **B. On-target, Off-tumor toxicity.** Target-antigen recognition that is also expressed on healthy tissue. **C. Immunogenicity.** Exogenous parts of the CARs can lead to severe autoimmune reactions. **D. On-target toxicity.** The intended antigen recognition might lead to an overwhelming immune response resulting in toxicity. Modified after Casucci *et al.* 2015 [93]

(A) Off-target, Off-tumor toxicities may originate from the binding interaction of the CAR molecule with receptors expressed on innate immune cells, leading to antigen-independent activation. With increasing potency of CARs, the risk for auto-reactivity in form of either activation of native T-cells or unspecific *off-tumor* activation increases. Each CAR contains parts of a monoclonal antibody; thus, it is not predictable whether parts of it might interact with epitopes on the surface of healthy human cells or not.

The hinge region in many CD19 CARs currently consists of a long spacer from the IgG1 or IgG4 CH₂CH₃ domain. They lead to dimerization and thereby increase CAR expression on the cell surface [94]. The CH₂CH₃ hinge was chosen because of its flexibility, lack of immunogenicity and easily adaptable modification of the length. One challenge of CAR therapy in clinical use is the effective cultivation and expansion of T-cells to ensure sufficient numbers for treatment. A major advantage of the CH₂CH₃ hinge is the possibility to detect CAR T-cells and purify T-cell populations with antibodies binding to the CH₂CH₃ domain. However, Hombach *et al.* demonstrated that the CH₂CH₃ domain of these CD19 CARs shows significant binding to Fc γ receptors i.e. the Fc γ RI (CD64) and the Fc γ RII (CD32) [94]. This leads to off-target activation of CAR T-cells and subsequently to activation induced cell death (AICD). AICD results in rapid loss of anti-tumor activity *in vivo* due to the loss of effector cells. As shown by Hudecek *et al.*, the interaction also activates immune cells which express Fc γ -receptors like monocytes or NK-cells and therefore leads to an unwanted immune response independent of the initial target cell. *In vivo* studies in mice demonstrated that Fc-receptors in the lungs activated CAR T-cells, which then disappeared due to AICD [94, 95]. This indicates that the spacer region can have significant effects on *in vivo* anti-tumor activity independent of costimulatory agents.

(B) Undesired On-target but Off-tumor toxicity can occur if the antigen is also expressed by other tissues or if cross-reaction with proteins on healthy tissue takes place [96, 97]. The consequences of on-target but off-tumor toxicities for the patient are partly dependent on whether the tissue expressing the target-antigen is essential or not for the survival of patients. For example, successful therapy with CD19 CARs against B-cell leukemic lines leads to the permanent depletion of B-cells, since healthy B-cells also express CD19 on their surface. Fortunately, this B-cell deficiency can partly be compensated by immunoglobulin infusions (IVIg) as replacement therapy [33, 47, 48, 89]. However, fatal lung toxicity after administration of anti-HER2 CARs to a patient with metastasized colon carcinoma might have been based on low-level HER2 expression on lung epithelia [98]. The patient was treated with a CAR based on the monoclonal antibody Trastuzumab, experienced respiratory distress within minutes after T-cell administration and died after 5 days. Possibly, anti-HER2 directed

T-cells recognized HER2 expressed by normal lung cells and released cytokines that caused pulmonary toxicity and edema followed by a cytokine storm which ultimately led to multiorgan failure [98, 99].

In comparison to CARs, TCRs are more prone to toxicity due to cross-reactions, since they detect much shorter epitopes which are therefore more likely to be part of other off-target receptors as well [93, 100]. This form of autoimmune toxicity led to the death of two patients that were treated with a TCR against melanoma targeting MAGE-A3 peptides presented on HLA-A*02. The TCR cross-reacted with MAGE-A12, which is expressed in the brain, and resulted in severe neurotoxicity [101]. In another study, two patients that were also treated with an affinity-enhanced TCR against MAGE-A3 that was presented on HLA-A*01 developed fatal cardiogenic shock, presumably due to the recognition of an epitope of Titin, a protein in cardiac tissue [96].

(C) As described in chapter 1.1.1, currently used CARs are assembled from pieces of different surface molecules of partly human and also murine origin. Therefore, **immunogenicity** of CARs can restrict the duration of treatment and limit the overall antitumor effect. Antitransgene rejection responses have previously been described as decisive factor for limited persistence of adoptively transferred CAR T-cells in humans [49]. Four patients with recurrent lymphoma were treated with CD19 and CD20 directed CAR T-cells, which were only detectable in the patient's blood stream for 1 to 7 days. Cellular antitransgene immune rejection responses that were mounted by the patient's endogenous T-cells were likely responsible for this lack of T-cell persistence.

Repeating doses of CARs that comprised parts of mouse monoclonal antibodies even led to severe immune reactions, like the development of IgE-mediated anaphylaxis [102]. Ideally, all non-human parts of a CAR should be replaced to minimize the risk of immunogenicity. This is intended by the use of proteins that are fully human, like CARs against the folate receptor α (α FR) in ovarian cancer [103], or via epitopes derived from humanized monoclonal antibodies.

(D) Cytokine release syndrome (CRS) is mainly characterized by high fever, tachycardia, hypotension, nausea, neurological syndromes, capillary leak syndrome and respiratory distress and may involve any organ including the central nervous system [34, 104, 105]. It is a potentially life-threatening toxicity caused by very high levels of pro-inflammatory cytokines like IFN- γ and IL-6, which are released by infused CAR T-cells after maximal and extensive cell activation. Patients with CRS were treated primarily with intensive supportive care and causal with the IL-6 receptor blocker Tocilizumab [108]. Prophylactic splitting of the

initial T-cell dose over 3 days and intensified monitoring during the first days after infusion to prevent CRS have proven to be effective, especially in combination with Tocilizumab and/or corticosteroids [104, 106].

1.2 The Suicide Gene System

1.2.1 Development of Suicide Gene Systems

With a growing amount of successful clinical trials with CARs and expanding scope of adoptive T-cell therapy, the demand for a system that facilitates *in vivo* control of the genetically modified cells has increased. One approach, which has been successfully tested in donor lymphocyte infusion (DLI) settings [107, 108], is to equip T-cells with a “safety switch” in form of a suicide gene system to allow selective destruction of these cells. The suicide gene encodes for an inert protein that converts a prodrug into a cytotoxic metabolite. Together with the CAR, the suicide gene can be transferred into T-cells and does not influence the cell metabolism until the matching prodrug is administered. Activation of the prodrug leads to the selective death of the CAR T-cell, which, in turn, ends severe side effects or the therapy itself as soon as a patient is considered to be cured [109]. Especially patients treated with CD19 CAR therapy against hematologic malignancies would benefit from such a therapy stop, since they experience the permanent B-cell depletion by the CAR T-cells. While administration of the prodrug initiates apoptosis in all suicide gene positive cells, non-transduced cells are not affected.

The first and best characterized system that was used *in vivo* to eliminate cells after HSCT or DLI, is the Herpes simplex virus – thymidine kinase (HSV-tk) in combination with its prodrug, Ganciclovir [110]. The viral enzyme thymidine kinase is essential for the first step of the intracellular phosphorylation of toxic Ganciclovir-triphosphate, which is then inserted as base-analog into the cellular DNA and induces apoptosis. This system was already successfully used in several clinical trials, but has also demonstrated its disadvantages [111, 112]. Due to its mechanism, the efficacy depends on cell proliferation and resting cells cannot be eliminated. The major disadvantage is that the HSV-tk protein is strongly immunogenic and led to rapid elimination of the T-cells after transfusion before a graft-vs-leukemia effect could evolve [113]. Also, Ganciclovir is an essential drug in the treatment of viral infections and reactivations like CMV after HSCT [107, 114].

Another suicide gene, iCASP9, is based on a fusion-protein of the human caspase 9 and a modified human FK-binding protein, AP1903. This fusion protein dimerizes upon exposure

with its drug, a synthetic small molecule. Dimerization of caspase 9 activates the downstream executioner caspase 3 molecule and therefore initiates apoptosis of the T-cell [109, 115]. In a clinical trial, more than 90% of the T-cells could be eliminated within less than an hour [109, 116].

An alternative system consists of a CD8 stalk with two Rituximab® binding sites from CD20 which are separated by the binding site for an antibody against CD34. This construct allows for the selection of transduced cells via CD34 antibodies. Additionally, these cells can be selectively eliminated via infusion of Rituximab®, a CD20 antibody. This system is highly promising since it leads to immediate cell death and is completely of human origin. Furthermore, Rituximab® is very well characterized and already approved for treatment of B-cell malignancies as well as autoimmune diseases [117].

1.2.2 CYP4B1-System

A recently developed new suicide gene system is the CYP4B1P+12 system with its prodrugs 4-*Ipomeanol* (4-IPO) and *Perilla ketone* (PK). The cytochrome P450 proteins are a superfamily of heme proteins which are present in virtually all organisms and catalyze reactions involved in drug metabolism and synthesis of cholesterol, steroids and other lipids [118, 119]. Like other CYP4 family cytochromes, the monooxygenase CYP4B1 ω -hydroxylates medium fatty acid chains [120] and metabolizes different xenobiotic substances like 4-*Ipomeanol* and aromatic amines, some of which led to tissue specific toxicity in animals [121-123].

In 1970, the phytoalexin 4-*Ipomeanol* was first identified as the cause of death in cattle that ingested mold-affected potatoes [124]. This furan-derivate (Figure 4) is produced naturally by the common sweet potato, *Ipomoea batatas*, in the presence of the mold *Fusarium solani* [125]. The enzyme CYP4B1 transfers an oxygen atom to the furan ring of 4-IPO and generates a highly toxic metabolite that causes DNA-protein cross links and DNA strand breaks resulting in apoptosis [120]. In mammals, CYP4B1 is predominantly expressed in lung cells and only low levels of mRNA can be detected in liver tissue and other tissues. Therefore, mammals die in respiratory distress after ingestion or administration of 4-*Ipomeanol* due to its tissue-selective activation by CYP4B1 in bronchiolar Clara cells and to a lesser degree in type II pneumocytes in the lung [126, 127]. The pulmonary toxicity of 4-*Ipomeanol* was also shown for laboratory animals and livestock [128]. Up to now, the exact chemical structure of the reactive intermediate is not known.

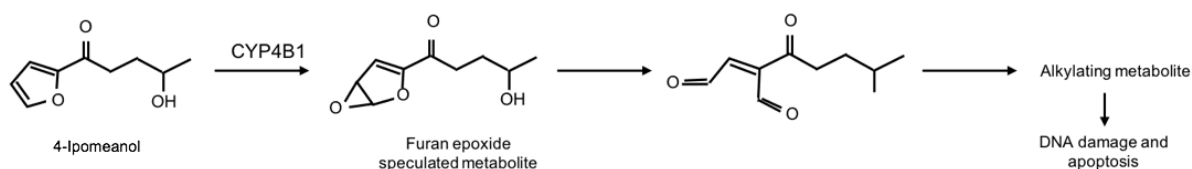


Figure 4. Bioactivation of 4-Ipomeanol via CYP4B1. The activation of 4-Ipomeanol via oxidative metabolisation of the furan ring leads to DNA-protein cross linking and DNA breaks, inducing apoptosis.

Due to its natural “lung-specific toxicity”, a result of the tissue-specific expression profile of CYP4B1, 4-Ipomeanol was viewed in the 1970ies as an ideal chemotherapeutic against lung tumors that would predominantly be activated in human lung tissue [127]. Here, one preliminary study in human non-small cell lung cancer lines demonstrated that incubation with 4-Ipomeanol led to metabolic activation and cytotoxicity of the cells *in vitro* [129]. Surprisingly, *in vivo* phase I/II studies showed no objective antitumor response against neither lung nor liver cancer. The dose limiting factor in those studies was hepatotoxicity [130]. Transient elevations in hepatocellular enzymes, predominantly alanine aminotransferase, occurred in the majority of patients [130]. When patients were treated with higher doses, hepatocellular toxicity was more severe and associated with right upper quadrant pain and severe reduction in general condition [127, 130-132]. A possible explanation for this toxic side effect was that the activation of 4-IPO was also catalyzed by other p450-cytochromes, since some of these cytochromes are highly expressed in liver tissue. However, this hypothesis was never proven in liver cells. Subsequent studies described a species difference between different mammals in 4-Ipomeanol metabolism and detected a decisive proline-to-serine transversion in the highly conserved meander region of the wild-type human protein CYP4B1 at position 427 [133]. This amino acid exchange renders the human CYP4B1 enzyme incapable of processing 4-IPO at all and explains the failed clinical studies [133, 134].

By contrast, the toxicity generated by the rabbit cytochrome P450 isozyme CYP4B1 (rCYP4B1) in combination with 4-Ipomeanol is very high. Therefore, this combination was tested as suicide gene system against gliosarcoma in rats [135]. *In vitro* experiments showed that only low concentrations of 4-IPO were needed to kill human and rat tumor cells that expressed rCYP4B1 with a direct correlation between the rCYP4B1 protein concentration and toxicity. The growth of rCYP4B1-expressing tumor cells that were implanted subcutaneously in mice was also stopped efficiently by intraperitoneal administration of 4-Ipomeanol [135]. When the rCYP4B1/4-IPO system was compared to the HSV-tk/Ganciclovir system *in vitro*, a significantly faster induction of apoptosis was measured [136, 137].

In order to avoid the potential immunogenicity of the rabbit enzyme, Wiek *et al.* re-engineered a human activated CYP4B1 by systematically exchanging different amino acids and thereby developed the concept of using the human CYP4B1 as a suicide gene [138]. The proline to serine change (hCYP4B1-P427) in the human protein already led to a higher enzyme activity towards 4-*Ipomeanol* and to a stabilized protein structure. The systematic exchange of 12 more single amino acids resulted in a modified human enzyme (hCYP4B1P+12) that metabolizes 4-*Ipomeanol* as effectively as the highly active rabbit CYP4B1. Since all altered amino acids are present in other human P450 enzymes at corresponding positions [138], the risk of generating immunogenicity via hCYP4B1P+12 is probably low.

Numerous other substrates like 3-methylindole or 2-aminofluorene are also known as potential prodrugs for CYP4B1 [120]. In a recent extensive biochemical characterization, different potential substrates were screened [139, 140]. Perilla ketone (PK), a naturally occurring pneumotoxin with very similar structure to 4-IPO (Figure 5), is a major ingredient in the oil of *Perilla frutescens*, a food plant in Asia, also known as ‘beef-steak plant’ or ‘perilla mint’ [141]. The chemical structure of PK resembles 4-IPO and only differs by a methyl group in position C5 instead of a hydroxyl group (Figure 5).

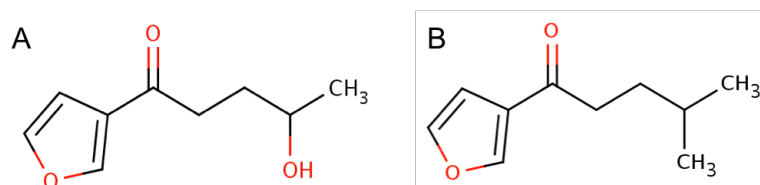


Figure 5. Chemical formulas of 4-*Ipomeanol* (A) and Perilla ketone (B). 4-IPO consists of a furan ring, which is substituted at the third carbon with a pentanone containing a hydroxyl group. The chemical structure of PK only differs from 4-IPO by a methyl group on position C5 instead of the hydroxyl group.

In the 1980s, studies on the effect of PK exposure in mammals showed that intoxication led to pulmonary edema and emphysema as well as liver toxicity [141, 142]. Importantly, PK proved to be more effective than 4-IPO in inducing apoptosis in genetically modified human T-cells that expressed CYP4B1 isoforms. There was no unspecific toxicity in control cells that did not express the rabbit or the humanized CYP4B1 protein [140]. In light of these findings, PK could be a suitable alternative prodrug for the hCYP4B1P+12 suicide gene.

1.3 Objective of this thesis

In vivo studies with CARs have demonstrated that the commonly used CH₂CH₃-derived fragment as hinge region can interact with the FcγR on myeloid cells leading to *off-target* activation and subsequent activation-induced cell death of the CAR T-cells. Hence, the first aim of this thesis was to design new hinge regions for CARs. Ideally, this hinge region should also be recognized by a monoclonal antibody that facilitates the detection and selection of CAR-expressing T-cells *in vitro* under GMP-compliant conditions.

Since clinical trials with CARs led to adverse events and toxicities, the inclusion of a safety switch that facilitates control of engineered T-cells *in vivo* would be of great benefit for clinical studies. To this end, a novel human suicide gene system utilizing the orphan human CYP4B1 enzyme changed at 13 amino acid positions has been rendered highly active to metabolize 4-*Ipomeanol* and a second prodrug, *Perilla ketone*. In order to potentially use either prodrug in combination with the activated hCYP4B1P+12 enzyme, it is important to understand which of the main cytochrome p450 enzymes in the liver were responsible for organ toxicities in the clinical trials with 4-*Ipomeanol*. Therefore, the second part of this thesis also investigated whether 4-*Ipomeanol* and *Perilla ketone* can be metabolized by different cytochromes that are naturally expressed in the human liver.

In the third part of this thesis, the newly created CARs were coexpressed together with the CYP4B1 suicide gene in human T-cells and tested for their efficiency in killing malignant B-cells. Finally, apoptosis of the CAR T-cells was induced by activation of the CYP4B1 suicide gene system.

2 MATERIAL AND METHODS

2.1 Material

2.1.1 Commercial Kits and enzymes

Table 1 Commercial Kits and Enzymes

Kits	Manufacturer
Plasmid DNA Purification NucleoBond Xtra Maxi	Macherey-Nagel (Düren), #740414100
High Pure PCR Product Purification Kit	Roche (Grenzach-Whylen), #11732676001
High Pure Plasmid Isolation Kit	Roche, #11754777001
DyeEX 2.0. Spin Kit	QIAGEN (Hilden), #63206
CD34 MicroBead Kit	Miltenyi Biotech, (Bergisch- Gladbach), #130-046-702
CD127 MicroBead Kit	Miltenyi Biotech, #130-092-283
Enzymes	Manufacturer
Pwo-DNA-Polymerase	Roche, #11644955001
T4-DNA-Ligase	New England Biolabs (NEB), (Frankfurt am Main), #M0202M
Restriction enzymes	NEB

2.1.2 Length and size standards

Table 2 Length and size standards

DNA-length standards	Manufacturer
1 kb plus DNA ladder	Thermo Fisher (Oberhausen) (#SM1333)
100 bp DNA ladder	Invitrogen (Karlsruhe), (#15628019)
Protein size standards	
PageRuler Plus Prestained Protein Ladder	Thermo Fisher (#26619)

2.1.3 Oligonucleotides

Oligonucleotides for Sequencing-PCRs of plasmids

Table 3 Oligonucleotides for Sequencing- PCRs of plasmids

No.	Sequence	Description
1561	CACCGCCATCTACTACTGCG	Forward-Primer, binds at the 5'End of the CL_CD19CAR
997	CATTAAAGCAGCGTATCCACATAGCG	Reverse-Primer, binds at the 3'End of the WPRE sequence
1260	CTCTCGGCATGGACGAGCTG	Forward-Primer, binds at the 5'End of EGFP
1565	CCTGGACTGGTGGCCCAAG	Forward-Primer, binds at the 5'End of the CL_CD19CAR

Oligonucleotides for PCR-amplification of plasmid fragments

Table 4 Oligonucleotides for PCR-amplification of plasmid fragments

No.	Sequence 5'-3'	Description
1903	CCAATTGAGATGCGCCTACGGCTACTAC CAGGACGAGACAAC	Forward-Primer, binds near the 5'End of Δ NGFR, encodes for the <i>MfeI</i> -cutting-site
1904	CACGCGTTCACACACGGTGTCTGCTTG TCTTGACAACCTGAACACC	Reverse-Primer, binds near the 3'End of Δ NGFR, encodes for the <i>MluI</i> -cutting-site
1905	CCAATTGGAGTGCCCCGACGGCACCTAC AGCGAC	Forward-Primer, binds near the 5'End of Δ NGFR, encodes for the <i>MfeI</i> -cutting-site
1906	CACGCGTTCGCACTCGGCATCGGCCCATC TGG	Reverse-Primer, binds near the 3'End of Δ NGFR, encodes for the <i>MluI</i> -cutting-site
1913	CACGCGTACTGTAGAGGCGATCAGATCC TGCTCGGG	Reverse-Primer, binds at the 3'End of Δ NGFR, encodes for the <i>MluI</i> -cutting-site
1914	CCAATTGCCCTGCCTGGACAGCGTGACC TTTAGCG	Forward-Primer, binds at the 5'End of Δ NGFR, encodes for the <i>MfeI</i> -cutting-site
1911	AATTGGAGCTGCCTACCCAGGGCACCTT CAGCAACGTGTCCACCAATGTGTCCCGA	Forward-Primer, binds near the 5'End of Δ CD34, encodes for the <i>MfeI</i> -cutting-site
1912	CGCGTCGGGACACATTGGTGGACACGTT GCTGAAGGTGCCCTGGGTAGGCAGCTCC	Reverse-Primer, binds near the 3'End of Δ CD34, encodes for the <i>MluI</i> -cutting-site
1907	GCCAATTGAGCCTGGACAACAACGGCAC CGCCACCC	Forward-Primer, binds near the 5'End of Δ CD34, encodes for the <i>MfeI</i> -cutting-site
1908	GCACGCGTGTGGTGGTTTCTGGTAGGA CACATTGGTGGACAC	Reverse-Primer, binds near the 3'End of Δ CD34, encodes for the <i>MluI</i> -cutting-site
1909	GCCAATTGGAGCTGCCTACCCAGGGCAC CTTCAGCAACG	Forward-Primer, binds near the 5'End of Δ CD34, encodes for the <i>MfeI</i> -cutting-site
1910	GCACGCGTACGGTTGTCTCGGTGATGTT GGTGGTGGCC	Reverse-Primer, binds near the 3'End of Δ CD34 encodes for the <i>MluI</i> -cutting-site
1915	GCACGCGTTGCACGCTGCTGTTGGTGT GCCGTACAC	Reverse-Primer, binds near the 3'End of Δ CD34 encodes for the <i>MluI</i> -cutting-site
1916	GCACGCGTCCGGGAGACAGGCTGGGCTT CAG	Reverse-Primer, binds near the 3'End of Δ CD34 encodes for the <i>MluI</i> -cutting-site
1917	GCACGCGTTCGGCCTGTTCTTCGCCACAC AGCACTCT	Reverse-Primer, binds near the 3'End of Δ CD34 encodes for the <i>MluI</i> -cutting-site

2.1.4 Plasmids

Table 5 Helper plasmids

Helper plasmids	Description
pCD/NL-BH	CMV-promoter driven expression vector for HIV gag/pol and accessory/regulatory genes; envelope & coating signals inactivated by deletion [143]
pczVSV-G wt	Construct to express the glycoprotein G of the vesicular stomatitis virus (VSV) [144]

2.1.5 Expression vectors

In this thesis, self-inactivating lentiviral expression vectors were used for gene transfer. Lentiviruses are part of the *Retroviridae* family, lead to a stable expression of transduced genes and facilitate quick and efficient transduction procedures compared to non-viral gene transfer [145, 146]. The vectors used in this thesis are replication deficient. They do not express viral proteins any more, instead they only contain *cis*-active sequences which are essential for e.g. reverse transcription and integration as well as for transcriptional control of the viral gene expression [146-148]. The necessary genes for the assembling of the virus particles are provided by separate expression plasmids *in trans* without separate packaging signal. Therefore, the newly created virus capsid only contains the packaging vector together with the transgene cassette and no enzymatic or regulatory genes. Without expression of those essential structural genes, no replicable virus can be produced in the transduced target cells. Furthermore, the used vectors are self-inactivating (SIN-) vectors with deleted promoter and enhancer sequences in the 3'LTR region [149]. After reverse transcription within the target cell, the deleted region serves as a template and is copied into the 5'LTR. Thereby, the generated 5'LTR is inactive what reduces the risk of unintended activation [150-152].

pMK-RQ_CD19_CAR is a cloning vector by Geneart life technologies that was used as a template for the R.CD19 CAR. The vector contains a Kanamycin resistance gene. The codon optimized R.CD19 CAR was developed in cooperation with Claudia Rössig, Münster [139].

p2CL21EGT2AR.CD19cowo is a lentiviral vector containing enhanced green fluorescent protein (EGFP) and the R.CD19 CAR, separated by a thosa assigna virus 2A (T2A) site.

Table 6 Inserts in p2CL21EGT2AR.CD19cowo

Plasmid name	Inserted cDNA
p2CL21 Δ CD34coT2AEGcowo	Δ CD34 and EGFP
p2CL21 Δ NGFRcoT2AR.CD19cowo	Δ NGFR and the R.CD19 CAR
p2CL21 Δ NGFRcoT2AEGcowo	Δ NGFR and EGFP
p2CL21 Δ NGFRcoT2AP+12cowo	Δ NGFR and the human CYP4B1 with aa changes
p2CL21P+12coT2A Δ CD34cowo	human CYP4B1 with 13 aa changes and Δ CD34
p2CL21R.CD19coT2AP+12cowo	R.CD19 CAR and the human CYP4B1 with 13 aa changes

p2CL21EGI2Pcowo is a lentiviral expression vector with EGFP and a codon-optimized puromycin resistance gene, separated by an IRES2-site.

Table 7 Inserts in p2CL21EGI2Pcowo

Plasmid name	Inserted cDNA
p2CL21r4B1EGI2Pcowo	rabbit CYP4B1
p2CL21h4B1P427EGI2Pcowo	human CYP4B1 with point mutation (h-P427)
p2CL21hCYP1A2EGI2Pcowo	human CYP1A2
p2CL21hCYP2E1EGI2Pcowo	human CYP2E1
p2CL21hCYP3A4EGI2Pcowo	human CYP3A4
p2CL21hCYP3A5EGI2Pcowo	human CYP3A5

2.1.6 Bacteria

One shot Top10 Competent *E. coli* cells by Invitrogen were used for the transformation of ligations.

2.1.7 Cell lines

Table 8 Cell lines

Cell lines	Characteristics	Reference
HEK293T	human embryonic kidney cells, transformed by adenovirus, contain the SV40 large T-antigen (allows for episomal replication of transfected plasmids containing the SV40 origin of replication)	[153, 154]
HepG2	human hepatocellular carcinoma cell line	[155]
Jurkat	human T-cell line, derived from a patient with acute lymphatic leukemia (ALL)	[156]
REH	human B-cell precursor leukemia cell line, derived from a patient with ALL	[157]

2.1.8 Primary cells

Primary human T-Lymphocytes were isolated from peripheral blood of healthy donors according to the Ficoll-protocol in Chapter 2.3.3. All volunteers provided written consent. The study was approved by the local ethics committee of the Heinrich-Heine-University of Düsseldorf (#4687).

2.1.9 Antibodies

The antibodies were used for FACS analysis, Western Blot and coating of cell culture vessels.

Table 9 Antibodies

Antibodies	Manufacturer	Concentration
<u>Western Blot:</u>		
Anti-EGFP (monoclonal)	Clontech, #632375	1:10000
Anti- β -Actin (monoclonal)	Sigma, #A2228	1:20000
Sheep anti-mouse IgG horseradish peroxidase	GE Healthcare, #RPN4201V	1:10000
<u>FACS cell sorting/analysis:</u>		
CD34 -PE	Thermo Fischer, #MA5-16927	0.5 mg/ml
Anti-Biotin-PE	Miltenyi Biotec # 130-090-756	0.5 mg/ml
CD271-PE	Miltenyi Biotec #130-091-885	0.5 mg/ml
Streptavidin conjugated to PE	BD Bioscience	0.5 mg/ml
Anti-Fcy-PE	Jackson Immunoresearch #109-115-098	0.5 mg/ml
Anti-Fab conjugated to Biotin-SP	Jackson Immunoresearch #115-065-072	0.5 mg/ml
<u>Coating of cell culture vessels:</u>		
CD3 (OKT-3)	eBioscience #19-0037-85	1 μ g/cm ²
CD28	BD Pharmingen™ #555725	1 μ g/cm ²

2.1.10 Buffer and solutions

Table 10 Buffers and solutions – cell culture

Buffer and solutions - cell culture

DMEM	Dulbecco's Modified Eagle Medium by Gibco™ (#31966-047)
IMDM	Iscove's Modified Dulbecco's Medium by Sigma Aldrich™ (#13390)
RPMI-1640	Originally by Roswell Park Memorial Institute, by GIBCO™ (#31870-074)
Supplements:	10 % inactivated FCS (fetal calf serum) by GIBCO™ (#10500-064), B-cell-cultivation: non-inactivated FCS by PAA (#A15-101) - 100 U/ml Penicillin - 100 μ l/ml Streptomycin => Pen/Strep-solution by GIBCO™ (#15140-122) - 2 mM L-Glutamine by GIBCO™ (#25030) - IL-2 (Chiron, Marburg)
Trypsin-EDTA	0.05 % Trypsin and 0.02 % EDTA by PAA™ (#L11-004)
DPBS	Dulbecco's Phosphate Buffered Saline by GIBCO™ (14190169)
Gelatin solution (0.1 %)	1 g gelatin by Sigma Alderich (#G1890) ad 1 l A. dest., mixed and autoclaved

Propidiumiodine stain	Propidiumiodine (PI) by Sigma-Aldrich (#P4864) diluted in DPBS up to a use concentration of 0.5 µg/ml
MACS buffer	0.5% albumin from Bovine Serum by Sigma Alderich (#A7906-10G) with 2 mM EDTA diluted in PBS, pH 7.2
Red blood cell lysis buffer	8.99 g NH ₄ CL, 1 g KHCO ₃ and 40 µl 0.5 M EDTA, ad 1 l A. dest., pH 7.3

Table 11 Buffers and solution – Analysis and Cloning of DNA

Buffer and solutions – Analysis and Cloning of DNA

LB-medium	20 g LB Broth Miller by Sigma-Aldrich (#L3022) filled up with 1 l A. dest
LB-agar	37 g LB Agar by Sigma-Aldrich(#L2897) filled up with 1 l A. dest
TAE-buffer (50x)	242 g Tris base 57.1 ml acetic acid 100 ml 0.5 M EDTA ad. 1 l A. dest, pH 8.5
Sample-buffer (10x)	250 mg Bromphenylblue 250 mg Xylene Cyanol 33 ml 150 mM Tris pH 7,6 60 ml Glycerine ad. 100 ml A. dest.

Table 12 Buffers and solution for protein-biochemical methods

Buffer and solutions for protein-biochemical methods

Protein-lysis buffer (10x)	10 ml 1M Tris/HCl, pH 8.0 8.2 g NaCl 0,25g NaN ₃ 10 ml Triton®X-100
Loading dye	NuPAGE® LDS Sample Buffer by novex® (#NP0007) NuPage® Sample reducing agent 10x by novex® (#NP0009)
Running buffer	NuPAGE® MES SDS Running Buffer 20x by novex® (#NP0002)
Transfer buffer	NuPAGE® Transfer Buffer 20x by novex® (#NP0006-1) 5 % Methanol
Ponceau S Staining solution	1 g Ponceau S 50 ml acetic acid ad. 1 l A. dest
Blocking solution	5 % milk powder by Roth (#T145) in PBS-T
PBS-T	PBS supplemented with 0.1 % Tween®20 by Sigma Aldrich (#1379)

2.2 Molecular biological methods

2.2.1 Primer annealing

Primer annealing was used to create a short, double-stranded DNA, which was subsequently inserted into a vector. 12.5 μ l (100 μ M) of two complementary primers were heated at 95 °C for 5 minutes and then slowly cooled down in stages using a Biometra T3 Thermocycler.

2.2.2 PCR amplification of plasmid fragments

All amplifications were carried out with Pwo-DNA-Polymerase.

Table 13 PCR reaction mix

Substrate	Concentration	Volume
DNA template	200 ng	2 μ l
Pwo-buffer	1x	2.5 μ l
ddNTP-mix	0,2 mM	1 μ l
Forward primer	100 pmol	1 μ l
Reverse primer	100 pmol	1 μ l
PWO-polymerase	2 U	2 μ l
fill up with A. dest.		25 μ l

Table 14 PCR reaction protocol

	Temperature	Duration	Cycle
Initial Denaturation	94 °C	3 min	1
Denaturation	94 °C	30 s	30
Annealing	65° - 68°	1 min	30
Elongation	72 °C	1 min	30
Final Elongation	72 °C	10 min	1
Cooling	4 °C	∞	

2.2.3 Gel electrophoresis

1 – 2 % agarose gels were used for analytical and preparative separation of DNA fragments. The agarose was diluted with 1x TAE buffer, boiled up and cooled down. 0.2 μ g/ml ethidium bromide were added allowing for detection of separated DNA-fragments under an UV-transilluminator. DNA fragments were excised from agarose gels under UV-light and subsequently extracted with the QIAquick Gel Extraction Kit (Qiagen, Hilden, Germany) according to the manufacturer's instructions.

2.2.4 Restriction digestion of plasmid DNA

Restriction digestion of plasmid DNA includes the specific cutting of DNA-sequences via restriction enzymes at specific palindromic sequences. This method was used for analytical identification of plasmids as well as for preparative cloning. The plasmid DNA was incubated

for 3 h at 37 °C with the chosen restriction enzymes and the appropriate restriction enzyme buffer according to the manufacturer's instructions. Success of digestion was tested using agarose gel electrophoresis.

Table 15 Digestion mix of plasmid DNA

	analytical	preparative
DNA	0,5 – 1 µg	5 µg
restriction buffer (10x)	2 µl	2,5 µl
restriction enzyme	2 – 5 U	10 U
filled up with A. dest.	20 µl	25 µl

2.2.5 Dephosphorylation of plasmid DNA

In some experiments, digested plasmid DNA was dephosphorylated to prevent self-ligation prior to ligation with insert DNA. Calf intestinal alkaline phosphatase (CIAP) dephosphorylates the phosphate at the 5' end. 10 Units of CIAP were added to the restricted DNA and incubated for 1h.

2.2.6 Ligation

A molar ratio of 1:3 of vector DNA to fragment DNA was used for all sticky end ligations. Ligations were carried out using 2 units T4 DNA ligase and ATP containing ligation buffer. This ligase binds the 3' hydroxyl group with the 5' phosphate group of the fragment DNA under usage of ATP. The ligations were incubated for 3 h at room temperature.

2.2.7 Transformation of plasmid-DNA in *E. coli*

Transformation is the artificially induced uptake of DNA by bacteria, which is then multiplied each time the bacteria divides. All plasmids used in this work contained a bacterial resistance gene (Ampicillin or Kanamycin) to prevent growth of non-transformed bacteria. Competent *E. coli* cells were thawed on ice. 5-30 µl of the ligation mixture was added with 50-70 µl bacteria suspension and incubated on ice for 20 minutes. The *E. coli* cells were then heat shocked for 45 seconds at 42°C and subsequently cooled down on ice for 2 minutes. 250 ml of LB-medium were added prior to shaking at 37 °C for 1 h. Afterwards the cells were spread on antibiotic agar plates and incubated at 37 °C over night.

2.2.8 Isolation of plasmid DNA from bacteria

The purification of DNA from small bacterial cultures (2-5 ml) was carried out with the High Pure PCR Product Purification Kit according to the manufacturer's instructions. For larger volumes (200 ml) and a higher amount of a high purity DNA, the DNA Purification NucleoBond Xtra Maxi Kit was used according to the manufacturer's instruction. The Plasmid DNA was dissolved in TE-buffer and quantified via spectrometry.

2.2.9 DNA sequencing

The sequencing service of the BMFZ Düsseldorf was used. A PCR reaction with DNA template, matching primer and the BigDye® Terminator v3.1 Cycle Sequencing Kit (Applied Biosystem) was started. The kit contains a DNA polymerase as well as fluorescence labeled ddNTPs. A typical reaction was made of 1 µg DNA, 4 µl BigDye® Terminator 1x, 10 pmol primer and H₂O in a volume of 20 µl. The PCR reaction was then purified with the DyeEx Spin Kit and Hi-Di™ Formamid (Applied Biosystems) was added, before the PCR reaction was handed to the BMFZ for sequencing.

2.3 Cell cultivation methods

2.3.1 Cultivation of cell lines

All cultured cells were grown at 37°C in 5 % CO₂ and 95 % humidified atmosphere. HT1080 cells, HEK293T cells and HepG2 cells were cultivated in tissue culture-treated culture dishes in DMEM medium with 4.5 mM glucose, 2 mM L-Glutamine, 10 % FBS, 100 U/ml penicillin and 100 µg/ml streptomycin. All culture dishes for cells that grow adherent were coated with 0.1 % gelatin solution. Jurkat and REH cells were grown in RPMI with 2 mM L-Glutamine, 10 % FBS, 100 U/ml penicillin and 100 µg/ml streptomycin.

Harvesting of adherent cells was performed as followed: At first, the cells were washed with 5 ml PBS solution and subsequently incubated with 1.5 ml trypsin-EDTA solution at 37 °C until they were fully detached. After the detachment of the cells, trypsin was inhibited by addition of fresh cell culture medium. The cells were resuspended and then split considering the growth rate on a new culture plate. To seed a certain number of cells, the resuspended cells were counted with a Neubauer counting chamber. The cell suspension was now diluted with fresh medium until the desired cell-concentration was reached.

2.3.2 Cryoconservation of eukaryotic cell lines

For storage, cell pellets were resuspended in freezing medium (culture medium, 6 % DMSO, 10 % additional FCS) and stored at $-80\text{ }^{\circ}\text{C}$ overnight. For re-cultivation, cells were defrosted at room temperature. After centrifugation, the medium with DMSO was removed and the thawed cells were seeded.

2.3.3 Isolation of primary T-cells

Primary human T-cells were collected from peripheral blood of healthy adult volunteers and separated by Ficoll-Paque centrifugation according to the manufacturer's protocol. In Ficoll-separation, two liquid phases (blood and Ficoll-Paque) with different densities were layered. The different types of blood cells were separated depending on their rate of sedimentation. After centrifugation, four layers are formed:

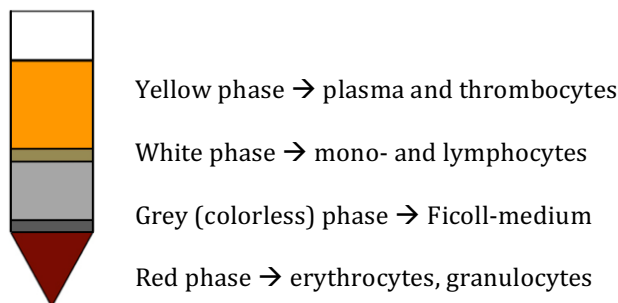


Figure 6. Ficoll hypaque density gradient centrifugation.

The white phase was carefully withdrawn and then underwent an additional lysis of remaining erythrocytes. The left-over cells were cultivated in IMDM supplemented with 10 % heat-inactivated FBS, 100 U/ml penicillin, 100 $\mu\text{g}/\text{ml}$ streptomycin and 2 mM L-Glutamin as well as 100 U/ml Interleukin 2. The non-tissue culture-treated 6-well-plates wells were previously coated with 1 $\mu\text{g}/\text{cm}^2$ CD3- and CD28-antibodies for T-cell-stimulation and incubated over night at $4\text{ }^{\circ}\text{C}$ before usage. Three days after cultivation of the mononuclear cells, 95 % of the total alive cell populations were T-lymphocytes.

2.3.4 Vector production and transduction

Transfection is the insertion of nucleic acid in eukaryotic cells. In this dissertation, Polyethylenimine (PEI) was used as transfection reagent. PEI is a cationic polymer, which binds and condenses nucleic acids. Cells absorb the complexes of nucleic acid and PEI efficiently, probably through endocytosis [158]. The day prior to transfection, 5×10^6 HEK

293T cells were seeded on a 10-cm culture plate in 10 ml medium and incubated at 37 °C over night.

Transfection via 293T

The next day, the medium was aspirated and replaced by 4 ml D-MEM with 15 % FCS.

Two dilutions were prepared:

Table 16 Transfection dilution

1.)	Volume	
DNA-Mix	985 µl	D-MEM without supplements
	5 µl	envelope plasmid VSV-G (1 µg/µl)
	5 µl	helper plasmid pCD/NL-BH (1 µg/µl)
	5 µl	lentiviral vector (1 µg/µl)
	1000 µl	
2.)	Volume	
PEI-Mix	955 µl	D-MEM without supplements
	45 µl	PEI (1 mg/ml)
	1000 µl	

The two dilutions were mixed and incubated for 20 min at RT. The complete transfection-mix (2 ml) was carefully dropped on the HEK 293T cells. Again, the cells were incubated overnight. The medium was changed to IMDM supplemented with 10 % FCS, Pen/Strep and 2 mM L-Glutamine 24 hours after transfection.

Harvest and Transduction

In order to harvest extracellular virus, all supernatant of the cell culture was absorbed with a disposable syringe and filtered through a filter with 0.45 µm wide pores. The now cell-free supernatant contains all extracellular virus particles. The target cells were then transduced with supernatant directly, or in appropriate dilutions. During each step of transduction, Protamine sulfate (8 µg/ml) was added to the medium of the target cells in order to enhance the efficiency of the transduction. The membrane of the virus particles and the target-cell membrane have equal membrane potential, leading to electrostatic repulsion. Protamine sulfate seems to stop this repulsion, and thus enhances the initial binding between cell and virus [159, 160]. 24 hours after transduction, medium was changed. Transfection and transduction efficiencies with EGFP-plasmids were controlled semi-quantitative via fluorescence microscope.

Transduction of HepG2 cells

One day before transduction, 3×10^6 HepG2 cells were seeded in 10 cm plates. The cells were incubated with 8 ml fresh virus supernatant. 24 hours later, medium was changed.

Transduction of cells in suspension

Using CH296-coated plates (Takara Bio Inc., Otsu, Japan) can increase the efficiency of transduction. CH296 is a recombinant fibronectin fragment with cell- and virus-binding domains. This ensures the physical proximity of cell and virus, which leads to a higher rate of transduction [161]. 6-well-plates were coated with CH296 and incubated for at least 2 hours at 37°C. Then the CH296 was withdrawn and the plates were washed with medium. Each well was filled with 2 ml of the virus supernatant and 1.5×10^5 primary T-cells were added. 16 hours later, fresh medium was added.

Since Jurkat cells show a very high efficiency of transduction, no fibronectin-coated plates were used in all Jurkat-experiments in this work. Standard tissue culture-treated wells were used, while the rest of the transduction-process remained the same as with T-cells.

2.3.5 FACS analysis

Fluorescence activated cell sorting (FACS)-analysis defines the size, granularity and fluorescence emitted by cells. This enables the differentiation of cell populations with marker genes such as fluorescence labeled antibodies.

Thus, the expression of marker genes can be examined and quantified. One cell at a time passes a focused laser and is sorted by light scattering and fluorescence. Before analysis, cells can be stained with a fluorescent-antibody, which marks certain cell structures. For example, cells expressing epitopes of CD34 and NGFR on their surface were stained with the matching CD34 or NGFR Phycoerythrin-bound antibodies. Phycoerythrin (PE) is a red protein isolated from the alga *Porphyridium cruentum* [162]. Its light emission can be detected via FACS; therefore, the amount of successfully stained cells can be determined. Additionally, EGFP (enhanced green fluorescent protein) was used as marker gene and propidium iodine (PI), a red stain, was used to stain dead cells. PI (50 µg/ml) penetrates the perforated cell membrane of dead cells only, thus living cells with an intact membrane will not be stained.

During FACS analysis, the mean fluorescent intensity (MFI), i.e. how positive the transduced cells are on average, is analysed. FACS measurements were evaluated using CellQuest Pro and FCS Express 5 (De Novo Software).

2.3.6 Cell separation via MACS

In this thesis, transduced T-cell samples were purified with the MACS® MicroBeads System according to the manufacturer's instructions. MACS® MicroBeads are paramagnetic particles that are conjugated to antibodies against a particular antigen on the cell surface. The cell samples were stained with the matching antibody against a surface antigen. Then the samples were applied to a column placed in a magnetic separator. The unlabeled cells passed through while the magnetically labeled cells were retained within the column. The flow-through was then collected as the unlabeled cell fraction. After a washing step, the column was removed from the separator, thus the magnet was not holding the labeled cells back any more, and the magnetically labeled cells were eluted from the column. Both cell fractions, labeled and unlabeled, were now ready to be used for further experiments.

2.3.7 Cytotoxicity assays

To analyse whether transduced T-cells with a modified CAR were able to kill the ALL-cell line REH (EGFP+), both cell lines were cocultured overnight in tissue-culture-treated, round bottom 96-well plates. The next day, B-cell survival was measured via FACS analysis.

Seeding of the cells

All transduced T-cells and the REH cells were harvested, centrifuged and resuspended in T-cell media (IMDM) without IL-2 to a concentration of 10^5 /ml. 100 μ l (i.e. 10^4 cells) of the REH cells were added to each well, except the T-cell control wells. Then 100 μ l T-cells were added at the following ratios:

- 3:1 (3×10^4 T-cells)
- 1:1 (10^4 T-cells)
- 0.3:1 (3×10^3 T-cells)
- 0.1:1 (10^3 T-cells)
- 0.03:1 (3×10^2 T-cells)
- 0.01:1 (10^2 T-cells)

Replicates of three wells per ratio were set up. Three T-cell control wells per transduced construct were filled with 100 μ l of the 1×10^4 T-cell-dilution and additional 100 μ l of IMDM without IL-2. Three REH B-cell control wells were filled with 100 μ l B-cell dilution and additional 100 μ l of T-cell media. Then the 96-well plates were centrifuged 30 secs at 200 xg and incubated over night at 37 °C.

Evaluation via FACS-analysis

After 16 hours, the percentage of surviving B- cells was determined via FACS. The three replicate wells were combined into one test tube and stained with 400 µL PI staining solution. Since the target cells expressed EGFP, no additional staining was required to discriminate between target cells and effector cells. The effector cells appeared as the EGFP negative population. Each sample was measured for 120 seconds. The number of living B-cells in each ratio was then compared with the number of living B-cells in the B-cell control sample.

2.3.8 Cell proliferation assays

Both transduced HepG2 cells and transduced primary human T-cells were tested for their survival after incubation with different prodrugs. Enzymes of the cytochrome P450 family convert the prodrug 4-Ipomeanol (4-IPO, provided by the National Cancer Institute, Drug Synthesis and Chemistry Branch) into a highly toxic alkylating metabolite, which triggers an apoptosis-mediated cell death [163]. The chemical structure of Perilla ketone (PK) differs only slightly from 4-Ipomeanol and was first synthesized in 1957 [140, 164].

With the following toxicity-assay, the rate of cell death in different cell types can be compared. The cells were incubated with varying concentrations of 4-IPO or PK and analysed after 24 and/or 48 hours.

Seeding of transduced cells

HepG2 cells: All cells were seeded in 12-Well plates in a volume of 500 µl:

- 2 x 10⁵ cells for day 1
- 1 x 10⁵ cells for day 2

Primary T-cells: All cells were seeded in 24-Well plates in a volume of 500 µl:

- 2 x 10⁵ cells for day 1

The cells were incubated at 37 °C for 3 hours, so that they could adhere to the plates.

Incubation with 4-Ipomeanol or Perilla ketone

The following concentrations of 4-IPO and PK were used in this work. They were added to the plated cells in a volume of 500 µl. The listed dilutions show the final concentration, i.e. the concentration of 4-IPO/PK in 1 ml medium:

- 0 µM
- 0.09 µM
- 0.9 µM
- 2.9 µM
- 9 µM
- 29 µM
- 90 µM
- 290 µM

After 24 and/or 48 h, the percentage of surviving cells was determined via flow cytometry. All cells were pelleted and stained with PI.

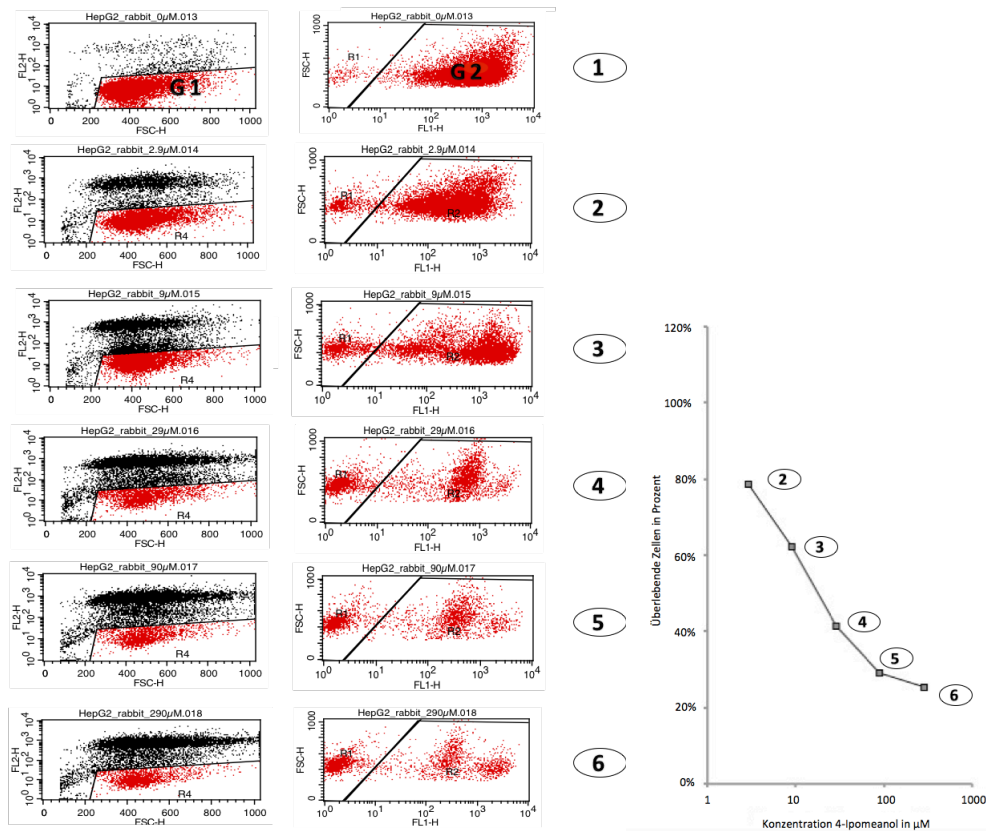


Figure 7. Schematic representation of FACS analysis. **A:** FSC-H (forward scattering, i.e. cell size) plotted against FLH-2 (PI-fluorescence, logarithmic). This raw data shows all events measured by the cytometer, i.e. living cells and cell debris. G1 was placed upon the living cells. **B:** FL1-H (EGFP-fluorescence, logarithmic) plotted against FSC-H (forward scattering, i.e. cell size). Out of all living cells (G1), only the EGFP-positive ones were taken into account for further evaluation. **C:** Graphic presentation of the mortality curve of cells incubated with 4-IPO concentrations from 2.9µM to 290µM

Evaluation of the toxicity-assays

The transgenic cells were incubated with different doses of 4-IPO or PK and analysed via flow cytometry after 1 or 2 days. For each sample, 3×10^4 cells were counted. The first Gate (G1) only showed living cells, i.e. no propidium iodine-stained cells. The second gate (G2) refers to G1 and shows all living cells, which also express EGFP. The number of cells in Gate 2 was used to create a mortality curve. The curve consists of 6 measuring points, each of which can be assigned to one specific concentration of 4-IPO/PK. For example, in Figure 7, the cells measured at measure point 2 were incubated with $2.9 \mu\text{M}$ 4-IPO and the cells at point 3 were incubated with $9 \mu\text{M}$ 4-IPO. The first measuring point ($0 \mu\text{M}$ 4-IPO or PK) was set as 100 % in each reference system, so that the amount of surviving, prodrug-treated cells referred to it. Flow cytometric data on EGFP and PI fluorescence was analysed in parallel to discriminate between living, dead, transduced and non-transduced cells.

The mortality curves consist of 4-6 measurements; each of them corresponding with one specific dilution of 4-IPO or PK. To determine the mortality rate, only EGFP+ (=genetically modified) and living cells were taken into account. The amount of living cells was counted and calculated relative to the untreated controls ($0 \mu\text{M}$ 4-IPO or PK), respectively.

2.4 Protein Biochemical Methods

2.4.1 Mild lysis of eukaryotic cells

Cell lysates were produced to control the protein expression in eukaryotic cells after transduction. First, the cells were washed with PBS and then incubated for 30 min with $500 \mu\text{l}$ lysis buffer. During lysis, the cell membrane becomes more permeable via Triton®X-100. Then the cells were frozen at $-20 \text{ }^\circ\text{C}$. After defrosting, nuclei and membrane fragments were separated by centrifugation (13000 rpm, 2 min). The supernatant was mixed with loading buffer and cooked at $95 \text{ }^\circ\text{C}$ for 10 min. These samples can be stored at $20 \text{ }^\circ\text{C}$.

2.4.2 Western Blot

To separate proteins via SDS-Gelelectrophoresis, the protein samples were plotted on 12 % or 4-12 % NuPAGE Bis-Tris-gel and separated in NuPAGE-MES-SDS-Running-Buffer for at least 45 minutes at 180 Volt. The separated proteins in SDS-gel were transferred to a nitrocellulose-membrane (Hybond-P PVDF membrane by GE Healthcare, #RPN303F) via Western Blot, i.e. via electric current. The gel was placed on top of the membrane and jammed between filter paper and sponges in a transfer-box. Transfer took place at 30 Volt for

1,5 h in transfer buffer. The membrane was stained with Ponceau red to visualize and confirm protein transfer. Afterwards, the membrane was rinsed with PBS-T and shaken for 1 hour in blocking solution at RT to stop unspecific binding of antibodies. After another washing with PBS-T, the membrane was incubated for at least 2 hours with the primary antibodies diluted in milk. Then the membrane was rinsed again with PBS-T to remove any free antibodies and incubated with secondary antibodies diluted in milk. After rinsing the membrane to remove unbound secondary antibody, detection could start. While the primary antibody binds the membrane-bound proteins, the secondary antibody detects the Fc-body of the primary antibody. Horseradish-peroxidase is linked to the secondary antibody and used to oxidize a chemiluminescent agent in the detection solution, and the reaction product produces luminescence in proportion to the amount of protein. Luminescence was detected via ECL system (Pierce, Thermo Fisher Scientific) and the Image Quant LAS 4000 mini (GE Healthcare).

3 RESULTS

3.1 Defining a new linker for CARs

At the start of my thesis, the hinge region of most CD19 CARs consisted of the CH₂CH₃ Fc-domain of human IgG1 or IgG4, as this conveniently allowed detection of the CAR on the surface of T-cells via monoclonal antibodies in flow cytometry. As reports of unintended interactions with the Fc γ -receptor of innate immune cells appeared [95], one aim of this thesis was to establish an alternative human sequence as a hinge that was less likely to cause unspecific off-target activation and still facilitated detection of the CAR by flow cytometry. Furthermore, the newly constructed CAR should be coexpressed together with a suicide gene in human T-cells without reducing the CARs efficacy against malignant cells.

3.1.1 Requirements for a new hinge region

As shown by Hudecek *et al.*, tailoring the length of the extracellular hinge can affect optimal tumor recognition for different target epitopes [42, 95]. Epitopes that are located proximal to the cell surface require CARs with a longer hinge domain, while epitopes that reach out further are ideally targeted with shorter CARs. For example, while some receptor tyrosine kinase-like orphan receptor 1 (ROR-1) epitopes on tumor cells can be reached with CARs with very short hinge regions, the R11 ROR-1 CAR is specific for a very membrane proximal epitope and therefore requires a longer hinge region [42, 95].

Additionally, a change in the amino acid sequence potentially can cause a change in the tertiary structure of the CAR and might thus interfere with the binding of epitope and antibody. Since the optimal length and composition of the spacer region can vary depending on the location of the targeted epitopes, numerous different spacer lengths were tested in this work.

The first step of this work was to modify the hinge domain of the pMK-RQ_CD19_CAR, then clone this new construct into a lentiviral vector together with the suicide gene hCYP4B1P+12. The alternative inserts in this thesis were derived from the truncated domains of two human surface molecules, the codon-optimized low-affinity nerve growth factor receptor (Δ NGFR/CD271) and the codon-optimized Δ CD34. Importantly, both proteins are not expressed on the surface of human T-cells. Cell samples expressing either construct can be

labeled via commercially available magnetic antibodies and purified with the MicroBeads® Kit by MACS Miltenyi.

The low affinity **nerve growth factor receptor p75**, a type I transmembrane protein, is a member of the tumor necrosis superfamily and takes part in the regulation of different neuronal functions like cell proliferation, survival and axon guidance in mammals [165]. NGFR p75 contains an extracellular domain which consists of four 40 amino acid long repeats with 6 cysteine residues at conserved positions followed by a serine/threonine-rich region, a single transmembrane domain, and a 155-amino acid cytoplasmic domain as depicted in Figure 8. Valtieri *et al.* established already in 1994, that the truncated NGFR can be used as a membrane marker for cell selection [166, 167].



Figure 8. The nerve growth factor receptor p75. A. Schematic model of NGFR. The truncated version Δ NGFR does not contain the chopper and death domain. **B. Protein sequence of the extracellular domain of Δ NGFR.** The cysteine-rich regions 1-4 are marked in red. The four different inserts are underlined/marked in color; Insert #N1 (cys-domain 3) in yellow; Insert #N2 (cys-domain 4) in black; Insert #N3 (cys-domain 3 and 4 plus 62aa at the C-Terminus) in blue; Insert #N4 (cys-domain 2, 3 and 4 plus 62aa at the C-Terminus) in green. Modified after Skeldal *et al.* 2011[168]

The epitope of the MACS selection Kit offered by Miltenyi Biotech GmbH at which their NGFR/CD271-antibody ME20.4 binds, is hypothesized to lie in the 3rd or 4th cysteine -rich domain (CRD) of the protein (personal communication). Therefore, four different sequences (#N1-N4) were designed in the extracellular region of NGFR (Figure 8) and cloned into the pMK-RQ_CD19_CAR (Figure 9). The first insert consists of the cysteine-rich region 3 (40 aa), the second one of the cysteine-rich region 4 (42 aa). Additionally, two longer inserts called #N3 (120 aa) and #N4 (162 aa) were chosen, in case the epitope lies in both regions or the tertiary structure of the epitope can only be preserved by using a longer sequence (Figure 8).

CD34 is a glycosylated Type I transmembrane-protein that is commonly known as marker for hematopoietic stem cells and progenitor cells as well as B-cell precursors [169]. It has also been detected on nonhematopoietic cell types, like vascular endothelial progenitor cells and embryonic fibroblasts [170]. Its extracellular domain is involved in cell-to-cell attachment and plays an important role in the attachment of hematopoietic stem cells to the bone

marrow extracellular matrix or to stromal cells [171]. The intracellular domain takes part in cell proliferation and regulation of differentiation [172]. Clinically, CD34 is used for the enrichment of stem cells during clinical trials, especially for transplantation purposes. A truncated form of CD34 has been identified as a naturally occurring splice variant which carries a partial deletion of the cytoplasmic domain for signal transduction [173]. The Qbend10 is a monoclonal antibody that detects human CD34. It presumably binds at an epitope which consists of 16 amino acids located at the position 42 - 57 in a serine-threonine-rich region of the N-terminus in human CD34 [117]. Figure 9 shows a structural model of CD34 and the amino acid sequence of the extracellular domain of the truncated CD34. A model of the tertiary structure of CD34 was used to design sequences, also considering the glycolisation sites of CD34.

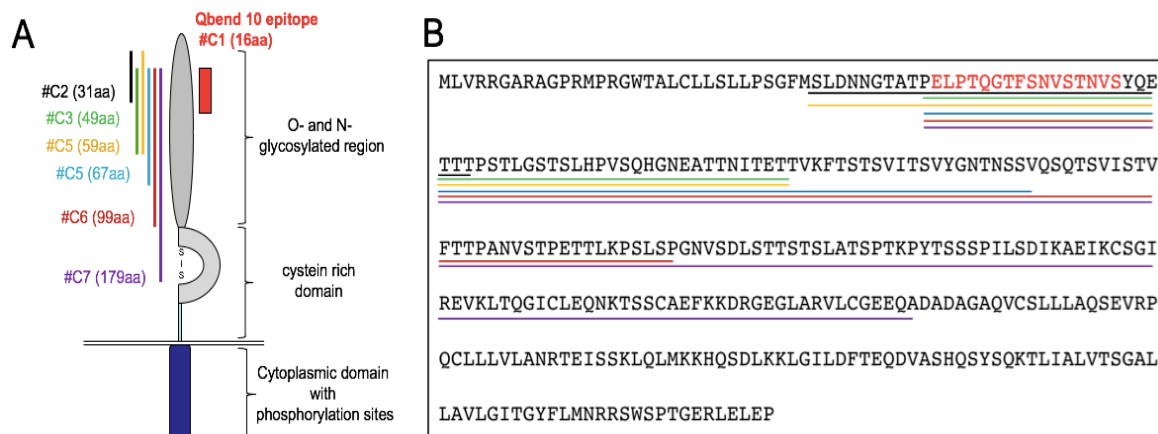


Figure 9. The human CD34 antigen A. Schematic model of CD34. The truncated version Δ CD34 contains an about 20kDa shorter cytoplasmic domain residue, Modified after Philip *et al.* [117] **B. Protein sequence of Δ CD34.** The epitope (16aa) #C1 is marked in red. The different inserts are underlined in color: Insert #C2 (31aa) in black; Insert #C3 (49aa) in green; Insert #C4 (59aa) in yellow; Insert #C5 (67aa) in blue; Insert #C6 (99aa) in dark red; Insert #C7 (179aa) in violet.

The experiments were carried out with truncated and human codon-optimized versions of CD34 and NGFR, labeled Δ NGFRco and Δ CD34co (by GeneArt). All vectors were generated using standard cloning techniques. The pMK-RQ_CD19_CAR vector was used as a template for an established CD19 CAR with the CH₂CH₃ linker, named R.CD19 CAR. pMK-RQ_CD19_CAR had been previously designed according to our needs and then synthesized by GeneArt (Figure 10). The CH₂CH₃ hinge was cut out of the pMK-RQ vector via *MfeI/MluI* and replaced by the ten different inserts designed from the surface units of CD34 and NGFR (Table 17). All inserts were generated by PCR amplification with p2CL21 Δ NGFRcoT2AEGcowo or p2CL21 Δ CD34coT2AEGcowo as templates and subsequently cloned into the *MfeI/MluI* restriction sites of the pMK-RQ_CD19_CAR. This interim cloning was necessary as a first step since the enzymes *MfeI* and *MluI* cut multiple times in the lentiviral vector

p2CL21EGT2AR.CD19cowo, what made it impossible to clone the new hinges directly in this vector.

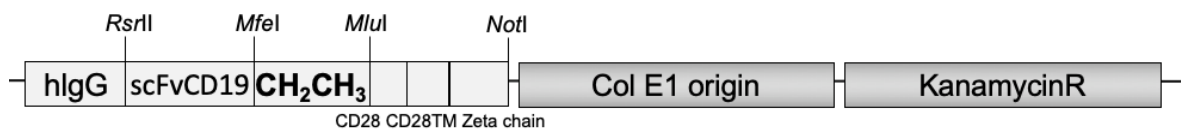


Figure 10. pMK-RQ_CD19_CAR The vector contains a kanamycin resistance gene and a Col E1 origin of replication. The codon optimized R.CD19 CAR was developed in cooperation with Claudia Rössig, Münster, with hlgG as leader sequence [139].

The PCR primers used for each construct are listed in Table 4. The R.CD19 CAR was cut out of p2CL21EGT2AR.CD19cowo, a 3rd generation lentiviral vector, with *RsrII/NotI* and replaced by the modified CARs (Figure 11). In several attempts, it was not possible to clone the minimal sequence of 16 aa called #C1, as ligations of the PCR product into the *MfeI-MluI* restriction site did not result in a stable DNA construct.

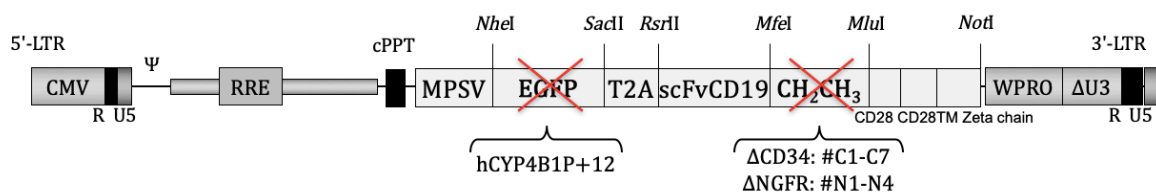


Figure 11. Scheme of p2CL21EGT2AR.CD19cowo Different cDNAs were inserted either in front or behind the T2A site using unique restriction enzymes. Ten new inserts replace the CH₂CH₃ region of the CD19 CAR, which was cut out by *MfeI/MluI*. EGFP was replaced by the suicide gene hCYP4B1P+12. The 5'-LTR contains the promoter of the human cytomegalovirus (CMV), the R region and the U5 region. The transgene is driven by a myeloproliferative sarcoma virus (MPSV) promoter. To express more than one transgene, an internal promoter, i.e. a 2A-derived sequence, was inserted. Ψ: packaging signal; RRE: rev response element; cPPT: central polypurine tract; WPRE: woodchuck hepatitis virus posttranscriptional element.

In the next step, the EGFP domain was replaced in each construct by the codon-optimized, modified human CYP4B1P+12 using *NheI* - *SacII* restriction sites. This was necessary for later experiments, in which transduction of T-cells with both, the new CAR and the suicide gene CYP4B1P+12, took place. Ten vectors containing the suicide gene and one of the new CD19 CAR version were created. Previous studies had shown, that neither the position of the suicide gene or EGFP nor the position of the CD19 CAR relative to the T2A site changes the enzymatic activity of EGFP or expression of the CAR or the suicide gene respectively [139]. Thus, it was not necessary to create alternative vector versions placing each construct in both positions relative to the T2A site. The final changes in both vectors are listed in Table 17.

Table 17 Constructed inserts cut out of NGFR or CD34 and newly created vectors

Name	Length	Position in NGFR/CD34	Cloning vector	Lentiviral vectors
#N1	40aa	108-147	pMK-RQ_CAR_#N1	p2CL21EGT2AR.CD19#N1cowo and p2CL21P+12T2AR.CD19#N1cowo
#N2	42aa	148-189	pMK-RQ_CAR_#N2	p2CL21EGT2AR.CD19#N2cowo and p2CL21P+12T2AR.CD19#N2cowo
#N3	120aa	108-227	pMK-RQ_CAR_#N3	p2CL21EGT2AR.CD19#N3cowo and p2CL21P+12T2AR.CD19#N3cowo
#N4	162aa	65-227	pMK-RQ_CAR_#N4	p2CL21EGT2AR.CD19#N4cowo and p2CL21P+12T2AR.CD19#N4cowo
#C1	16aa	42-57	pMK-RQ_CAR_#C1	p2CL21EGT2AR.CD19#C1cowo
#C2	32aa	32-63	pMK-RQ_CAR_#C2	p2CL21EGT2AR.CD19#C2cowo and p2CL21P+12T2AR.CD19#C2cowo
#C3	49aa	42-90	pMK-RQ_CAR_#C3	p2CL21EGT2AR.CD19#C3cowo and p2CL21P+12T2AR.CD19#C3cowo
#C4	59aa	32-90	pMK-RQ_CAR_#C4	p2CL21EGT2AR.CD19#C4cowo and p2CL21P+12T2AR.CD19#C4cowo
#C5	69aa	42-110	pMK-RQ_CAR_#C5	p2CL21EGT2AR.CD19#C5cowo and p2CL21P+12T2AR.CD19#C5cowo
#C6	99aa	42-140	pMK-RQ_CAR_#C6	p2CL21EGT2AR.CD19#C6cowo and p2CL21P+12T2AR.CD19#C6cowo
#C7	179aa	42-220	pMK-RQ_CAR_#C6	p2CL21EGT2AR.CD19#C7cowo and p2CL21P+12T2AR.CD19#C7cowo

3.1.2 Functional tests in Jurkat cells

To test whether the CD34 and NGFR antibodies were able to detect the different CAR constructs expressed on cells, I used a T-cell ALL line, Jurkat, as a first screening tool. The newly created vector plasmids with EGFP were transfected into HEK293T cells via PEI transfection. Viral particles in the supernatant were collected after 48 hours and used to transduce Jurkat cells as described in chapter 2.3.4. In all Jurkat experiments, a similar MOI determined by viral titration was used.

3.1.2.1 Expression of CARs in Jurkat cells

Jurkat cells coexpressing one of the new CARs together with EGFP were stained with either Phycoerythrin-labeled CD271 (NGFR) or CD34 antibody. EGFP served as a control to discriminate between transduced and non-transduced cells and to compare expression of

both transgenes semi-quantitatively. Of the four constructs containing sequences from NGFR as hinge, CD19 CARs with the spacer domain comprised out of either the 3rd or 4th cysteine rich region (#N1 and #N2) were not stained with the NGFR antibody, although EGFP expression clearly indicated positive transduction and expression of the mRNA for EGFP and the CD19 CAR construct. Only the two longer constructs (#N3 and #N4) were expressed on the surface of Jurkat cells, as the cells were successfully stained with PE (Figure 12). Importantly, there was a clear direct correlation between the positivity for EGFP and for NGFR. Hence, I only considered the two longer versions of the NGFR constructs (#N3 and #N4) in the next experiments. All CD19 CAR constructs with inserts derived from CD34 (#C2-C7) were successfully stained with the QBend-10 antibody with a clear direct correlation between the positivity for EGFP and for NGFR. Therefore, I continued to work with all six constructs.

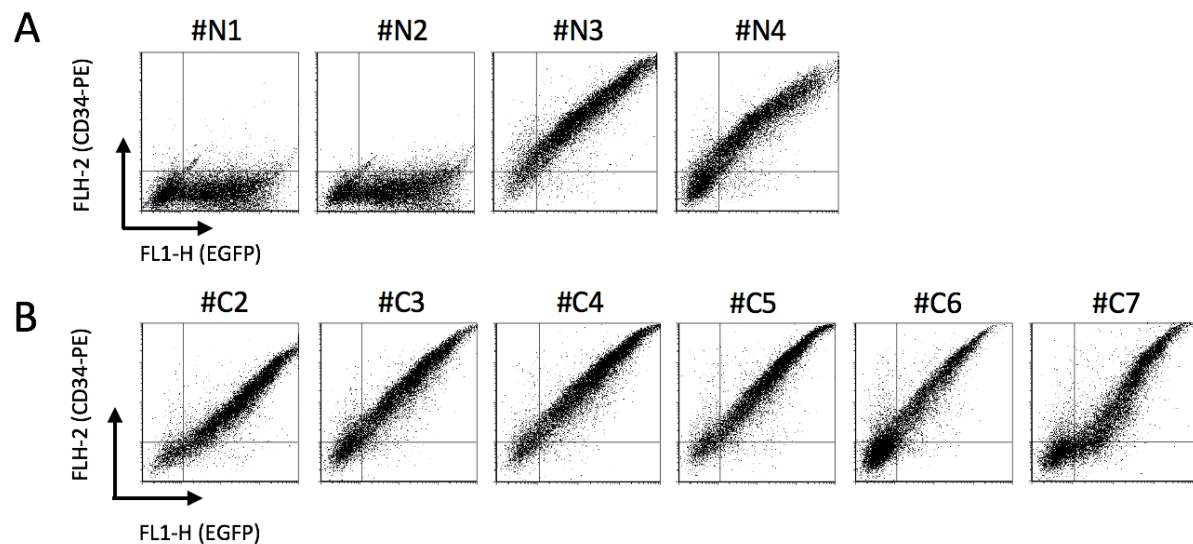


Figure 12. FACS results of Jurkat cells transduced with CD19 CAR constructs with 10 different hinge regions. All cells were stained with PE-bound antibodies. FL1-H (EGFP fluorescence, logarithmic) is plotted against FLH-2 (PE fluorescence, logarithmic). A: Polyclonal Jurkat cells transduced with CAR #N1-N4, respectively, were stained with NGFR-antibody B: Six cell lines transduced with CAR #C2-C7 respectively, stained with CD34-antibody. A representative FACS analysis for each construct is shown, n=4

3.1.2.2 MACS selection of transduced Jurkat cells

As shown in Figure 12, in each successfully stained cell population, only a part of the Jurkat cells express the transduced gene. Next, I tested whether the expression of the CD34 or NGFR hinge region was sufficient to facilitate cell separation. Magnetic cell sorting (MACS) allows cell separation via magnetic nanoparticles coated with antibodies against a particular surface antigen. In this work, it was then tested whether the antibody binding of the CD19 CARs with NGFR-hinge #N3 and #N4 and the CD19 CARs with the CD34-hinge #C2-C7 was strong enough to facilitate cell separation via commercially available CD34- or NGFR-microbeads.

Prior to MACS separation, a cell sample was analysed via FACS to determine the transduction efficacy (before MACS column). Then, the cell populations were purified via MACS separation using directly beads-labeled antibodies. Samples were collected from the flow-through of the columns after one round of selection (flow-through = negative selection) and also from the eluates obtained from the columns after release of the cells bound in the columns (eluate = positive selection). The efficacy of the MACs selection was analysed using EGFP as a marker for transduced cells by flow cytometry as both EGFP and the CARs are translated from the same mRNA. As shown in Figure 13. CD34- and NGFR-derived hinge regions facilitated enrichment of transduced cells with only one run over the column. However, there were marked differences in the efficiencies of the cell separation (Figure 13).

NGFR hinge

Although there was a clear enrichment of positive cells expressing the CARs with #N3 or #N4 in the eluate, the numbers of positive cells recovered from the column were very low (Figure 13A). The vast majority of positive cells were passing through the column into the flow-through. Based on FACS analysis, the percentage of CAR positive cells only decreased from $60.1 \pm 2.6\%$ before separation to $57.2 \pm 1.8\%$ in the flow through for #N3 and from $51.4 \pm 11.5\%$ to $49.7 \pm 11.7\%$ for #N4, respectively. Thus, less than 5% of the positive cells were successfully enriched and selected from the cell samples. This shows, that while the few eliminated cells in the eluate were strongly positive for the CD19 CAR #N3 or #N4, the efficiency of cell enrichment was very poor and the majority of transgene positive cells was lost in the flow through.

CD34 hinge

Only few of the positive Jurkat cells expressing the #C2 CD19 CAR could be separated in the flow-through, the percentage of positive cells decreased from $68.7 \pm 2.7\%$ (before column) to $68.1 \pm 3.0\%$ (flow-through). With increasing length of the inserted amino acid sequences from CD34, less transduced cells were passing through the column in the flow-through. From #C3 ($61.6 \pm 2.7\%$ to $47.6 \pm 2.1\%$) to #C4 ($64.3 \pm 25.3\%$ to $47.0 \pm 6.3\%$) to #C5 ($65.5 \pm 2.1\%$ to $41.1 \pm 5.0\%$), more successfully transduced cells could be enriched in the eluate. There were only minimal differences in the efficiency of cell sample purification between the three constructs. The best enrichment was achieved with CAR #C6 ($50.7 \pm 10.5\%$ to $28.3 \pm 6.8\%$) (Figure 13B). Cells expressing the CAR with the longest insert, #C7, were enriched less efficiently than the #C6 construct. $78.4 \pm 3.2\%$ were positive before sorting, $67.1 \pm 3.5\%$ in the flow-through. The overlay in Figure 13 visualizes the three different fractions in one figure, before MACS sorting (blue), the flow-through (green) and the eluate (red).

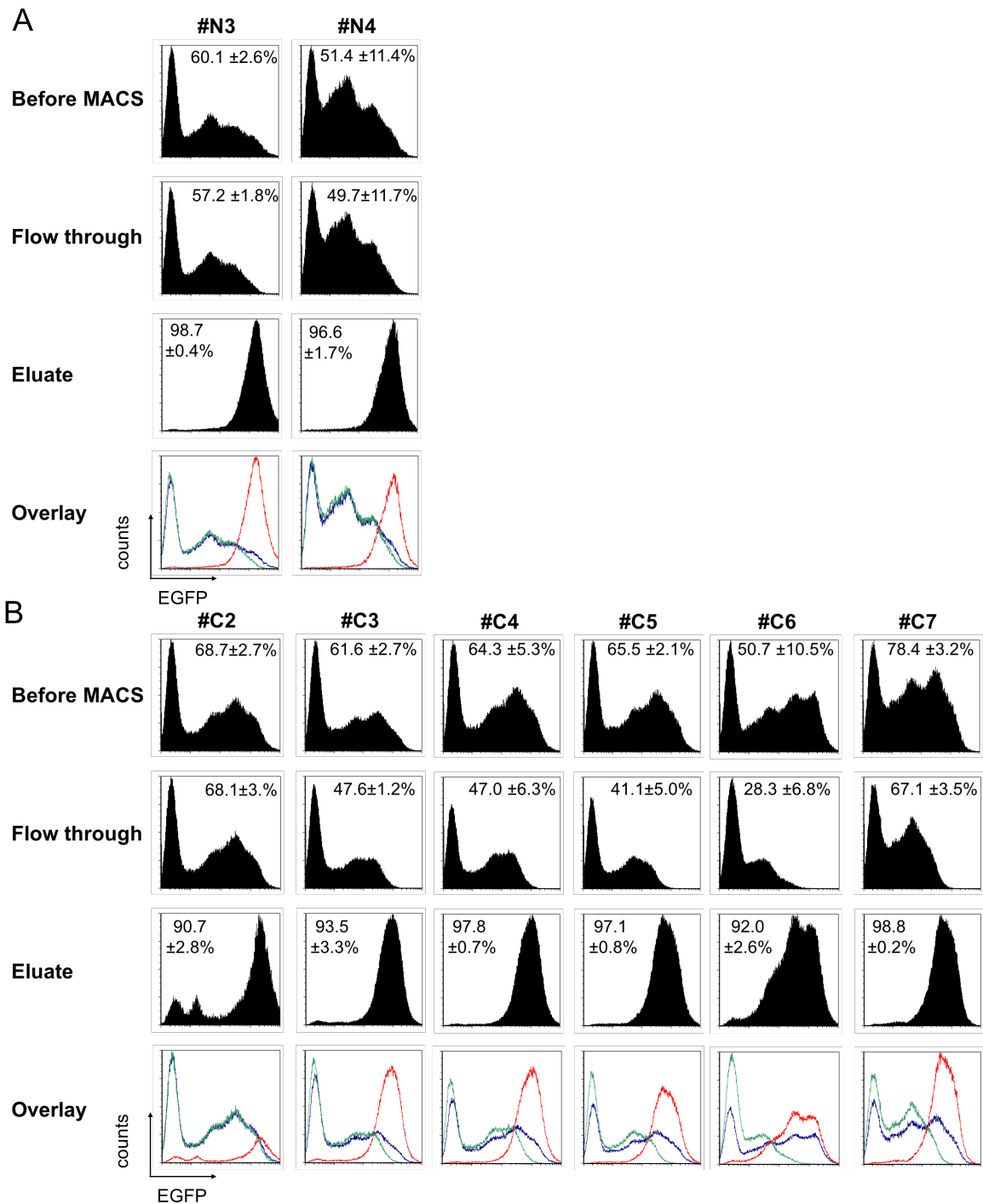


Figure 13. FACS results after MACS cell separation of transduced Jurkat cell lines. In all histograms, the same EGFP-fluorescence is plotted against the cell count. Cell samples were collected before MACS separation and from the eluate after removing the columns out of the magnetic field as well as from the flow-through. The eluate contains the strongly positive enriched cells, while the flow-through contains the negative cells. **A** shows all constructs separated with NGFR microbeads. **B** shows all constructs separated with CD34 microbeads. The numbers indicate the percentage of positive cells in each sample. The overlays show the three different fractions: before MACS (blue), flow-through (green) and eluate (red). Mean ± SEM is shown from at least three experiments.

In the #C2 experiments, the curves representing the populations before cell separation and in the flow-through are nearly identical, i.e. the enrichment of positive cells in the column was

very inefficient. Therefore, no further experiments were conducted with that construct. In the #C6 experiments the blue and green curves differed the most, suggesting #C6 as the best hinge for enrichment.

3.1.3 Functional tests in primary human T-cells

To confirm these results in primary human T-cells, cells from healthy donors were isolated from peripheral blood via Ficoll according to the protocol in Chapter 2.3.3. Mononuclear cells were stimulated on immobilized CD3/CD28 monoclonal antibodies for 2-3 days and subsequently transduced on RetroNectin-coated plates with lentiviral vectors expressing modified CD19 CARs with #N3-4 or #C3-7 spacer regions.

3.1.3.1 Expression of CARs in primary human T-cells

In analogy with the Jurkat cell experiments described above, T-cells coexpressing the modified CARs #N1, #N4 and #C2-#C7 and EGFP were stained with either PE-conjugated CD271 or CD34 antibody in order to test whether the antibodies were able to detect the matching epitope in the context of the CD19 CAR on primary human T-cells. All tested domains (#N3-N4, #C3-C7) were successfully stained with the corresponding antibody (data not shown).

3.1.3.2 MACS selection of primary human T-cells

As the next step, transduced T-cell samples were purified via MACS selection (Figure 14). In the NGFR-experiments, the percentages of positive T-cells only decreased from $53.7 \pm 1.8\%$ (Before MACS sorting) to $50.6 \pm 0.8\%$ (flow-through) for #N3 and from $53.9 \pm 2.5\%$ (before MACS sorting) to $50.5 \pm 2.3\%$ (flow-through) for #N4. Therefore, only $5.73 \pm 1.06\%$ (#N3) or $6.31 \pm 0.02\%$ (#N4) of the positive cells were enriched by the column, the rest was lost in the flow-through. Due to these disappointing results, the NGFR-derived constructs were not included in further experiments.

In line with the Jurkat experiments, increasing the length of the CD34-derived hinge region led to less loss of positive cells in the flow-through. The cells containing the CARs with shorter constructs, #C3 ($54.7 \pm 8.7\%$ to $47.8 \pm 8.8\%$), #C4 ($63.3 \pm 11.3\%$ to $52.9 \pm 11.9\%$) and #C5 ($56.2 \pm 10.7\%$ to $39.2 \pm 10.8\%$) were not enriched as efficiently as the cells expressing CARs with the longer hinge regions #C6 and #C7. The CAR with the #C6 hinge region resulted in the strongest enrichment of positive cells in the eluate. Here, the percentage of positive cells decreased from $41.2 \pm 6.2\%$ before separation to $11.7 \pm 3.9\%$ in the flow-through.

Therefore, $74.13 \pm 5.57\%$ of the positive cells were successfully enriched, while the CAR with #C7 led to less ($50.97 \pm 5.72\%$) enriched positive cells.

Overall, the constructs #C3 to #C5 showed only minimal differences in efficacy. Therefore, all of the following experiments were first carried out with the CD19 CAR with the shorter #C3 hinge region and then with the #C6 CAR, which was the most efficient construct during cell sorting. Since #C7 is the longest construct and CAR #C7+ cells were less efficiently enriched than CAR #C6+ cells, it was not considered for the following experiments.

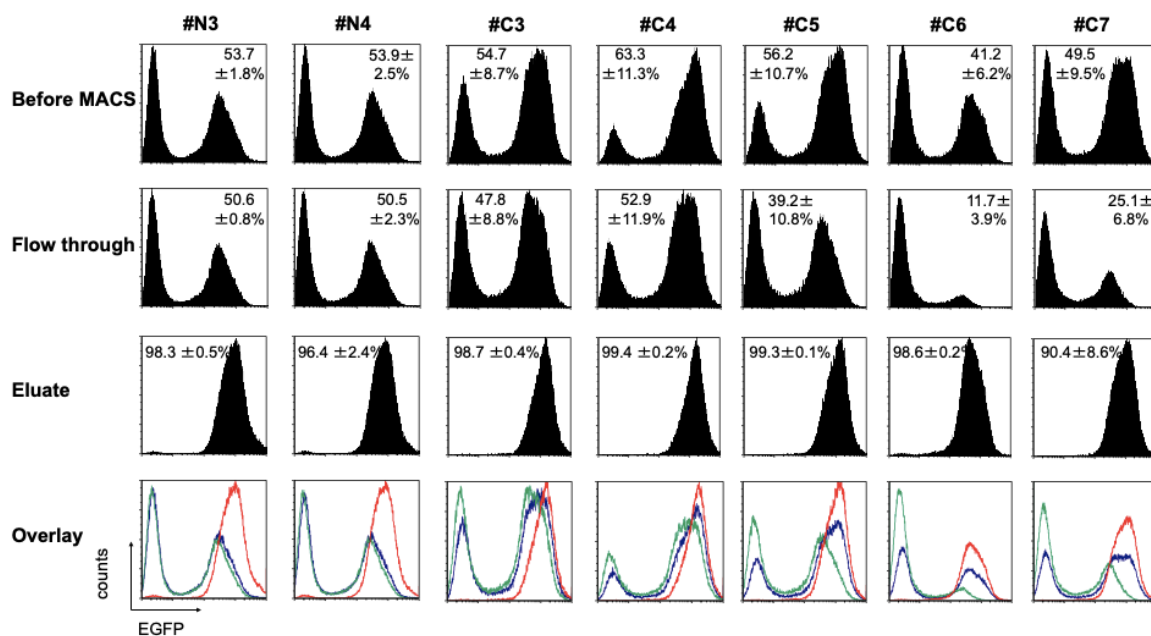


Figure 14. FACS results after MACS cell separation of transduced primary human T-cells. EGFP fluorescence is plotted against the relative cell count. Cell samples were collected before MACS separation and from the eluate as well as from the flow-through. The eluate contains the strongly positive cells, while the flow-through predominantly contains the negative cells. All constructs were separated by using either NGFR or CD34 microbeads. The numbers show the percentage of positive cells in each sample from 3 different experiments. The overlays show the three different fractions: before MACS (blue), flow-through (green) and eluate (red). Mean \pm SEM is shown from at least three experiments.

3.1.3.3 Cytotoxicity assay with leukemic B-cells

To test whether the cytotoxicity of the CD19 CAR is also preserved in the CAR with #C3 or #C6 as hinge region, CAR-expressing cells were incubated with a leukemic CD19+ B-cell line. Subsequently, their efficiency in killing the leukemic cells was measured. The following experiments were carried out with cells expressing the suicide gene hCYP4B1P+12 instead of EGFP, because in a later step, it was intended to eliminate the T-cells using the suicide gene system.

T-cells from healthy donors were isolated from peripheral blood and prestimulated on CD3/CD28 monoclonal antibodies. After 2-3 days, they were transduced with lentiviral

vectors that contained the cDNAs of hCYP4B1P+12 and either the #C3 CAR, the #C6 CAR or the original R.CD19 CAR with CH₂CH₃ as hinge region (Figure 15). As negative control, T-cells were transduced with the vector construct p2CL21P+12coT2AΔCD34cowo, since this construct expressed no CAR but could be enriched via CD34 microbeads. All transduced T-cells were enriched by staining with either CD34-labeled MACS microbeads (#C3 and #C6 CAR, negative control) or with biotinylated Fab antibodies followed by streptavidin MACS microbeads (CH₂CH₃ CAR) and then cocultivated in different ratios with the leukemic B-cell line REH. These REH cells express CD19 on their surface and were genetically modified to express EGFP, therefore they are called REH-EG in the rest of this thesis. The REH-EG cells can easily be distinguished from the non-fluorescent T-cells by FACS analysis [157]. After cocultivation, all samples were analysed by flow cytometry.

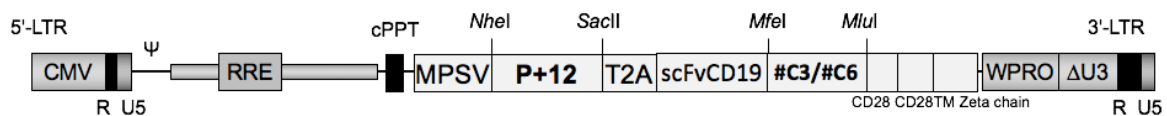


Figure 15. Scheme of p2CL21P+12T2AR.CD19#C3cowo and p2CL21P+12T2AR.CD19#C6cowo. Either the #C3 or the #C6 hinge replaces the CH₂CH₃ region of the CD19 CAR, as shown in Figure 11. EGFP was cut out of p2CL21EGT2AR.CD19cowo via *NheI/SacII* and replaced by the suicide gene hCYP4B1P+12.

CD19 CAR #C3

First, I compared the cytotoxicity of T-cells expressing the #C3 CD19 CAR to those cells expressing the CD19 CAR with CH₂CH₃ as hinge region. The CD19 CAR with the CH₂CH₃-hinge served as a positive control for cytotoxicity towards CD19⁺ target cells, since its cytotoxicity had already been analyzed and quantified before [139]. Transduced T-cells that did not express any CAR were used as negative control. Cocultivation and FACS analysis were carried out as described in chapter 2.3. The survival curves of the REH-EG B-cells are shown in Figure 16. The negative control showed only little toxicity towards malignant B-cells at high effector to target cell ratios. Numerically, those T-cells mediated lysis of 12.4±8.2% of the target B-cells at the highest ratio (3:1), and minimal lysis (<10%) at all lower ratios in all 3 experiments. An effector to target cell ratio of 3:1 lead to the death of 92.64±1.2% of the B-cells by T-cells expressing the construct #C3 compared to 91.6±2.4% when cocultivated with T-cells expressing the CH₂CH₃ CD19 CAR. At lower ratios like 1:1 (88.3±3.2) and 0.3:1 (76.9±1.6), the #C3 CAR led to the lysis of more than 70% of the B-cells. At a ratio of 0.1:1, the #C3 CAR T-cells induced apoptosis in 62.0±4.8% of the tumor cells. Even at the lowest ratio (0.03:1) of effector to target cells, 30.0%±12.4% (CH₂CH₃ CAR: 34.8±14.3%) of the B-cells cocultivated with #C3 CAR T-cells were dead after 24 hours. Therefore, the efficacy of both constructs, the #C3 CD19 CAR and the CH₂CH₃ CD19 CAR was comparable at any effector to target cell ratio.

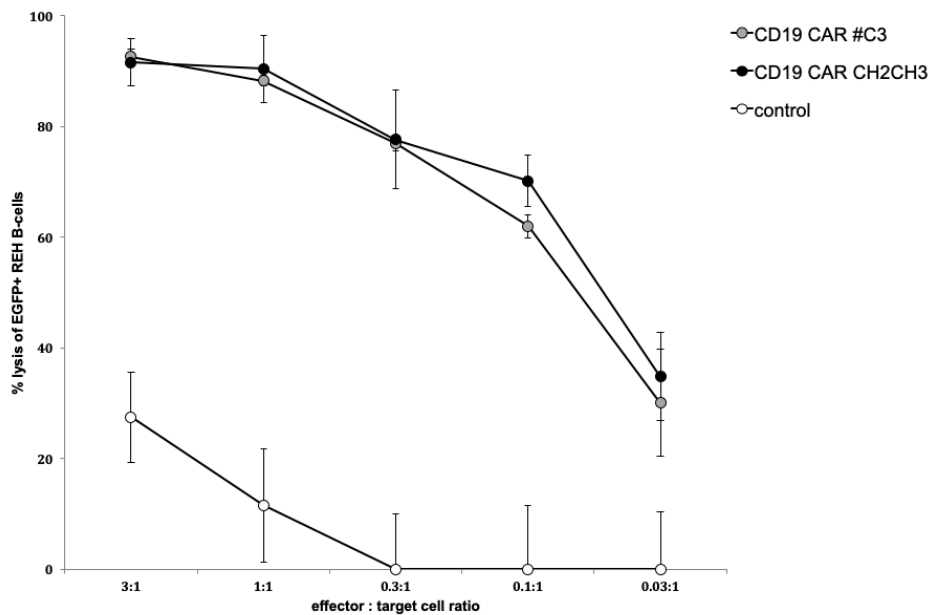


Figure 16. Cell lysis induced in REH-EG cells by #C3 CAR-expressing human T-cells. EGFP positive REH cells were incubated at different ratios with primary T-cells. T-cells were transduced with either the CH₂CH₃ CAR or the #C3 CAR construct. As control, REH-EG cells were incubated with T-cells not expressing any CAR. After 24 hours, REH-EG-cell survival was measured with FACS analysis via PI staining. Mean \pm SEM is shown from at least three experiments.

CD19 CAR #C6

Next, the cytotoxicity assays were carried out with the CD19 CAR containing the #C6 hinge (Figure 17). Since the #C3 experiments were carried out first, and the T-cells equipped with CD19 CAR #C3 induced lysis in significant numbers of T-cells at the lowest effector to target cell ratio, a lower ratio (0.01:1) was added for the #C6 experiments. At high effector to target ratios (3:1 and 1:1), T-cells with the modified #C6 CAR induced cell lysis in 89.4 \pm 1.3% and 85.7 \pm 0.9% of the target cells after 24 h. The CD19 CAR with the CH₂CH₃ hinge resulted in the death of 89.1 \pm 4.3% (ratio 3:1) and 85.0 \pm 6.1% (ratio 1:1) REH cells. A ratio of 0.3:1 led to the death of 76.3 \pm 1.3% B-cells during cocultivation with CAR #C6 expressing T-cells, while the CH₂CH₃ hinge CAR T-cells eliminated 72.1 \pm 9.0% of the B-cells. With lower ratios, the efficiency of B-cell killing decreased, e.g. lysis of 56.8 \pm 2.0% (#C6) and 48.9 \pm 5.0% (CH₂CH₃) of the B-cells at 0.1:1 effector to target cell ratios. At a ratio of 0.03:1 (0.01:1) the #C6 CAR led to the killing of 35.8 \pm 9.7% (18.1 \pm 7.0%), the CH₂CH₃ CAR showed similar efficiency.

In summary, transduced T-cells with the #C3 or #C6 CAR showed similar toxicity as the very efficient and previously published CD19 CAR with CH₂CH₃ hinge towards malignant CD19+ B-cells [140]. Thus, *in vitro*, the changed hinge region did not lead to a decrease of CAR-mediated cytotoxicity.

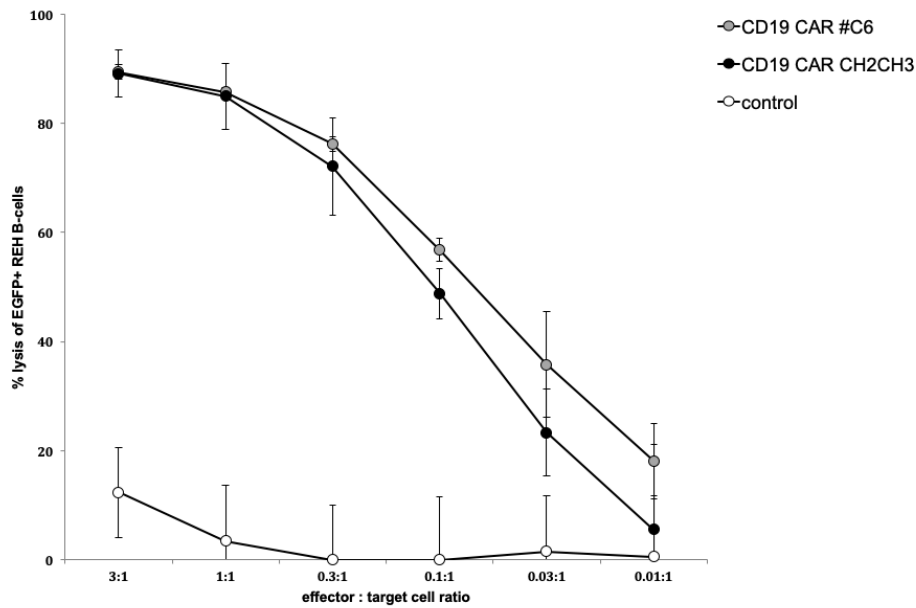


Figure 17. Cell lysis induced in REH-EG cells by #C6 CD19 CAR expressing human T-cells. EGFP positive REH cells were incubated in different ratios with primary T-cells from different healthy donors. The T-cells were transduced with either the CH₂CH₃ CAR or the #C6 CAR construct. As control, REH-EG cells were incubated with T-cells not expressing any CAR. After 24 hours, REH-EG-cell survival was measured by FACS analysis via PI staining. Mean \pm SEM is shown from at least three experiments.

3.1.3.4 Toxassays with 4-Ipomeanol and Perilla ketone

In order to test whether the viral vector shown in Figure 15 not only facilitates selection and cytotoxicity against CD19+ leukemic cells, but also allows for elimination of transduced T-cells by incubation with Perilla ketone or 4-Ipomeanol, the MACS-enriched CAR T-cells from the previous cytotoxicity assays were subsequently incubated with one of the two prodrugs. T-cells expressing hCYP4B1P+12 and none of the new CARs were used as positive control for apoptosis, non-transduced T-cells without suicide gene served as negative control. Cells were incubated with PK or 4-IPO in 24-well-plates. 24 hours later, the cultures were harvested and all cells were stained with PI for life/dead discrimination. The percentage of dead T-cells compared to T-cells that were not incubated with either prodrug was analysed by flow cytometry.

CD19 CAR #C3

Cells expressing the #C3 CAR together with the human suicide gene were incubated with 4-IPO or PK at final concentrations of 2.9 μ M, 9 μ M, 29 μ M and 90 μ M, respectively (Figure 18). T-cells expressing the suicide gene as well as the truncated version of CD34 (Δ CD34) were used as a positive control, since Δ CD34 enabled MACs separation of these cells prior to the toxicity assays. T-cells that did not express hCYP4B1P+12 were not sensitive to PK or 4-IPO in any of the tested concentrations (Figure 18). Toxicity assays with 4-IPO showed that there is no significant difference in T-cell apoptosis whether the #C3 CAR was coexpressed with the

suicide gene or not. 24 hours after incubation with 90 μ M 4-IPO, 79.6 \pm 3.5% of the CAR T-cells were killed. Lower concentrations led to decreasing numbers of dead cells. Already 50.5 \pm 1.4% of the T-cells coexpressing the #C3 CAR and the suicide gene were killed at the lowest concentration (2.9 μ M). Toxicity assays with Perilla ketone (PK) also showed no difference whether the suicide gene was coexpressed with the #C3 CAR or not. PK proved to be far more toxic than 4-IPO, which is in line with the results of Roellecke *et al.* [139]. The highest concentration (90 μ M) killed 90.0 \pm 4.0% of the transduced T-cells expressing the #C3 CAR, reducing the concentration to 2.9 μ M of PK still led to apoptosis in 81.3 \pm 5.5% of the transduced and MACS-enriched T-cells.

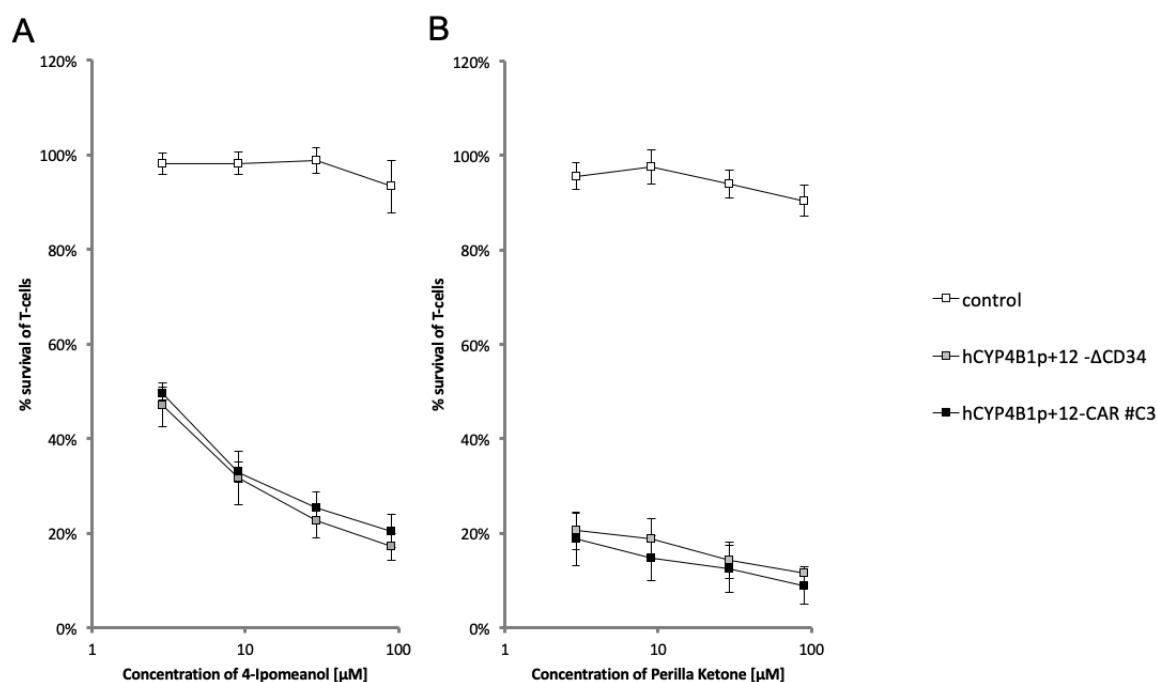


Figure 18. Cytotoxicity assay of #C3 T-cells expressing hCYP4B1P+12. Survival of T-cells expressing hCYP4B1P+12 and either the #C3 CAR or Δ CD34. **A.** Mortality curves after incubation with increasing concentrations of 4-Ipomeanol. **B.** Survival curves after incubation with increasing concentrations of Perilla ketone. Non-transduced T-cells served as negative control. Survival was measured after 24h by flow cytometry and PI staining. For each construct, the mean value \pm SEM is shown from at least 3 experiments.

CD19 CAR #C6

In the next step, the cytotoxicity assays were carried out with T-cells expressing the CD19 CAR #C6 as well as the suicide gene hCYP4B1P+12. Since Perilla ketone proved to be much more efficient in the #C3 experiments, all suicide gene experiments with the #C6 CAR were carried out only with PK, starting at lower concentrations (0.09 μ M, 0.9 μ M, 9 μ M and 90 μ M). T-cells expressing the suicide gene as well as the CD19 CAR with the CH₂CH₃ hinge served as positive control. The #C6 experiments showed that 24 hours of incubation with 90 μ M PK led to the death of 93.9 \pm 1.6% of the cells expressing #C6 and 94.9 \pm 2.7% of the cells expressing

the original CD19 CAR with CH₂CH₃ hinge. Concentrations of 9 μM PK still killed 87.4±2.7% (#C6) to 90.5±2.4% (CH₂CH₃) of the T-cells. As expected, lower concentrations led to a significant decrease in PK-induced apoptosis. At a concentration of 0.9 μM, 46.4±8.3% (#C6) and 60.9±11.0% (CH₂CH₃) of the T-cell populations were dead. Incubation with the lowest concentration (0.09 μM) led to the death of only 1.7±10.9% CAR #C6 T-cells and 6.2±5.7% CAR T-cells with CH₂CH₃-hinge.

Overall, both C19 CARs with the #C3 or the #C6 hinge, can be coexpressed with the suicide gene CYP4B1P+12 on primary human T-cells that are still highly cytotoxic after MACS enrichment and can be effectively eliminated *in vitro* via application of PK.

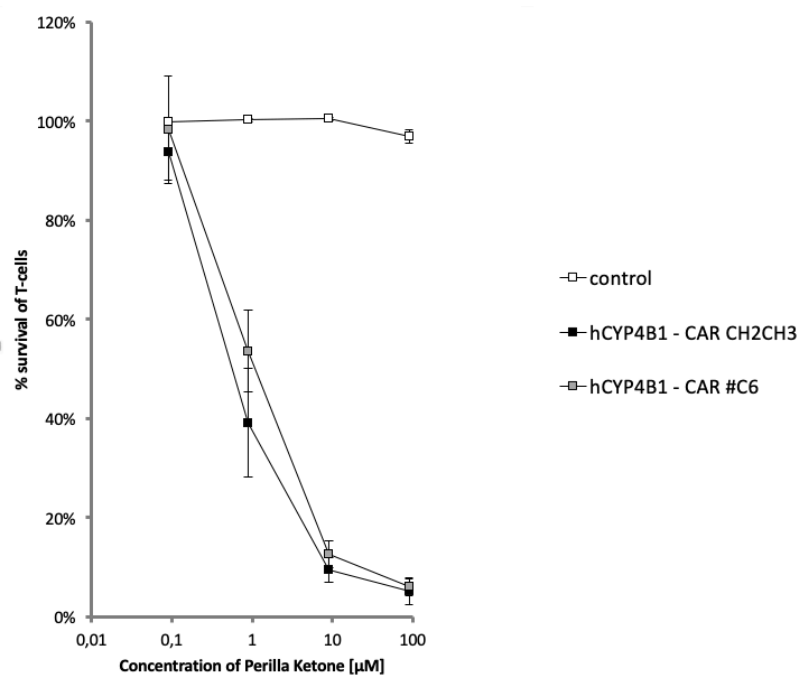


Figure 19. Cytotoxicity assay of #C6 T-cells expressing hCYP4B1P+12 Survival of T-cells expressing hCYP4B1P+12 and either the #C6 CAR or the CAR with CH₂CH₃ hinge after incubation with increasing concentrations of Perilla ketone. Non-transduced T-cells served as negative control. Survival was measured after 24h by flow cytometry and PI staining. For each construct, the mean value ±SEM is shown from at least 3 experiments.

3.2 Hepatotoxicity assays with different cytochromes

While CAR therapy extends the possibilities in the treatment of hematologic malignancies, its potentially life-threatening side effects increase the demand for a system that facilitates control over the genetically modified cells *in vivo*. One approach is the parallel expression of so-called “suicide genes” that facilitate the selective destruction of modified cells *in vivo*. A novel human suicide gene, hCYP4B1P+12, was recently developed and converts different

prodrugs into highly toxic DNA-alkylating metabolites [138]. While 4-*Ipomeanol* is a well-established prodrug for CYP4B1, *Perilla* ketone was not tested in *in vivo*-studies yet but showed a higher toxicity towards cells that expressed hCYP4B1P+12 *in vitro* [139].

One obstacle in the use of both prodrugs, 4-IPO and PK, is that the role of other human cytochrome P450 enzymes, which potentially metabolize these substrates, has not been widely explored yet. In fact, hepatotoxicity was a dose-limiting factor in clinical phase I/II studies with 4-*Ipomeanol* [130]. Since CYP4B1 is not expressed in human liver cells, other liver enzymes must have activated the prodrug 4-*Ipomeanol*. The enzymes CYP 1A2, 2E1, 3A4 and 3A5 are amongst the highest expressed cytochrome forms in liver tissue [174], therefore it is likely that one of them metabolized 4-*Ipomeanol* in *in vivo* studies. Those four different liver enzymes were overexpressed in HepG2 cells, a human hepatoma cell line that shows characteristics of primary human hepatocytes [155]. Subsequently, these transduced cells were tested for processing of the prodrugs PK and 4-IPO.

The cDNAs of the human cytochromes 1A2, 2E1, 3A4 and 3A5 were cloned as fusion proteins with EGFP into a 3rd generation lentiviral expression vector with an IRES-Puromycin expression cassette, p2CL21EGI2Pcowo. The vector coexpresses EGFP as a fusion gene with the cytochromes as well as a puromycin selection gene, connected by an IRES site. EGFP was needed as a selection marker for FACS analysis, since specific fluorescent antibodies against all four liver cytochromes are not available. The IRES site enables the expression of two transgenes from a single mRNA [175]. This combination ensured that each fluorescent cell also expressed the human cytochrome. The puromycin gene enabled selection of transduced HepG2-cells, therefore all experiments were carried out with puromycin resistant HepG2-populations.



Figure 20. Scheme of p2CL21EGI2Pcowo Different cytochromes were inserted in front of the EGFP sequence, a puromycin resistance gene is located after the IRES-site. The 5'LTR contains the promoter of the human cytomegalovirus (CMV), the R region and the U5 region. The transgene is driven by a myeloproliferative sarcoma virus (MPSV) promoter. Ψ: packaging signal; RRE: rev response element; cPPT: central polypurine tract; WPRE: *woodchuck hepatitis virus* posttranscriptional element

HepG2 cells were transduced as described in chapter 2.3.4 with medium containing protamine sulfate. Cells transduced with the control vector p2CL21EGI2Pcowo without cytochrome as well as non-transduced HepG2 cells served as negative controls. The very active rabbit CYP4B1 is already well characterized and was used as a positive control for efficient activation of the prodrug. It shows a very high processing of 4-IPO and PK. Another control was the mutated human CYP4B1-P427 that contains a proline at position 427 instead

of a serine. In previous studies, hCYP4B1 showed a lower level of activity than the rabbit cytochrome [138]. To analyse the enzymatic activity of the different liver cytochromes in the presence of 4-Ipomeanol and Perilla ketone, the constructs in Table 18 were used for transduction of HepG2 cells.

Insert	Vector construct
No new insert (negative control)	p2CL21EG12Pcowo
rCYP4B1 (positive control)	p2CL21rCYP4B1EG12Pcowo
hCYP4B1-P427 (positive control)	p2CL21hCYP4B1P427EG12Pcowo
hCYP1A2	p2CL21hCYP1A2EG12Pcowo
hCYP2E1	p2CL21hCYP2E1EG12Pcowo
hCYP3A4	p2CL21hCYP3A4EG12Pcowo
hCYP3A5	p2CL21hCYP3A5EG12Pcowo

Table 18. Vector constructs used to express different CYP-enzymes in HepG2 cells.

3.2.1 Hepatotoxicity assays with 4-Ipomeanol and Perilla ketone

Transduced HepG2 cells were incubated with increasing concentrations of 4-IPO or PK for 24 and 48h. The cell death rate was measured via flow cytometry. As shown in Figure 21, the non-transduced cells and cells transduced with the control vector were unaffected by the incubation with either prodrug.

When incubated with 4-IPO at low doses, the positive control rCYP4B1 already showed significant toxicity. 2.9 μ M of 4-IPO led to apoptosis of 30.2 \pm 4.3% after 24h and 50.6 \pm 7.1% after 48h. The highest concentration (290 μ M) of 4-IPO induced apoptosis of more than 80% of the cells expressing rCYP4B1 on both days. However, out of the human liver enzymes, only hCYP1A2 showed measurable toxicity when incubated with 4-Ipomeanol. 11.62 \pm 5.1% of the hCYP1A2-transduced cells died after 24h of incubation with 290 μ M 4-IPO. Expression of the other enzymes CYP2E1, CYP3A4 and CYP3A5 did not lead to the death of transduced cells, the survival rates were comparable to those of non-transduced cells.

Even at low concentrations (2.9 μ M), PK already induced apoptosis in 53.3 \pm 5.3% of the HepG2 cells expressing the positive control rCYP4B1 after 24h and 73.5 \pm 1.9% after 48h. All four tested liver enzymes induced measurable apoptosis during incubation with Perilla ketone. HepG2 cells expressing **hCYP3A5** showed the lowest activation rate of PK. Concentrations of 290 μ M were necessary to induce cell death in more than 10% of the cells. After 24 hours, the highest concentration led to the death of only 13.8 \pm 5.1% of the cells, after 48 hours, 23.6 \pm 1.8% died at the same concentration. **hCYP3A4** and **hCYP2E1** showed a similar rate of metabolism of PK. Concentrations from 2.9 μ M to 29 μ M lead to the death of

less than 10% of the transduced cells on both days. After 24 hours, 290 μ M of PK induced apoptosis in 30.1 \pm 3.1% of the cells overexpressing hCYP3A4 and 36.1 \pm 0.2% of those overexpressing hCYP2E1. The same concentration led to the death of 66.5 \pm 2.9% (3A4) and 42.4 \pm 2.9% (2E1) after 48 hours. Thus, high concentrations of PK were needed to induce significant cell death in the cell lines expressing these two constructs. Overexpression of **hCYP1A2** led to the highest toxicity in HepG2 cells. Concentrations of 90 μ M PK caused cell death in 42.4 \pm 7.1% of the population after 24 hours, 290 μ M PK induced apoptosis in nearly 60% of the cells. After 48h, 290 μ M PK induced cell death in 77.6 \pm 3.4% of the hCYP1A2 HepG2 cells.

Therefore, while the positive control rCYP4B1 showed significant toxicity when incubated with each substrate at low doses, PK was more toxic than 4-Ipomeanol. The other positive control, hCYP4B1-P427, showed a slightly lower sensitivity towards both prodrugs. This is in line with the results of Wiek *et al.* and Roellecke *et al.* [138, 140]. While PK induced significant apoptosis in all four tested liver enzymes even at low concentrations, 4-IPO only induced measurable toxicity when incubated with the enzyme hCYP1A2.

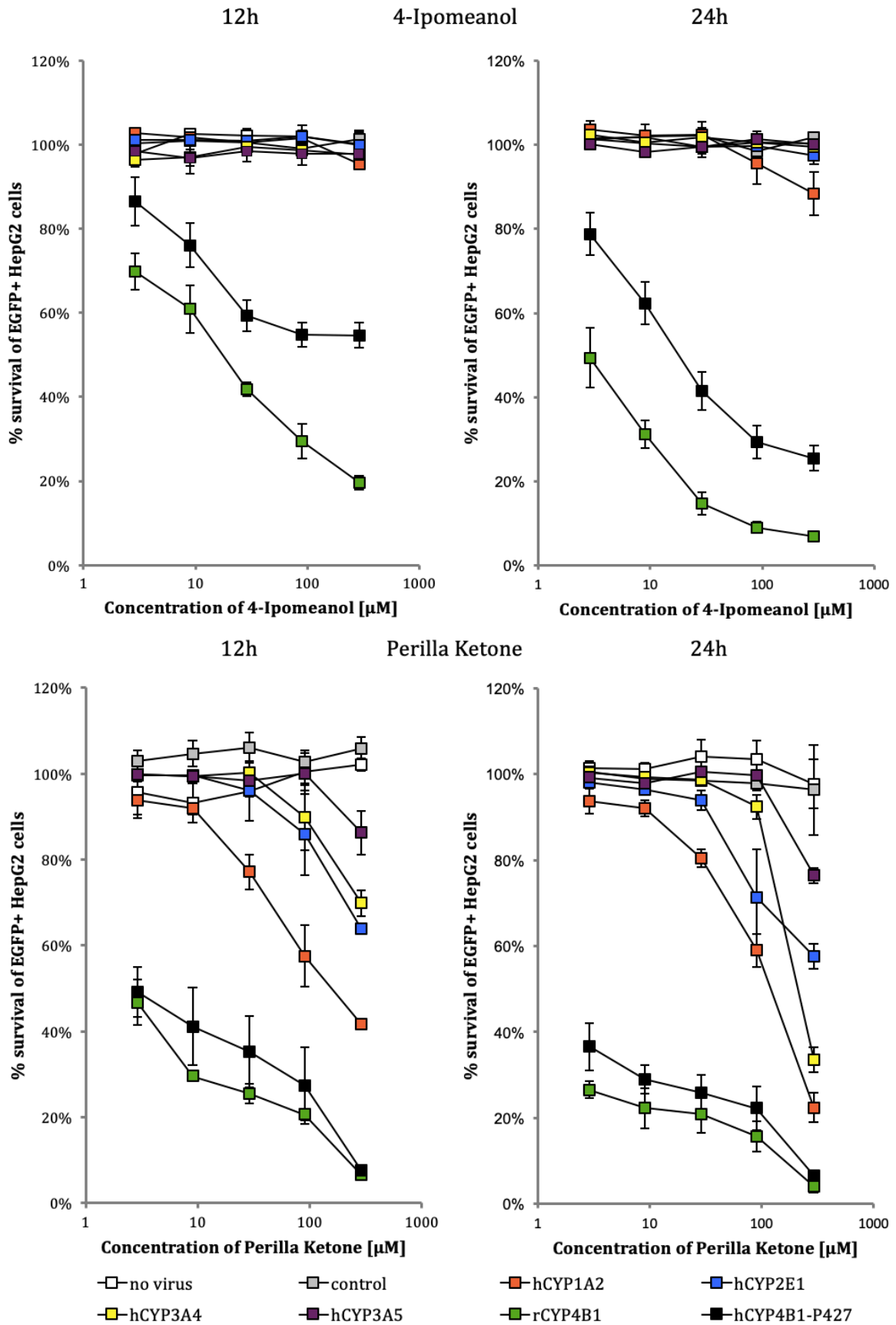


Figure 21. Toxicity assay - Liver enzyme activity. Survival of HepG2 cells transduced with hCYP1A2-hCYP2E1-, hCYP3A4-, hCYP3A5-, hCYP4B1-P427- and rCYP4B1-EGFP fusion enzymes after incubation with 4-IPO (A) or PK (B). Non-transduced cells and cells transduced with EGFP were used as negative control. The percentage of surviving cells is depicted after 24h and 48h. For each construct, the mean value \pm SEM is shown from at least 3 experiments.

3.2.2 Western Blot and MFI

To compare the protein expression levels of the different cytochromes transduced in HepG2 cells with the activity results shown in Figure 21, cells expressing EGFP as a fusion with rCYP4B1, hCYB4B1-P427, hCYP1A2, hCYP2E1, hCYP3A4 and hCYP3A5 and cells expressing only the EGFP vector control were lysed. The lysates were analysed via Western Blot. Importantly, as EGFP was used as a protein tag, semi-quantitative comparison of the protein expression levels in the cells was possible. Beta-Actin has a molecular weight of 42 kDa and was used to visualize equal protein loading. The different CYP enzymes only have a molecular weight of about 58 kDa, the fusion constructs with EGFP weigh about 27kDa more. Thus, the CYP – EGFP fusion constructs could be detected as bands at about 85kDa. p2CL21EG12Pcowo was used as control vector, its EGFP-band was detected at 27kDa (lane 1).

Western Blot analysis of the different lysates with the monoclonal EGFP antibody demonstrated that the rabbit CYP4B1 (lane 2) had the most prominent protein band, i.e. had the strongest protein expression. The modified human CYP4B1-P427 (lane 3) and hCYP1A2 (lane 4) also showed good expression levels, while cells transduced with hCYP3A4 (lane 6) and hCYP3A5 (lane 7) constructs have lower expression of the CYP450 protein. hCYP2E1 (lane 5) has the weakest protein band, which surprisingly appeared as a double band. Overall, in Western Blot analysis, the protein expression of the liver cytochrome fusion-constructs was lower compared to the fusion-construct containing the rabbit CYP4B1.

In addition, using the EGFP tag as a fluorescent marker in flow cytometry allows us to determine the mean fluorescent intensity (MFI) of all transduced cell samples, indicating how positive the transduced cells were on average. MFI of the fusion constructs varied between 745.5 ± 92.4 (rCYP4B1) and 139.7 ± 20.7 (hCYP2E1). Cells that were transduced with EGFP only had a significantly stronger protein expression and much higher MFI of 2114.1 ± 91.0 than all cells transduced with EGFP fusion proteins. Importantly, the half-life of EGFP (about 26 h) is longer than the half-life of the modified human CYP4B1-P427, which was determined in our working group at about 16.5h [176]. However, half-lives of all 4 liver enzymes used in these experiments have been determined in different publications to lie at least in the same range as the half-life of EGFP [177], what makes a direct comparison of the results possible. In summary, the calculated MFIs correspond with the Western Blot results.

Those results prompt to the conclusion, that the different levels of activity in combination with both prodrugs are linked to the amount of protein existing in the transduced cells in a steady state mood.

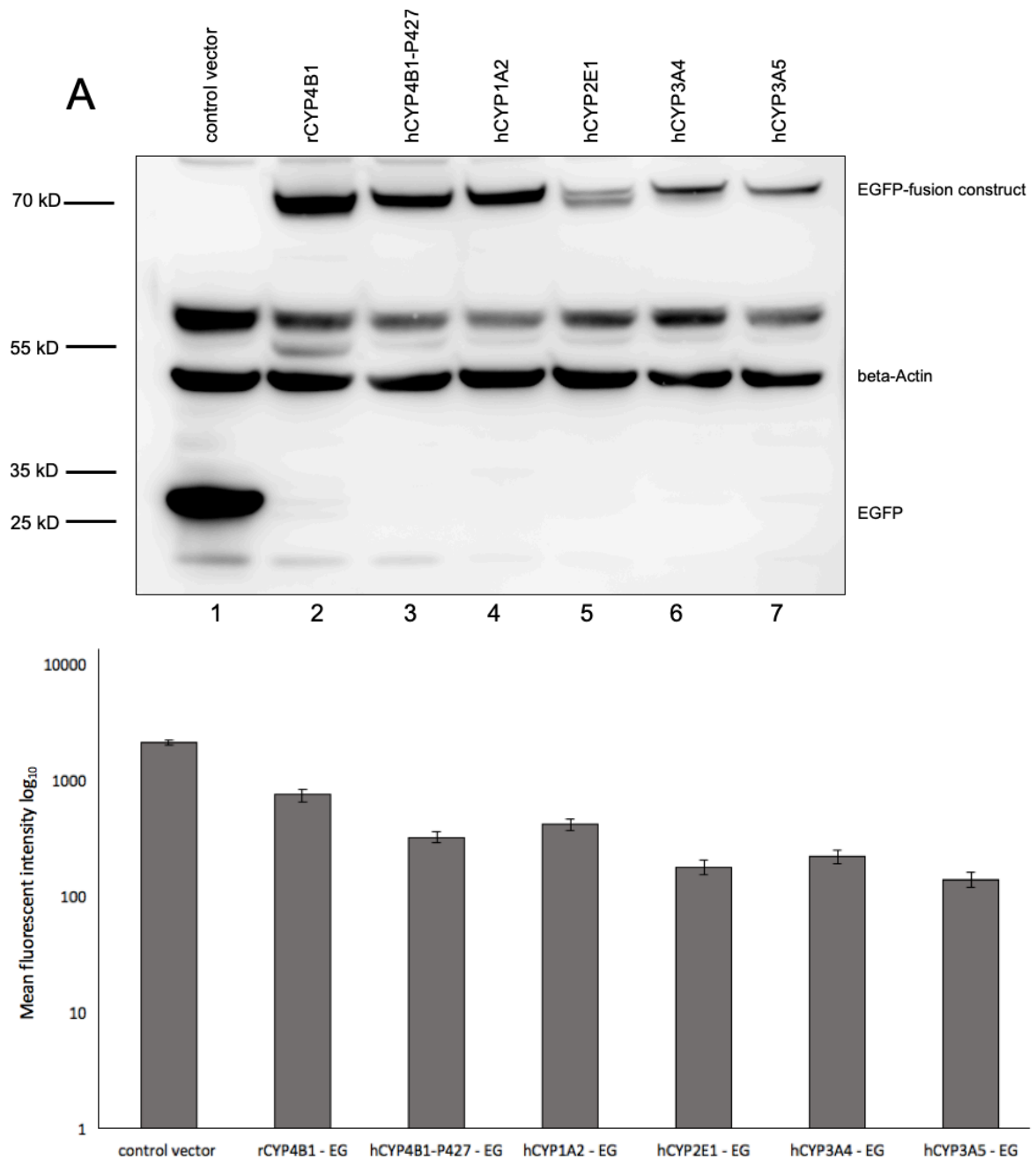


Figure 22 A. Western Blot. Analysis of HepG2 cells transduced with lentiviral vectors expressing EGFP as a fusion protein with different CYP-species. Detection via EGFP antibody. β -actin staining was used to visualize equal protein loading. **B. MFI of transduced HepG2 cells.** MFI displayed as \log_{10} . All cells were transduced with the same constructs that were used for the Western Blot. MFI \pm SEM is shown from at least 6 experiments.

4 DISCUSSION

In 2013, Science magazine selected cancer immunotherapy as “Science breakthrough of the year”, stating that „immunotherapy marks an entirely different way of treating cancer - by targeting the immune system, not the tumor itself“ [178]. The term “cancer immunotherapy“ included checkpoint immunotherapy as well as treatment with chimeric antigen receptors. Antibody therapy directed against negative immunologic regulators (checkpoints) on the surface of tumor cells or the immune effector cells has shown significant success in a large variety of malignancies and is likely to be a standard component in the treatment especially of solid tumor patients [179]. Typical examples for checkpoint inhibitors are antibodies that target the cytotoxic T-cell-associated antigen 4 (CTLA-4) in patients with metastatic melanoma [180] or antibodies against the programmed cell death protein 1 pathway (PD-1). The later one is a negative regulator of T-cell activity whose ligands PD-L1 and PD-L2 are present on some tumor cells and would normally downregulate the innate anti-tumor response when activated. The deactivation of PD-1 has improved the overall survival of patients with advanced melanoma as well as solid tumors like renal cell carcinoma [181].

The possibility to genetically engineer autologous human T-cells and use these cells to individually fight tumor cells has led to new developments that tremendously extended the field of adoptive T-cell therapy. Genetically modifying the immune effector cells with CARs seems to be a promising new approach in the treatment of various malignancies and a possible treatment option even after failure of the intensive first line and second line chemotherapies (including hematopoietic stem cell transplantation). T-cells expressing a CAR specifically and efficiently recognize an antigen on the surface of tumor cells, are activated solely upon engagement of the scFv fragment in the CAR in a MHC-independent manner and subsequently kill the cells [75]. Activation of CAR T-cells leads to an enhanced overall immune response, resulting in specific killing of all cells – malignant and nonmalignant cells - expressing the TAA and in addition to activation of other innate immune cells like monocytes and NK-cells. CAR-engineered T-cells proliferate *in vivo* and therefore can last much longer in the patient than all chemical and molecular therapeutics [22, 75]. Another advantage of CAR therapy is that they facilitate detection of other structures than proteins like carbohydrates and glycolipids which increases the pool of potential epitopes and target antigens. Significant quantities of tumor-antigen specific T-cells can readily be generated *in vitro*, for example by lentiviral gene transfer. After expansion, these genetically modified cells are (re-) infused into the patients and start attacking all cells that express the TAA.

In August 2017, Kymirah®, a CD19 CAR T-cell product, received FDA approval as a regular drug against relapse or refractory ALL in pediatric and young adult patients [182]. A second CD19 CAR against large B-cell lymphoma by Kite Pharma called Yescarta® received FDA approval in October 2017 [183].

At the moment, CAR therapy is a form of personalized therapy that is still time-consuming and extremely expensive, since it has to be adapted individually to every patient and the modification of T-cells *in vitro* with integrating lentiviral vectors remains a very complex process. The price for one dose of Kymirah® by Novartis was set at 373.000 US Dollar in December 2018 and the patient's cell samples have to be send to a central manufacturing center to genetically engineer the T-cells. Due to the low number and heterogeneity of patients in each study as well as different gene-transfer methods, treatment protocols and CAR structure, the results of the clinical trials are not directly comparable yet. Therefore, a specific T-cell component that allows enumeration and even purification of CAR T-cells with already established methods could be of great benefit and a step forward in the direction of "off-the-shelf" adoptive cell therapy. This would probably lower the costs of T-cell engineering, speed up the therapeutic process *in vitro* and facilitate comparability of different trials.

4.1 Establishing a new detection sequence as part of a CAR

An obstacle in the search for an ideal CAR construct is the design of an optimal hinge region. It gives the CAR the necessary mobility to stick out of the glycocalyx covering the T-cell to reach the antigen on the tumor cell surface. Although there is no ubiquitously used hinge region [42, 46], an ideal spacer needs to fulfill certain criteria. It should be of human origin to reduce the risk of immunogenicity, has to provide the necessary flexibility to reach antigens on the tumor cell surface and should be non-signaling when the CAR is not engaged. Hudecek *et al.* demonstrated that the length of the spacer domain can have a major effect on T-cell function as well as on efficacy after target recognition [95]. The frequently used CH₂CH₃ domain derived from IgG leads to off-target activation of CAR T-cells through Fcγ-bearing cells. In mice and probably also in humans, this can lead to an unintended immune response independent of tumor cell recognition and subsequently to AICD of the engineered T-cells as well as to activation of innate immune cells. Correspondingly, the T-cells were unable to attack their intended targets [94].

The hinge region within a CAR can also serve as a marker region for experimental immunology and gene therapy. In general, marker genes facilitate detection and positive selection of transduced cells. Thereby, after administration, transduced cells can be readily tracked in peripheral blood, liquor or bone marrow. Conservative T-cell stimulation during transduction leads to varying rates of successfully transduced T-cells. The amount of CAR positive T-cells in a sample that is retransfused to a patient differs a lot even within one trial. According to a review by Hartmann *et al.*, the percentage of CAR+ T-cells in each sample even varied between 20 and 90% in different trials [92]. Via positive selection *in vitro*, a sample of completely transduced cells would be administered to the patient, therefore the efficacy could be monitored more closely and comparison of different trials would be facilitated. *In vitro* studies commonly use EGFP as a coexpressed marker for successful transduction. However, EGFP transgenic expression *in vivo* is not biologically inert and its effects on human metabolic pathways remain unclear [184]. Commonly used marker genes in human trials are mainly type I transmembrane proteins like truncated CD19 [109], the truncated low-affinity nerve growth factor (Δ LNGFR) [185] or truncated CD34 (Δ CD34), they are expressed as independent molecules on the cell surface [173]. Similar to an ideal hinge region, an ideal detection site would be of human origin to avoid immune reactions against genetically modified T-cells. Since adoptive T-cell therapies are highly complex, many parameters like cell cultivation *in vitro* or transgene production need to be optimized before phase I/II clinical trials can be developed. To enable rapid and repetitive experiments and to minimize changes in the T-cell culture that appear after long-term *ex vivo* cultivation, the selection of transduced cells should be a quick process.

In this thesis, I developed new hinge regions with an integrated detection site that will facilitate clinical grade and GMP approved purification, thereby combining the therapeutical benefit of a CAR with the need for a selection marker in one molecule. In addition, both receptor templates are of human origin, this reduces the risk of immunogenicity. Antibody epitopes of both NGFR and CD34, which were previously used as selection marker, were tested [139].

NGFR

The low-affinity nerve growth factor receptor (LNGFR, CD271) serves as a receptor for neurotrophins which are protein growth factors that stimulate neuronal cells to differentiate [186]. LNGFR is not expressed on human hematopoietic T-cells, what makes its truncated surface domain Δ NGFR suitable for usage as selection marker in T-cell experiments. In 2002, Li *et al.* reported a leukemic transformation in murine bone marrow after integration of a

retroviral vector and suggested that in addition to the insertional mutagenesis the expression of Δ NGFR contributed to the progression of the disease [187]. However, concerns that the expression of Δ NGFR might work as an oncogene could not be confirmed by Bonini *et al.*, when they compared numerous preclinical experiments and a clinical trial that used retroviral vectors to express Δ NGFR [188]. Over 300 mice transplants and more than 100 transductions of human lymphocytes showed no change in differentiation of progenitor cells and no adverse events.

The exact epitope of the LNGFR in which the ME20.4 CD271 antibody binds is not known, but the manufacturer Miltenyi Biotech confirmed that it probably is located somewhere in the 3rd or 4th cysteine rich domain (personal communication). To localize the epitope more exactly, I inserted four different templates containing different sequences of the 3rd and 4th CRD of Δ NGFR into the CD19 CAR (kindly obtained from Claudia Rössig) between *MfeI* and *MluI*. After transduction, neither CAR #N1 (40 aa) nor CAR #N2 (42 aa) was stained by the NGFR-antibody. The other two CAR constructs with longer sequences (the #N3-hinge contained 120 aa, the #N4-hinge contained 162 aa) were successfully stained, suggesting that the epitope lies in both regions or the tertiary structure of the epitope can only be preserved by using a longer sequence. Surprisingly, when using the NGFR hinge in the CD19 CAR, the vast majority of transduced cells were not efficiently enriched via MicroBead selection with the anti NGFR-mAb ME20.4. Since an efficient selection process is a key feature of an ideal spacer region, I conducted no further experiments with these constructs and proceeded with the CD34 - experiments. Therefore, although all available information about the NGFR epitope was considered in this work, it was not possible to identify an ideal sequence for the hinge region that could serve as a marker for CARs.

After the experiments in this thesis had already been carried out, Casucci *et al.* stated that their group successfully tested different parts of the cysteine-rich regions of LNGFR as alternative spacer regions for CARs *in vitro* and in murine models [189]. Their tested spacers were between 140 and 222 aa long and were all derived from the 4 cysteine rich regions plus the serine/threonine-rich stalk. While all their constructs were successfully stained by the anti NGFR mAb C40-1457, the ME20.4 antibody only bound to the 222 aa long construct that contained all four unchanged CRDs plus stalk [189]. The CD19 CARs with hinges from NGFR tested in this thesis contained less amino acids (40 aa to 162 aa) and none of them included all 4 cysteine-rich regions. Therefore, a much longer aa-sequence of NGFR might be necessary for sufficient binding of the ME20.4 antibody. Bondanza *et al.* continued to work only with the C40-1457 monoclonal antibody by BD Bioscience, which cannot be used directly in the CliniMACS devices to purify cell populations.

CD34

CD34 is a glycosylated type I transmembrane protein [171]. Since it is already widely used for HSC selection as well as for quality control in HSCT, a GMP-compatible CliniMACS selection device is commercially available [190]. Interestingly, the exact function of CD34 and its family members has not been fully determined yet [191-193]. However, it is known that CD34 is an adhesion molecule that participates in differentiation and attachment of stem cells [171]. Studies in murine models have shown that CD34 limits the migration abilities of bone marrow stem cells, an effect that was more distinct in cells with full-length CD34 than in cells expressing the truncated variant Δ CD34 [194]. When used as hinge in the CAR, the transduced T-cell will only express a minor part of the Δ CD34 molecule, therefore changes in migration ability and adhesion characteristics of T-cells seem rather unlikely. In 2014, Philip *et al.* proposed the central amino acid sequence of the epitope for the CD34 type I monoclonal antibody Qbend10. Importantly, this antibody labelled with supramagnetic beads is already FDA approved for selection of CD34 positive cells by a CliniMACS device. By sequential deletion of the amino and carboxyl termini of the amino-terminal 40 aa of Δ CD34, they concluded that only a sequence of 16 aa is necessary for efficient antigen binding. Philip *et al.* used this sequence in combination with parts of CD20 and CD8 to create a new suicide gene called RQR8 that includes a selection marker [117].

In contrast, in this thesis sequences around the epitope for the QBEND10 antibody were inserted into a CD19 CAR as hinge region. As Philip *et al.* pointed out, depending on the target antigen, a 16 amino acids long sequence might not be long enough to ensure the CARs necessary flexibility to reach its target on the tumor surface [117]. Adjacent amino acids were systematically added to the amino- and carboxyl-terminal of the 16 amino acids long epitope, which served as "core sequence". While #C1 (16 aa) was not stable even in bacteria, the final six variants (#C2-#C7) were cloned as linker regions in the CD19 CAR. Consecutive staining experiments with the Jurkat T-cell line and primary human T-cells revealed that cells expressing CARs with any of the six inserts #C2-#C7 as linker were successfully stained by the CD34 antibody. In the next set of experiments, selection of transduced cells by MACS, the #C6 construct with 99 aa led to most efficient cell separation with excellent enrichment and little loss of positive cells. CARs with the #C3-5 hinge showed lower, rather similar efficacy in cell separation. This might be due to the tertiary structure of CD34 relative to the CD19 CAR, possibly shorter inserts limited the antibodies direct access to the epitope. The longer #C7 with 179 aa was the second most efficient construct. Therefore, #C7 could be of use for CARs that need a longer hinge region to reach their target, such as some ROR1 CARs [42].

Importantly, these results show that the efficiency of MACS selection does not necessarily correlate with the length of the insert.

The experiments in this work were carried out with CARs directed against CD19. Guest *et al.* showed that CD19 CARs without long spacer efficiently eliminated malignant cells and even showed a higher IFN γ -expression *in vitro* than CD19 CARs with longer spacer regions [46]. Therefore, I continued to work not only with CARs including #C6 (99 aa), which showed the best enrichment in MACS experiments, but also with CAR #C3 (49 aa) T-cell populations, which were purified less efficiently but only contain 49 new amino acids.

An alternative approach to solve the problem of unwanted T-cell activation is the modification of the already established extracellular CH₂CH₃ spacer region. *In vivo* tests with CD19 CARs in murine models showed that a shorter spacer consisting only of the IgG4 hinge region without CH₂CH₃ domain led to enhanced cytokine production and a higher proliferation rate of engineered T-cells without antigen-independent cell activation [95]. Another changed version of this spacer was created by Hombach *et al* [94]. They replaced amino acids of the Fc γ R detection site in the CH₂ domain of the IgG1 spacer. Since both the Fc γ RII and the Fc γ RIII can bind to other residues besides this known epitope, they additionally changed single amino acids in the CH₂ region that coded for alternative binding sites [187, 195, 196]. CARs expressing this modified spacer did kill malignant cells efficiently *in vitro* and were not activated by other immune cells.

By replacing the complete Fc-part with a CD34 derived hinge, any risk of Fc γ R-dependent off-target activation should be eliminated. In addition, this approach provides an alternative and shorter detection site that can be used to efficiently enrich and select genetically modified T-cells with clinically approved CD34 selection kits.

4.2 Metabolisation of 4-IPO and PK by different liver enzymes

Parallel to the development of more advanced *in vivo* CAR-therapy strategies, the demand for an “off-switch” for engineered T-cells increases. A strategy to control CAR therapy is necessary for multiple reasons. Most importantly, numerous adverse events like cytokine release syndrome, sepsis or on-target off-organ toxicity might occur [34, 96, 99]. If the CAR therapy cannot be inhibited as soon as an adverse event occurs, this might lead to severe morbidity and even mortality of the patient [96, 99]. Individual variations in T-cell responses and in risks for toxicities make it impossible to predict the optimal number of T-cells per infusion for each patient [197]. Based on the use of HSV-tk and iCASP-9, potentially life-

threatening situations can be stopped by fast elimination of all genetically manipulated T-cells [109, 114, 198]. Also, successfully treated patients with CD19 CAR T-cells suffer permanently from B-cell aplasia, which can only be partly compensated with frequent immunoglobulin infusions. If a complete therapy stop via elimination of all genetically engineered T-cells was achieved, the patient would develop his own B-cells again.

A possible solution for this problem is the use of so-called suicide genes as safety-switch. Most of these genes code for proteins which convert a non-toxic prodrug into a toxic metabolite that leads to the death of suicide gene positive cells. In this thesis, the hCYP4B1P+12 suicide gene system was used [138]. hCYP4B1P+12 meets several requirements of an ideal suicide gene. Since all 13 amino acid changes are conserved in corresponding positions in other human CYP4-family proteins, the risk of causing immunogenicity is rather low. The activated prodrug 4-*Ipomeanol* induces apoptosis independent of cell division and shows no bystander activity [137]. 4-IPO was initially thought to be a potent therapeutic against lung or liver cancer and was therefore tested in clinical trials [127, 131, 132]. An alternative prodrug, *Perilla ketone*, that resembles 4-IPO closely in its chemical structure, has recently been tested *in vitro* [139]. In our laboratory, it was shown that PK is more potent in T-cells with the hCYP4B1P+12 suicide gene, induces apoptosis faster than 4-IPO and leads to no unspecific toxicity towards non-transduced T-cells [139, 140]. Both combinations, hCYP4B1/4-IPO and hCYP4B1/PK lead to fast and efficient elimination of T-cells *in vitro* [138, 139].

One obstacle in the use of hCYP4B1P+12 as a suicide gene in humans is that the role of other human CYP450 enzymes in the liver, which potentially metabolize substrates like 4-IPO or PK, has not been widely explored yet. Hepatotoxicity induced by 4-IPO was dose limiting in patients [130], but the dose where this occurred in clinical trials is likely to exceed the necessary dose rates to eliminate CAR T-cells. Therefore, additional information about the metabolism of 4-IPO in humans would be beneficial to avoid possible adverse events in further experiments with the hCYP4B1P+12 system. *Perilla ketone* has not been tested in clinical trials yet, and it remains unknown if it induces toxicity due to catalysation via other cytochromes. Due to its structural similarity to 4-IPO, it is likely metabolized by a similar portfolio of enzymes.

In this thesis, four different liver enzymes were overexpressed in HepG2 cells, a hepatocellular carcinoma cell line [199], and tested for their metabolism of 4-IPO as well as PK. HepG2 cells are a suitable *in vitro* model system for the study of human hepatocytes, since they resemble the characteristics of primary human hepatocytes and are well

established as a model system for studies of liver metabolism and hepatotoxicity [200]. The human enzymes CYP2E1, CYP3A4/3A5 and CYP1A2 are some of the main P450 enzymes in the liver and responsible for the metabolism of a large number of toxic environmental chemicals and carcinogens that enter the body [201]. hCYP2E1 is a membrane protein in hepatocytes that is also involved in the metabolism of ethanol and fatty acids [202]. hCYP3A4, the most abundant of the CYP3A enzyme family in the human liver, plays an important role in the oxidative metabolism of a large number of essential drugs. Different hCYP3A5 alleles in varying ethnic populations metabolize xenobiotics at different rates [203, 204]. The main function of hCYP1A2 is to activate polycyclic aromatic hydrocarbons and its expression is enhanced by the presence of these metabolites [205, 206]. The expression levels of all four enzymes depend on genetics and external influences [118, 204, 207, 208].

In order to understand the reason for liver toxicity of 4-IPO, HepG2 cells expressing the four P450 enzymes described above were generated and incubated with different concentrations of 4-*Ipomeanol* for 24 or 48 hours. Previous clinical studies with 4-IPO reached serum peak concentrations of 100 μ M with doses up to 1290 mg/m² of the prodrug and treated patients for a period of three weeks with doses up to 1032 mg/m² [130, 132]. *In vitro* experiments in this work needed doses up to 90 μ M 4-IPO to efficiently induce apoptosis in more than 90% of engineered CAR T-cells within 24 hours. The results of the experiments in HepG2 cells indicate that the concentrations used in this thesis lie within an applicable range for clinical trials.

In this thesis, hCYP1A2 was the only tested enzyme that induced significant cytotoxicity in transduced HepG2 cells at high concentrations of 4-IPO. It was already demonstrated that hCYP1A2 does metabolize 4-IPO, albeit far less efficient than e.g. the rabbit CYP4B1 [209]. Surprisingly, in the experiments in this thesis, hCYP1A2 positive cells showed less measurable toxicity compared to those experiments when incubated with 4-IPO. In CYP4B1 knock-out mice, the expression of CYP1A2 in the mouse liver tissue was not affected by the elimination of CYP4B1 and no toxicity at all was observed in any CYP4B1^{-/-} mice after infusion of 4-IPO [210]. This indicates a lack of significant CYP1A2 activity mediated by 4-IPO in mouse hepatocytes *in vivo*. Hepatotoxicity was a dose-limiting factor in clinical studies in some, but not in all trial patients [130]. If CYP1A2 alone was responsible for activation of 4-IPO, all patients in the trial would have experienced hepatotoxicity, albeit in various degrees, since CYP1A2 is expressed in every human liver cell. Additionally, individual genetic variabilities like Single Nucleotide Polymorphisms (SNPs) and other mutations in patients might lead to a more or less efficient metabolism of 4-IPO.

All Hep-G2 cells transduced with a liver cytochrome showed measurable toxicity when incubated with high doses of Perilla ketone. Again, hCYP1A2 metabolized PK most efficiently but far less effective than the rabbit CYP4B1 or the human CYP4B1P+12. In line with earlier results of our work group, PK proved to be more toxic and induced apoptosis faster than 4-IPO in combination with the suicide gene [139].

The expression of cytochrome-P450-oxidoreductase (POR) might also contribute to the low levels of enzyme activity in these experiments. The activity of cytochromes as monooxygenases is highly dependent on sufficient electron transfer to the hem-group of the enzyme via the NADPH-dependent enzyme POR [211]. All CYP enzymes in a cell interact with the same POR and it has been shown that CYP enzymes outnumber the POR proteins in human hepatocytes [212-214]. Overexpression of cytochromes might therefore lead to an imbalance between electron donators and acceptors. Unpublished *in vitro* experiments in our work group showed that while activity of the different CYP4B1 versions cannot be enhanced via simultaneous overexpression of POR, the activity of hCYP1A2 alone does indeed increase when POR is overexpressed. Therefore, hCYP1A2 and other tested enzymes might have competed for electrons by the POR and maximum activity of these cytochromes during the experiments cannot be guaranteed.

The low metabolisation rate of 4-IPO by human liver enzymes may partly be due to the use of EGFP- cytochrome fusion proteins that were used in this thesis. Earlier experiments in our group and others demonstrated that EGFP-fusion constructs lead to slightly reduced activity of the enzyme that is fused to EGFP, compared to constructs in which the enzyme and EGFP are expressed separately [138]. These findings are supported by the weak protein expression of all fusion-protein constructs in Western Blot analysis and the corresponding MFIs. Therefore, the lower levels of enzyme activity in combination with both prodrugs could be linked to the amount of existing protein.

To confirm or disprove the hepatotoxicity results in this thesis, the experiments should be repeated without fusion protein and maybe should be carried out with overexpressed POR. Furthermore, the *in vivo* efficacy of the hCYP4B1P+12 system needs to be tested in the previously mentioned *CYP4B1* knock-out mice [210]. Additionally, alternative faster and more precise ways of delivering the prodrug to the engineered T-cells need to be tested. Ultimately, the question which concentration is needed to ensure a therapy stop and which concentration might induce toxic side effects needs to be readdressed in *in vivo* preclinical studies.

Other suicide genes have already been successfully employed in clinical trials [109, 111]. HSV-tk with its prodrug Ganciclovir has the advantage that it is the most widely tested suicide gene and therefore well characterized [114, 215, 216]. Unfortunately, due to the high immunogenicity of the viral HSV-tk protein, genetically modified T-cells are often eliminated rapidly, especially in immunocompetent hosts [113]. Furthermore, the HSV-tk/Ganciclovir system has a bystander effect [217], its efficacy is dependent on cell division and Ganciclovir is an essential drug in the treatment of post-transplant CMV infections.

The iCASP system consists of the human caspase 9 which is fused to the dimerizing domain of the FK506 binding-protein as a suicide gene together with an applicable dimerizing drug [109]. The drug AP1903 is not needed as therapeutic drug otherwise and seems to be biologically inert in human [109, 218]. Budde *et al.* also showed that induction of cell death requires a high expression of iCASP in T-cells and that T-cells need to be activated for efficient elimination [219]. However, this suicide gene works independent of the cell cycle and eliminates cells rapidly via activation of the mitochondrial apoptotic cascade. Activation of the iCASP-system led to eradication of genetically engineered T cells *in vivo* within 2 hours after administration of AP1903 [109]. This is a major advantage of the iCASP system, since a very fast elimination of genetically engineered cells can be decisive when acute adverse events occur. The prodrug AP1903 is synthetic [220] and theoretically could cause immunogenicity [221]. However, studies *in vivo* with a long-term follow up of 3.5 years have not shown any significant adverse events caused by immunogenicity [109, 218]. At the moment, the iCASP system is one of the most promising approaches for a standardized suicide gene system in CAR T-cell therapy.

4.3 Cytotoxicity and subsequent elimination of modified CAR T-cells

To ensure both safe and efficient CAR therapy at the same time, T-cells can be equipped with an effective, non-immunogenic CAR together with a suicide gene. In this thesis, primary human T-cells were transduced with a lentiviral vector containing the new #C3 CD19 CAR or #C6 CD19 CAR construct and the hCYP4B1P+12 suicide gene. The whole population of cells engineered with a CAR should express the suicide gene to facilitate an effective elimination if necessary. In all lentiviral vectors, the two transgenes were separated by a T2A site, which codes for a so-called “self-cleaving” peptide and generates two discontinuous protein fragments from one mRNA translation driven by a single promoter [222]. Therefore, equal expression of both, the suicide gene and the CAR, was ensured.

Importantly, T-cells expressing CD19 CARs with the #C3 or the #C6 hinge proved to be as efficient in eliminating CD19+ leukemic cells as the CD19 CAR with the IgG4 CH₂CH₃ hinge. In addition, the T-cells that killed the leukemic cells can still be efficiently eliminated by hCYP4B1P+12 via exposure to 4-*Ipomeanol* or *Perilla* ketone as prodrug. These results prompted me to conclude that the new CAR constructs fight tumor cells as efficient as the one with the IgG4 hinge, and that the suicide gene functionality is not impaired when transduced in the same vector as the CAR. This work also shows that it is possible to integrate additional information into the already complex CAR structure without limiting its functions. The signaling cascade that activates the CAR after detection of an antigen does not seem to be influenced by the additional amino acids of the hinge. On the other hand, the CD34 epitope is successfully detected by the Qbend10 antibody even though it is embedded in the CAR structure. With this form of adoptive cell therapy, a crucial part of the therapeutic process is the positive selection of transduced T-cells *in vitro*. Additionally, the different lengths of the #C3 and #C6 inserts give us the possibility to adapt the length of the CAR individually depending on the targeted epitope. Hypothetically, the #C3 hinge could even be sufficient for experiments in which detection of the transduced T-cells without additional selection is required.

Nevertheless, while one reason for *off-target* activation in the new CAR construct was eliminated in this thesis and selection and detection possibilities were included, immunogenicity still represents a potential limitation to this form of therapy. Ultimately, only clinical trials can determine the actual consequences of immunogenicity of any T-cell engineering component and the hCYP4B1P+12 suicide gene could be an efficient tool to control these consequences.

4.4 Future directions of CAR therapy

ALTERNATIVE TARGETS

All alternative hinge regions tested in this work were inserted into a second generation CD19 CAR. However, chimeric antigen receptors directed at different antigens have been developed for clinical trials and the #C3 CD19 CAR and #C6 CD19 CAR developed in this thesis could be beneficial in many of them.

The search for an ideal target on the surface of acute myeloid leukemia (AML) proves to be difficult, since AML is a very heterogenic form of leukemia and many antigens are only present in subpopulations of the AML. Myeloid blasts do express myeloid specific but not

AML specific target surface antigens like CD33 or CD123. The main problem of these two possible targets is that humans can neither live without CD33+ nor without CD123+ cells.

In our work group, it has already been confirmed that the #C6 spacer domain is also functioning for MACS selection in other CARs directed against two forms of CD123 and against CD33 and does not alter the cytotoxic activity of these CAR constructs [223]. Since the expression of both antigens is not restricted to AML blasts, the potential of major adverse events resulting in toxicity and severe impairment of normal hematopoiesis is very high [224, 225]. The suicide gene tested in this thesis would increase the safety of patients treated with different CARs, potential adverse side effects such as the destruction of hematopoiesis would become a temporary problem during treatment and could be stopped by elimination of all genetically modified T-cells after therapeutic success.

An alternative target on the surface of B-cell malignancies is ROR1, a receptor expressed on prevalent B-lymphoid and epithelial cancers [226]. It is known to be expressed during embryogenesis but not on adult tissue or mature B-cells, what would be an advantage compared to CD19 [227]. For ALL and lung cancer, *in vitro* research showed that ROR-1 tumor cells did not tolerate the loss of ROR-1 on their surface [228, 229]. ROR-1 CARs against hematopoietic tumors were already successfully designed and tested in mice. The required length of the hinge region to ideally target ROR-1 on tumor cells largely depends on the selected target epitope within the ROR-1 molecule [42, 227]. While some ROR-1 epitopes can be reached with very short CARs, i.e. short hinge regions like the #C3 region, the R11 ROR-1 CAR is specific for an epitope in a more membrane proximale domain [95]. Therefore, R11 requires a longer spacer and the #C6 or #C7 hinge region could be an alternative hinge region for R11 ROR-1 CARs.

IMPROVED CONSTRUCT

The CARs that were tested in clinical trials so far were directed at a single antigen. In those trials, relapses were due to the fact that the malignant cells were mutated and did no longer express the target antigen CD19 on their surface, for example during treatment with a CAR against ALL in children [34, 87, 105, 230]. This risk of immune escape of current CAR therapies is high because only one structure is targeted and the malignant cells often exhibit marked genetic instability [231]. Administration of T-cells that express different CARs against multiple antigens or a tandem CAR that detects two epitopes might prevent such events and facilitate the detection of tumor cells with lower density of surface molecules [232, 233]. Zah *et al.* created a so-called "CD19-OR-CD20" CAR that led to cytotoxicity when either CD19 or CD20 was detected on the the target cell [234]. On the contrary, Kloss *et al.* created a

genetically modified T-cell that coexpressed two CARs against two prostate cancer antigens on their surface which were connected to the same intracellular domain [235]. This construct was only activated when both antigens were detected on a tumor cell but did not affect cells expressing either antigen alone. This approach would enhance CAR-specificity towards tumor cells and reduce the risk of *off-target* activation. These two studies highlight one major challenge that CAR T-cell therapy faces at the moment: To keep the balance between an efficient target recognition in order to cure the patient on the one hand and the dangers of *off-target* activation that could possibly harm the patient on the other hand.

Recently, alternative approaches to control CAR T-cells without a suicide gene have been developed. A so-called "ON-switch" CAR only dimerizes in the presence of a small molecule and therefore needs the presence of the targeted epitope as well as the heterodimerizing molecule to be activated. Thus, by titrating the amount of small molecule in the patient's blood, the CAR on the surface of engineered T-cells is activated or deactivated [236]. This allows for more detailed control over dose and timing of the anti-tumor response. Ultimately, the ideal mechanism of control for CAR T-cell therapy still needs to be identified and characterized more precisely in the future.

CHEAPER ALTERNATIVE

Since a single CAR cell treatment could prove curative, CAR therapies, unlike most pharmaceuticals, have the potential to be a "one and done" therapy. Therefore, costs cannot be split up into many smaller treatments. However, CAR T-cells have immense manufacturing costs and need to be individualized for every patient, this leads to very high price tags for insurances and patients. In addition, the patients need further treatment like chemotherapy and antibody infusions. It has proven to be difficult to calculate the costs of any gene therapy regime in advance.

A cheaper alternative is the use of monoclonal antibodies against antigens on the tumor cell surface. For example, Rituximab® against CD20 or Trastuzumab® against the epidermal growth receptor HER2 are already widely and successfully used in the treatment of hematologic malignancies and breast cancer, respectively [14, 237]. They do not need to be personalized, have been tested in large clinical trials and are easily available [238-240]. In addition, no immune cells need to be genetically engineered, therefore no viral gene transfer is necessary and all obstacles associated with DNA modification of cells are bypassed.

However, the monoclonal antibodies do not involve T-cells in their activation of the immune system. A T-cell engaging approach to actively point the immune system towards tumor cells

are bispecific antibodies (BsAbs) [241]. These antibodies commonly bind to a tumor cell antigen with one segment and to an effector cell with their other segment. Therefore, antitumor-activity can be enhanced by the bridging of T-cells with tumor cells in an MHC-independent way by a small molecule. The BsAb Blinatumomab® was successfully tested in studies against B-cell ALL and other lymphomas and received FDA approval in 2014 [242]. The bispecific antibody consists of two single-chain variable fragments that detect CD19, which is present on many B-cell malignancies, and CD3, which is expressed on T-cells [242]. While monotherapy with Blinatumomab® led to remission in patients with different types of lymphoma as well as ALL, the median response duration was less than a year [243, 244]. BsAbs carry the risk of immunogenicity and are not resistant to immune-evading mechanisms like antigen loss, but since BsAbs are an “off-the-shelf product”, their major advantage compared to CARs are the much lower costs.

Importantly, T-cells expressing CARs directed at the same or related antigens additionally offer the benefits of active trafficking to tumor sites. They expand *in vivo* and enhance the overall response of the immune system. Most antibodies have a rather short half-life, while CARs lead to a long-term persistence of engineered T-cells in the body, resulting in a highly amplified response and eradication of large numbers of tumor cells within weeks [47].

One principle to cut the costs of CAR therapy by making the product easily applicable to a large scale of patients is the editing of the genome of donor T-cells so that genes that normally code for the TCR are knocked out. This would limit the risk of GvHD after administration of third party (unrelated) T-cells, therefore neither individual donor-derived nor autologous T-cells would be needed any more and CARs would become so called “off-the-shelf” products. Transcription activator-like effector nucleases (TALEN®) are restriction enzymes that can be engineered to cut specific sequences of DNA [245, 246]. Poirot *et al.* used electrocorporated TALEN® mRNA to functionally inactivate genes coding for the TCR and CD52, the target of Alemtuzumab, a lymphodepleting immunosuppressive chemotherapeutic [247]. These T-cells were then equipped with a CD19 CAR and efficiently fought leukemic cells in murine models. Without TCR, no Graft versus Host effect was induced by the CAR T-cells. Since they did not express CD52, Alemtuzumab targeting other white blood cells could be administered simultaneously to enhance the engraftment of these engineered T-cells. In this context, the idea of an emergency stop like the hCYP4B1P+12 suicide gene to stop therapy appears very attractive if any form of immune rejection appears despite TCR depletion. In addition, since the 3rd party T-cells are a potential immune risk, it is advisable to infuse a CAR T-cell positive population without TCR that has been separated before administration.

Ongoing international trials use the TALEN® system by Collectis to create universal allogenic CD19 CARs without TCR and CD52 gene for patients with relapsed or refractory CD19+ B-ALL [248, 249]. These “UCART19” T-cells are additionally engineered to express the previously mentioned suicide gene RQR8 as a safety switch and therefore can be eliminated by the infusion of Rituximab into the patient’s blood [117]. Two children treated with UCART19 as a “bridge to transplant” achieved molecular remission and remained in remission after allogenic stem cell transplantation with a follow-up of 24 months [250]. The ongoing phase I trial (NCT02808442) is supposed to continue until March 2020 and preliminary results showed no serious GvHD [248]. This approach would therefore combine the idea of “off-the-shelf” CARs with a suicide gene system as a “safety switch”.

In the long term, a combination of different control strategies for CAR T-cells might lead to “smart T-cells” with individual exogenous control over their key therapeutic features. Ultimately, the future of CAR therapy will depend on the successful development and implementation of CAR T-cells with increasing safety and cost efficiency.

5 BIBLIOGRAPHY

1. Hanahan, D. and R.A. Weinberg, *The hallmarks of cancer*. Cell, 2000. **100**(1): p. 57-70.
2. Hanahan, D. and R.A. Weinberg, *Hallmarks of cancer: the next generation*. Cell, 2011. **144**(5): p. 646-74.
3. Teng, M.W., J.B. Swann, C.M. Koebel, R.D. Schreiber, and M.J. Smyth, *Immune-mediated dormancy: an equilibrium with cancer*. J Leukoc Biol, 2008. **84**(4): p. 988-93.
4. Kim, R., M. Emi, and K. Tanabe, *Cancer immunoediting from immune surveillance to immune escape*. Immunology, 2007. **121**(1): p. 1-14.
5. Vitale, M., G. Pelusi, B. Taroni, G. Gobbi, C. Micheloni, R. Rezzani, et al., *HLA class I antigen down-regulation in primary ovary carcinoma lesions: association with disease stage*. Clin Cancer Res, 2005. **11**(1): p. 67-72.
6. Kurd, N. and E.A. Robey, *T-cell selection in the thymus: a spatial and temporal perspective*. Immunol Rev, 2016. **271**(1): p. 114-26.
7. Perry, J.S. and C.S. Hsieh, *Development of T-cell tolerance utilizes both cell-autonomous and cooperative presentation of self-antigen*. Immunol Rev, 2016. **271**(1): p. 141-55.
8. Shurin, G.V., V. Gerein, M.T. Lotze, and E.M. Barksdale, Jr., *Apoptosis induced in T cells by human neuroblastoma cells: role of Fas ligand*. Nat Immun, 1998. **16**(5-6): p. 263-74.
9. Pardoll, D.M., *The blockade of immune checkpoints in cancer immunotherapy*. Nat Rev Cancer, 2012. **12**(4): p. 252-64.
10. Mougiakakos, D., A. Choudhury, A. Lladser, R. Kiessling, and C.C. Johansson, *Regulatory T cells in cancer*. Adv Cancer Res, 2010. **107**: p. 57-117.
11. Coley, W.B., *The treatment of malignant tumors by repeated inoculations of erysipelas. With a report of ten original cases. 1893*. Clin Orthop Relat Res, 1991(262): p. 3-11.
12. Pardoll, D., *Does the immune system see tumors as foreign or self?* Annu Rev Immunol, 2003. **21**: p. 807-39.
13. Vigneron, N. and B.J. Van den Eynde, *Insights into the processing of MHC class I ligands gained from the study of human tumor epitopes*. Cell Mol Life Sci, 2011. **68**(9): p. 1503-20.
14. Anderson, D.R., A. Grillo-Lopez, C. Varns, K.S. Chambers, and N. Hanna, *Targeted anti-cancer therapy using rituximab, a chimaeric anti-CD20 antibody (IDEC-C2B8) in the treatment of non-Hodgkin's B-cell lymphoma*. Biochem Soc Trans, 1997. **25**(2): p. 705-8.
15. Chatenoud, L. and J.A. Bluestone, *CD3-specific antibodies: a portal to the treatment of autoimmunity*. Nat Rev Immunol, 2007. **7**(8): p. 622-32.
16. Arnaud, P., *[The interferons: pharmacology, mechanism of action, tolerance and side effects]*. Rev Med Interne, 2002. **23 Suppl 4**: p. 449s-458s.
17. Talpaz, M., R. Hehlmann, A. Quintas-Cardama, J. Mercer, and J. Cortes, *Re-emergence of interferon-alpha in the treatment of chronic myeloid leukemia*. Leukemia, 2013. **27**(4): p. 803-12.
18. Simonsson, B., H. Hjorth-Hansen, O.W. Bjerrum, and K. Porkka, *Interferon alpha for treatment of chronic myeloid leukemia*. Curr Drug Targets, 2011. **12**(3): p. 420-8.

19. Hansel, T.T., H. Kropshofer, T. Singer, J.A. Mitchell, and A.J. George, *The safety and side effects of monoclonal antibodies*. Nat Rev Drug Discov, 2010. **9**(4): p. 325-38.
20. Sleijfer, S., M. Bannink, A.R. Van Gool, W.H. Kruit, and G. Stoter, *Side effects of interferon-alpha therapy*. Pharm World Sci, 2005. **27**(6): p. 423-31.
21. Rosenberg, S.A., N.P. Restifo, J.C. Yang, R.A. Morgan, and M.E. Dudley, *Adoptive cell transfer: a clinical path to effective cancer immunotherapy*. Nat Rev Cancer, 2008. **8**(4): p. 299-308.
22. Dotti, G., S. Gottschalk, B. Savoldo, and M.K. Brenner, *Design and development of therapies using chimeric antigen receptor-expressing T cells*. Immunol Rev, 2014. **257**(1): p. 107-26.
23. Besser, M.J., R. Shapira-Frommer, A.J. Treves, D. Zippel, O. Itzhaki, L. Hershkovitz, et al., *Clinical responses in a phase II study using adoptive transfer of short-term cultured tumor infiltration lymphocytes in metastatic melanoma patients*. Clin Cancer Res, 2010. **16**(9): p. 2646-55.
24. Rosenberg, S.A., J.C. Yang, R.M. Sherry, U.S. Kammula, M.S. Hughes, G.Q. Phan, et al., *Durable complete responses in heavily pretreated patients with metastatic melanoma using T-cell transfer immunotherapy*. Clin Cancer Res, 2011. **17**(13): p. 4550-7.
25. Coccoris, M., T. Straetemans, C. Govers, C. Lamers, S. Sleijfer, and R. Debets, *T cell receptor (TCR) gene therapy to treat melanoma: lessons from clinical and preclinical studies*. Expert Opin Biol Ther, 2010. **10**(4): p. 547-62.
26. Karpanen, T. and J. Olweus, *T-cell receptor gene therapy--ready to go viral?* Mol Oncol, 2015. **9**(10): p. 2019-42.
27. Schmitt, T.M., D.H. Aggen, I.M. Stromnes, M.L. Dossett, S.A. Richman, D.M. Kranz, et al., *Enhanced-affinity murine T-cell receptors for tumor/self-antigens can be safe in gene therapy despite surpassing the threshold for thymic selection*. Blood, 2013. **122**(3): p. 348-56.
28. Bendle, G.M., C. Linnemann, A.I. Hooijkaas, L. Bies, M.A. de Witte, A. Jorritsma, et al., *Lethal graft-versus-host disease in mouse models of T cell receptor gene therapy*. Nat Med, 2010. **16**(5): p. 565-70, 1p following 570.
29. van Loenen, M.M., R. de Boer, A.L. Amir, R.S. Hagedoorn, G.L. Volbeda, R. Willemze, et al., *Mixed T cell receptor dimers harbor potentially harmful neoreactivity*. Proc Natl Acad Sci U S A, 2010. **107**(24): p. 10972-7.
30. Sadelain, M., R. Brentjens, and I. Riviere, *The promise and potential pitfalls of chimeric antigen receptors*. Curr Opin Immunol, 2009. **21**(2): p. 215-23.
31. Sadelain, M., I. Riviere, and R. Brentjens, *Targeting tumours with genetically enhanced T lymphocytes*. Nat Rev Cancer, 2003. **3**(1): p. 35-45.
32. Seliger, B., *Different regulation of MHC class I antigen processing components in human tumors*. J Immunotoxicol, 2008. **5**(4): p. 361-7.
33. Porter, D.L., B.L. Levine, M. Kalos, A. Bagg, and C.H. June, *Chimeric antigen receptor-modified T cells in chronic lymphoid leukemia*. N Engl J Med, 2011. **365**(8): p. 725-33.
34. Maude, S.L., N. Frey, P.A. Shaw, R. Aplenc, D.M. Barrett, N.J. Bunin, et al., *Chimeric antigen receptor T cells for sustained remissions in leukemia*. N Engl J Med, 2014. **371**(16): p. 1507-17.
35. Kochenderfer, J.N., M.E. Dudley, S.H. Kassim, R.P. Somerville, R.O. Carpenter, M. Stetler-Stevenson, et al., *Chemotherapy-refractory diffuse large B-cell lymphoma and*

- indolent B-cell malignancies can be effectively treated with autologous T cells expressing an anti-CD19 chimeric antigen receptor.* J Clin Oncol, 2015. **33**(6): p. 540-9.
36. Fujita, Y., C.M. Rooney, and H.E. Heslop, *Adoptive cellular immunotherapy for viral diseases.* Bone Marrow Transplant, 2008. **41**(2): p. 193-8.
37. Chmielewski, M. and H. Abken, *TRUCKs: the fourth generation of CARs.* Expert Opin Biol Ther, 2015. **15**(8): p. 1145-54.
38. Mitsuyasu, R.T., P.A. Anton, S.G. Deeks, D.T. Scadden, E. Connick, M.T. Downs, et al., *Prolonged survival and tissue trafficking following adoptive transfer of CD4zeta gene-modified autologous CD4(+) and CD8(+) T cells in human immunodeficiency virus-infected subjects.* Blood, 2000. **96**(3): p. 785-93.
39. Roberts, M.R., L. Qin, D. Zhang, D.H. Smith, A.C. Tran, T.J. Dull, et al., *Targeting of human immunodeficiency virus-infected cells by CD8+ T lymphocytes armed with universal T-cell receptors.* Blood, 1994. **84**(9): p. 2878-89.
40. Kumaresan, P.R., P.R. Manuri, N.D. Albert, S. Maiti, H. Singh, T. Mi, et al., *Bioengineering T cells to target carbohydrate to treat opportunistic fungal infection.* Proc Natl Acad Sci U S A, 2014. **111**(29): p. 10660-5.
41. Krebs, K., N. Bottinger, L.R. Huang, M. Chmielewski, S. Arzberger, G. Gasteiger, et al., *T cells expressing a chimeric antigen receptor that binds hepatitis B virus envelope proteins control virus replication in mice.* Gastroenterology, 2013. **145**(2): p. 456-65.
42. Hudecek, M., M.T. Lupo-Stanghellini, P.L. Kosasih, D. Sommermeyer, M.C. Jensen, C. Rader, et al., *Receptor affinity and extracellular domain modifications affect tumor recognition by ROR1-specific chimeric antigen receptor T cells.* Clin Cancer Res, 2013. **19**(12): p. 3153-64.
43. Beckman, R.A., L.M. Weiner, and H.M. Davis, *Antibody constructs in cancer therapy: protein engineering strategies to improve exposure in solid tumors.* Cancer, 2007. **109**(2): p. 170-9.
44. Chmielewski, M., A. Hombach, C. Heuser, G.P. Adams, and H. Abken, *T cell activation by antibody-like immunoreceptors: increase in affinity of the single-chain fragment domain above threshold does not increase T cell activation against antigen-positive target cells but decreases selectivity.* J Immunol, 2004. **173**(12): p. 7647-53.
45. Moritz, D. and B. Groner, *A spacer region between the single chain antibody- and the CD3 zeta-chain domain of chimeric T cell receptor components is required for efficient ligand binding and signaling activity.* Gene Ther, 1995. **2**(8): p. 539-46.
46. Guest, R.D., R.E. Hawkins, N. Kirillova, E.J. Cheadle, J. Arnold, A. O'Neill, et al., *The role of extracellular spacer regions in the optimal design of chimeric immune receptors: evaluation of four different scFvs and antigens.* J Immunother, 2005. **28**(3): p. 203-11.
47. Kalos, M., B.L. Levine, D.L. Porter, S. Katz, S.A. Grupp, A. Bagg, et al., *T cells with chimeric antigen receptors have potent antitumor effects and can establish memory in patients with advanced leukemia.* Sci Transl Med, 2011. **3**(95): p. 95ra73.
48. Savoldo, B., C.A. Ramos, E. Liu, M.P. Mims, M.J. Keating, G. Carrum, et al., *CD28 costimulation improves expansion and persistence of chimeric antigen receptor-modified T cells in lymphoma patients.* J Clin Invest, 2011. **121**(5): p. 1822-6.
49. Jensen, M.C., L. Popplewell, L.J. Cooper, D. DiGiusto, M. Kalos, J.R. Ostberg, et al., *Antitransgene rejection responses contribute to attenuated persistence of adoptively transferred CD20/CD19-specific chimeric antigen receptor redirected T cells in humans.* Biol Blood Marrow Transplant, 2010. **16**(9): p. 1245-56.

50. Cruz, C.R., K.P. Micklethwaite, B. Savoldo, C.A. Ramos, S. Lam, S. Ku, et al., *Infusion of donor-derived CD19-redirected virus-specific T cells for B-cell malignancies relapsed after allogeneic stem cell transplant: a phase 1 study*. *Blood*, 2013. **122**(17): p. 2965-73.
51. Campana, D., H. Schwarz, and C. Imai, *4-1BB chimeric antigen receptors*. *Cancer J*, 2014. **20**(2): p. 134-40.
52. Haynes, N.M., M.B. Snook, J.A. Trapani, L. Cerruti, S.M. Jane, M.J. Smyth, et al., *Redirecting mouse CTL against colon carcinoma: superior signaling efficacy of single-chain variable domain chimeras containing TCR-zeta vs Fc epsilon RI-gamma*. *J Immunol*, 2001. **166**(1): p. 182-7.
53. Brocker, T. and K. Karjalainen, *Adoptive tumor immunity mediated by lymphocytes bearing modified antigen-specific receptors*. *Adv Immunol*, 1998. **68**: p. 257-69.
54. Brocker, T., *Chimeric Fv-zeta or Fv-epsilon receptors are not sufficient to induce activation or cytokine production in peripheral T cells*. *Blood*, 2000. **96**(5): p. 1999-2001.
55. Hombach, A., D. Sent, C. Schneider, C. Heuser, D. Koch, C. Pohl, et al., *T-cell activation by recombinant receptors: CD28 costimulation is required for interleukin 2 secretion and receptor-mediated T-cell proliferation but does not affect receptor-mediated target cell lysis*. *Cancer Res*, 2001. **61**(5): p. 1976-82.
56. Hombach, A., A. Wierzchowiec, T. Marquardt, C. Heuser, L. Usai, C. Pohl, et al., *Tumor-specific T cell activation by recombinant immunoreceptors: CD3 zeta signaling and CD28 costimulation are simultaneously required for efficient IL-2 secretion and can be integrated into one combined CD28/CD3 zeta signaling receptor molecule*. *J Immunol*, 2001. **167**(11): p. 6123-31.
57. Beecham, E.J., Q. Ma, R. Ripley, and R.P. Junghans, *Coupling CD28 co-stimulation to immunoglobulin T-cell receptor molecules: the dynamics of T-cell proliferation and death*. *J Immunother*, 2000. **23**(6): p. 631-42.
58. Maher, J., R.J. Brentjens, G. Gunset, I. Riviere, and M. Sadelain, *Human T-lymphocyte cytotoxicity and proliferation directed by a single chimeric TCRzeta /CD28 receptor*. *Nat Biotechnol*, 2002. **20**(1): p. 70-5.
59. Altvater, B., S. Landmeier, S. Pscherer, J. Temme, H. Juergens, M. Pule, et al., *2B4 (CD244) signaling via chimeric receptors costimulates tumor-antigen specific proliferation and in vitro expansion of human T cells*. *Cancer Immunol Immunother*, 2009. **58**(12): p. 1991-2001.
60. Brentjens, R.J., E. Santos, Y. Nikhamin, R. Yeh, M. Matsushita, K. La Perle, et al., *Genetically targeted T cells eradicate systemic acute lymphoblastic leukemia xenografts*. *Clin Cancer Res*, 2007. **13**(18 Pt 1): p. 5426-35.
61. Hombach, A.A., M. Chmielewski, G. Rappl, and H. Abken, *Adoptive immunotherapy with redirected T cells produces CCR7- cells that are trapped in the periphery and benefit from combined CD28-OX40 costimulation*. *Hum Gene Ther*, 2013. **24**(3): p. 259-69.
62. Hombach, A.A., J. Heiders, M. Foppe, M. Chmielewski, and H. Abken, *OX40 costimulation by a chimeric antigen receptor abrogates CD28 and IL-2 induced IL-10 secretion by redirected CD4(+) T cells*. *Oncoimmunology*, 2012. **1**(4): p. 458-466.
63. Redmond, W.L., C.E. Ruby, and A.D. Weinberg, *The role of OX40-mediated co-stimulation in T-cell activation and survival*. *Crit Rev Immunol*, 2009. **29**(3): p. 187-201.

64. Chmielewski, M., C. Kopecky, A.A. Hombach, and H. Abken, *IL-12 release by engineered T cells expressing chimeric antigen receptors can effectively Muster an antigen-independent macrophage response on tumor cells that have shut down tumor antigen expression*. *Cancer Res*, 2011. **71**(17): p. 5697-706.
65. Cheadle, E.J., R.E. Hawkins, H. Batha, D.G. Rothwell, G. Ashton, and D.E. Gilham, *Eradication of established B-cell lymphoma by CD19-specific murine T cells is dependent on host lymphopenic environment and can be mediated by CD4+ and CD8+ T cells*. *J Immunother*, 2009. **32**(3): p. 207-18.
66. Antony, P.A., C.A. Piccirillo, A. Akpınarli, S.E. Finkelstein, P.J. Speiss, D.R. Surman, et al., *CD8+ T cell immunity against a tumor/self-antigen is augmented by CD4+ T helper cells and hindered by naturally occurring T regulatory cells*. *J Immunol*, 2005. **174**(5): p. 2591-601.
67. Gattinoni, L., S.E. Finkelstein, C.A. Klebanoff, P.A. Antony, D.C. Palmer, P.J. Spiess, et al., *Removal of homeostatic cytokine sinks by lymphodepletion enhances the efficacy of adoptively transferred tumor-specific CD8+ T cells*. *J Exp Med*, 2005. **202**(7): p. 907-12.
68. Dudley, M.E., J.R. Wunderlich, P.F. Robbins, J.C. Yang, P. Hwu, D.J. Schwartzentruber, et al., *Cancer regression and autoimmunity in patients after clonal repopulation with antitumor lymphocytes*. *Science*, 2002. **298**(5594): p. 850-4.
69. Muranski, P., A. Boni, C. Wrzesinski, D.E. Citrin, S.A. Rosenberg, R. Childs, et al., *Increased intensity lymphodepletion and adoptive immunotherapy--how far can we go?* *Nat Clin Pract Oncol*, 2006. **3**(12): p. 668-81.
70. Bear, A.S., R.A. Morgan, K. Cornetta, C.H. June, G. Binder-Scholl, M.E. Dudley, et al., *Replication-competent retroviruses in gene-modified T cells used in clinical trials: is it time to revise the testing requirements?* *Mol Ther*, 2012. **20**(2): p. 246-9.
71. Baum, C., J. Dullmann, Z. Li, B. Fehse, J. Meyer, D.A. Williams, et al., *Side effects of retroviral gene transfer into hematopoietic stem cells*. *Blood*, 2003. **101**(6): p. 2099-114.
72. Cavalieri, S., S. Cazzaniga, M. Geuna, Z. Magnani, C. Bordignon, L. Naldini, et al., *Human T lymphocytes transduced by lentiviral vectors in the absence of TCR activation maintain an intact immune competence*. *Blood*, 2003. **102**(2): p. 497-505.
73. Morgan, D.A., F.W. Ruscetti, and R. Gallo, *Selective in vitro growth of T lymphocytes from normal human bone marrows*. *Science*, 1976. **193**(4257): p. 1007-8.
74. Smyth, M.J. and J.A. Trapani, *Granzymes: exogenous proteinases that induce target cell apoptosis*. *Immunol Today*, 1995. **16**(4): p. 202-6.
75. Cartellieri, M., M. Bachmann, A. Feldmann, C. Bippes, S. Stamova, R. Wehner, et al., *Chimeric antigen receptor-engineered T cells for immunotherapy of cancer*. *J Biomed Biotechnol*, 2010. **2010**: p. 956304.
76. Kochenderfer, J.N., M.E. Dudley, R.O. Carpenter, S.H. Kassim, J.J. Rose, W.G. Telford, et al., *Donor-derived CD19-targeted T cells cause regression of malignancy persisting after allogeneic hematopoietic stem cell transplantation*. *Blood*, 2013. **122**(25): p. 4129-39.
77. Anwer, F., A.A. Shaikat, U. Zahid, M. Husnain, A. McBride, D. Persky, et al., *Donor origin CAR T cells: graft versus malignancy effect without GVHD, a systematic review*. *Immunotherapy*, 2017. **9**(2): p. 123-130.
78. Till, B.G., M.C. Jensen, J. Wang, E.Y. Chen, B.L. Wood, H.A. Greisman, et al., *Adoptive immunotherapy for indolent non-Hodgkin lymphoma and mantle cell lymphoma using genetically modified autologous CD20-specific T cells*. *Blood*, 2008. **112**(6): p. 2261-71.

79. Haso, W., D.W. Lee, N.N. Shah, M. Stetler-Stevenson, C.M. Yuan, I.H. Pastan, et al., *Anti-CD22-chimeric antigen receptors targeting B-cell precursor acute lymphoblastic leukemia*. *Blood*, 2013. **121**(7): p. 1165-74.
80. Mansfield, E., P. Amlot, I. Pastan, and D.J. FitzGerald, *Recombinant RFB4 immunotoxins exhibit potent cytotoxic activity for CD22-bearing cells and tumors*. *Blood*, 1997. **90**(5): p. 2020-6.
81. FitzGerald, D.J., A.S. Wayne, R.J. Kreitman, and I. Pastan, *Treatment of hematologic malignancies with immunotoxins and antibody-drug conjugates*. *Cancer Res*, 2011. **71**(20): p. 6300-9.
82. Blanc, V., A. Bousseau, A. Caron, C. Carrez, R.J. Lutz, and J.M. Lambert, *SAR3419: an anti-CD19-Maytansinoid Immunoconjugate for the treatment of B-cell malignancies*. *Clin Cancer Res*, 2011. **17**(20): p. 6448-58.
83. Ramos, C.A., B. Savoldo, and G. Dotti, *CD19-CAR trials*. *Cancer J*, 2014. **20**(2): p. 112-8.
84. Scheuermann, R.H. and E. Racila, *CD19 antigen in leukemia and lymphoma diagnosis and immunotherapy*. *Leuk Lymphoma*, 1995. **18**(5-6): p. 385-97.
85. Medicine, U.S.N.L.o. *Clinical Trials with CD19 Chimeric antigen receptors*. [cited 2019 6th March]; Available from: <https://clinicaltrials.gov/ct2/results?cond=&term=Chimeric+antigen+receptors+CD19&cntry=&state=&city=&dist=>.
86. Brentjens, R.J., J.B. Latouche, E. Santos, F. Marti, M.C. Gong, C. Lyddane, et al., *Eradication of systemic B-cell tumors by genetically targeted human T lymphocytes co-stimulated by CD80 and interleukin-15*. *Nat Med*, 2003. **9**(3): p. 279-86.
87. Grupp, S.A., M. Kalos, D. Barrett, R. Aplenc, D.L. Porter, S.R. Rheingold, et al., *Chimeric antigen receptor-modified T cells for acute lymphoid leukemia*. *N Engl J Med*, 2013. **368**(16): p. 1509-18.
88. Kochenderfer, J.N., M.E. Dudley, S.A. Feldman, W.H. Wilson, D.E. Spaner, I. Maric, et al., *B-cell depletion and remissions of malignancy along with cytokine-associated toxicity in a clinical trial of anti-CD19 chimeric-antigen-receptor-transduced T cells*. *Blood*, 2012. **119**(12): p. 2709-20.
89. Brentjens, R.J., M.L. Davila, I. Riviere, J. Park, X. Wang, L.G. Cowell, et al., *CD19-targeted T cells rapidly induce molecular remissions in adults with chemotherapy-refractory acute lymphoblastic leukemia*. *Sci Transl Med*, 2013. **5**(177): p. 177ra38.
90. DeFrancesco, L., *Juno's wild ride*. *Nat Biotechnol*, 2016. **34**(8): p. 793.
91. DeFrancesco, L., *CAR-T's forge ahead, despite Juno deaths*. *Nat Biotechnol*, 2017. **35**(1): p. 6-7.
92. Hartmann, J., M. Schussler-Lenz, A. Bondanza, and C.J. Buchholz, *Clinical development of CAR T cells-challenges and opportunities in translating innovative treatment concepts*. *EMBO Mol Med*, 2017. **9**(9): p. 1183-1197.
93. Casucci, M., R.E. Hawkins, G. Dotti, and A. Bondanza, *Overcoming the toxicity hurdles of genetically targeted T cells*. *Cancer Immunol Immunother*, 2015. **64**(1): p. 123-30.
94. Hombach, A., A.A. Hombach, and H. Abken, *Adoptive immunotherapy with genetically engineered T cells: modification of the IgG1 Fc 'spacer' domain in the extracellular moiety of chimeric antigen receptors avoids 'off-target' activation and unintended initiation of an innate immune response*. *Gene Ther*, 2010. **17**(10): p. 1206-13.

95. Hudecek, M., D. Sommermeyer, P.L. Kosasih, A. Silva-Benedict, L. Liu, C. Rader, et al., *The nonsignaling extracellular spacer domain of chimeric antigen receptors is decisive for in vivo antitumor activity*. *Cancer Immunol Res*, 2015. **3**(2): p. 125-35.
96. Linette, G.P., E.A. Stadtmauer, M.V. Maus, A.P. Rapoport, B.L. Levine, L. Emery, et al., *Cardiovascular toxicity and titin cross-reactivity of affinity-enhanced T cells in myeloma and melanoma*. *Blood*, 2013. **122**(6): p. 863-71.
97. Lamers, C.H., S. Sleijfer, S. van Steenberg, P. van Elzakker, B. van Krimpen, C. Groot, et al., *Treatment of metastatic renal cell carcinoma with CAIX CAR-engineered T cells: clinical evaluation and management of on-target toxicity*. *Mol Ther*, 2013. **21**(4): p. 904-12.
98. Morgan, R.A., J.C. Yang, M. Kitano, M.E. Dudley, C.M. Laurencot, and S.A. Rosenberg, *Case report of a serious adverse event following the administration of T cells transduced with a chimeric antigen receptor recognizing ERBB2*. *Mol Ther*, 2010. **18**(4): p. 843-51.
99. Brudno, J.N. and J.N. Kochenderfer, *Toxicities of chimeric antigen receptor T cells: recognition and management*. *Blood*, 2016. **127**(26): p. 3321-30.
100. Janeway, C. and P. Travers, *Immunobiology : the immune system in health and disease*. 2nd ed. 1996, London ; San Francisco ; New York: Current Biology ; Garland Pub.
101. Morgan, R.A., N. Chinnasamy, D. Abate-Daga, A. Gros, P.F. Robbins, Z. Zheng, et al., *Cancer regression and neurological toxicity following anti-MAGE-A3 TCR gene therapy*. *J Immunother*, 2013. **36**(2): p. 133-51.
102. Maus, M.V., S.A. Grupp, D.L. Porter, and C.H. June, *Antibody-modified T cells: CARs take the front seat for hematologic malignancies*. *Blood*, 2014. **123**(17): p. 2625-35.
103. Song, D.G., Q. Ye, M. Poussin, L. Liu, M. Figini, and D.J. Powell, Jr., *A fully human chimeric antigen receptor with potent activity against cancer cells but reduced risk for off-tumor toxicity*. *Oncotarget*, 2015. **6**(25): p. 21533-46.
104. Davila, M.L., I. Riviere, X. Wang, S. Bartido, J. Park, K. Curran, et al., *Efficacy and toxicity management of 19-28z CAR T cell therapy in B cell acute lymphoblastic leukemia*. *Sci Transl Med*, 2014. **6**(224): p. 224ra25.
105. Lee, D.W., J.N. Kochenderfer, M. Stetler-Stevenson, Y.K. Cui, C. Delbrook, S.A. Feldman, et al., *T cells expressing CD19 chimeric antigen receptors for acute lymphoblastic leukaemia in children and young adults: a phase 1 dose-escalation trial*. *Lancet*, 2015. **385**(9967): p. 517-528.
106. Ertl, H.C., J. Zaia, S.A. Rosenberg, C.H. June, G. Dotti, J. Kahn, et al., *Considerations for the clinical application of chimeric antigen receptor T cells: observations from a recombinant DNA Advisory Committee Symposium held June 15, 2010*. *Cancer Res*, 2011. **71**(9): p. 3175-81.
107. Ciceri, F., C. Bonini, C. Gallo-Stampino, and C. Bordignon, *Modulation of GvHD by suicide-gene transduced donor T lymphocytes: clinical applications in mismatched transplantation*. *Cytotherapy*, 2005. **7**(2): p. 144-9.
108. Tiberghien, P., *"Suicide" gene for the control of graft-versus-host disease*. *Curr Opin Hematol*, 1998. **5**(6): p. 478-82.
109. Di Stasi, A., S.K. Tey, G. Dotti, Y. Fujita, A. Kennedy-Nasser, C. Martinez, et al., *Inducible apoptosis as a safety switch for adoptive cell therapy*. *N Engl J Med*, 2011. **365**(18): p. 1673-83.
110. Ciceri, F., C. Bonini, M.T. Stanghellini, A. Bondanza, C. Traversari, M. Salomoni, et al., *Infusion of suicide-gene-engineered donor lymphocytes after family haploidentical*

- haemopoietic stem-cell transplantation for leukaemia (the TK007 trial): a non-randomised phase I-II study*. *Lancet Oncol*, 2009. **10**(5): p. 489-500.
111. Immonen, A., M. Vapalahti, K. Tyynela, H. Hurskainen, A. Sandmair, R. Vanninen, et al., *AdvHSV-tk gene therapy with intravenous ganciclovir improves survival in human malignant glioma: a randomised, controlled study*. *Mol Ther*, 2004. **10**(5): p. 967-72.
112. Shalev, M., D. Kadmon, B.S. Teh, E.B. Butler, E. Aguilar-Cordova, T.C. Thompson, et al., *Suicide gene therapy toxicity after multiple and repeat injections in patients with localized prostate cancer*. *J Urol*, 2000. **163**(6): p. 1747-50.
113. Berger, C., M.E. Flowers, E.H. Warren, and S.R. Riddell, *Analysis of transgene-specific immune responses that limit the in vivo persistence of adoptively transferred HSV-TK-modified donor T cells after allogeneic hematopoietic cell transplantation*. *Blood*, 2006. **107**(6): p. 2294-302.
114. Bonini, C., G. Ferrari, S. Verzeletti, P. Servida, E. Zappone, L. Ruggieri, et al., *HSV-TK gene transfer into donor lymphocytes for control of allogeneic graft-versus-leukemia*. *Science*, 1997. **276**(5319): p. 1719-24.
115. Fan, L., K.W. Freeman, T. Khan, E. Pham, and D.M. Spencer, *Improved artificial death switches based on caspases and FADD*. *Hum Gene Ther*, 1999. **10**(14): p. 2273-85.
116. Tey, S.K., G. Dotti, C.M. Rooney, H.E. Heslop, and M.K. Brenner, *Inducible caspase 9 suicide gene to improve the safety of allodepleted T cells after haploidentical stem cell transplantation*. *Biol Blood Marrow Transplant*, 2007. **13**(8): p. 913-24.
117. Philip, B., E. Kokalaki, L. Mekkaoui, S. Thomas, K. Straathof, B. Flutter, et al., *A highly compact epitope-based marker/suicide gene for easier and safer T-cell therapy*. *Blood*, 2014. **124**(8): p. 1277-87.
118. Hasler, J.A., *Pharmacogenetics of cytochromes P450*. *Mol Aspects Med*, 1999. **20**(1-2): p. 12-24, 25-137.
119. Nelson, D.R., *Progress in tracing the evolutionary paths of cytochrome P450*. *Biochim Biophys Acta*, 2011. **1814**(1): p. 14-8.
120. Baer, B.R. and A.E. Rettie, *CYP4B1: an enigmatic P450 at the interface between xenobiotic and endobiotic metabolism*. *Drug Metab Rev*, 2006. **38**(3): p. 451-76.
121. Robertson, I.G., C. Serabjit-Singh, J.E. Croft, and R.M. Philpot, *The relationship between increases in the hepatic content of cytochrome P-450, form 5, and in the metabolism of aromatic amines to mutagenic products following treatment of rabbits with phenobarbital*. *Mol Pharmacol*, 1983. **24**(1): p. 156-62.
122. Vanderslice, R.R., J.A. Boyd, T.E. Eling, and R.M. Philpot, *The cytochrome P-450 monooxygenase system of rabbit bladder mucosa: enzyme components and isozyme 5-dependent metabolism of 2-aminofluorene*. *Cancer Res*, 1985. **45**(11 Pt 2): p. 5851-8.
123. Imaoka, S., T. Hiroi, Y. Tamura, H. Yamazaki, T. Shimada, M. Komori, et al., *Mutagenic activation of 3-methoxy-4-aminoazobenzene by mouse renal cytochrome P450 CYP4B1: cloning and characterization of mouse CYP4B1*. *Arch Biochem Biophys*, 1995. **321**(1): p. 255-62.
124. Wilson, B.J., D.T. Yang, and M.R. Boyd, *Toxicity of mould-damaged sweet potatoes (*Ipomoea batatas*)*. *Nature*, 1970. **227**(5257): p. 521-2.
125. Hansen, A.A., *Two Fatal Cases of Potato Poisoning*. *Science*, 1925. **61**(1578): p. 340-1.
126. Verschoyle, R.D., R.M. Philpot, C.R. Wolf, and D. Dinsdale, *CYP4B1 activates 4-ipomeanol in rat lung*. *Toxicol Appl Pharmacol*, 1993. **123**(2): p. 193-8.

127. Christian, M.C., R.E. Wittes, B. Leyland-Jones, T.L. McLemore, A.C. Smith, C.K. Grieshaber, et al., *4-Ipomeanol: a novel investigational new drug for lung cancer*. J Natl Cancer Inst, 1989. **81**(15): p. 1133-43.
128. Boyd, M.R., *Role of metabolic activation in the pathogenesis of chemically induced pulmonary disease: mechanism of action of the lung-toxic furan, 4-ipomeanol*. Environ Health Perspect, 1976. **16**: p. 127-38.
129. Falzon, M., J.B. McMahon, H.M. Schuller, and M.R. Boyd, *Metabolic activation and cytotoxicity of 4-ipomeanol in human non-small cell lung cancer lines*. Cancer Res, 1986. **46**(7): p. 3484-9.
130. Rowinsky, E.K., D.A. Noe, D.S. Ettinger, M.C. Christian, B.G. Lubejko, E.K. Fishman, et al., *Phase I and pharmacological study of the pulmonary cytotoxin 4-ipomeanol on a single dose schedule in lung cancer patients: hepatotoxicity is dose limiting in humans*. Cancer Res, 1993. **53**(8): p. 1794-801.
131. Kasturi, V.K., M.P. Dearing, S.C. Piscitelli, E.K. Russell, G.G. Sladek, K. O'Neil, et al., *Phase I study of a five-day dose schedule of 4-Ipomeanol in patients with non-small cell lung cancer*. Clin Cancer Res, 1998. **4**(9): p. 2095-102.
132. Lakhanpal, S., R.C. Donehower, and E.K. Rowinsky, *Phase II study of 4-ipomeanol, a naturally occurring alkylating furan, in patients with advanced hepatocellular carcinoma*. Invest New Drugs, 2001. **19**(1): p. 69-76.
133. Zheng, Y.M., K.R. Henne, P. Charmley, R.B. Kim, D.G. McCarver, E.T. Cabacungan, et al., *Genotyping and site-directed mutagenesis of a cytochrome P450 meander Pro-X-Arg motif critical to CYP4B1 catalysis*. Toxicol Appl Pharmacol, 2003. **186**(2): p. 119-26.
134. Czerwinski, M., T.L. McLemore, R.M. Philpot, P.T. Nhamburo, K. Korzekwa, H.V. Gelboin, et al., *Metabolic activation of 4-ipomeanol by complementary DNA-expressed human cytochromes P-450: evidence for species-specific metabolism*. Cancer Res, 1991. **51**(17): p. 4636-8.
135. Rainov, N.G., K.U. Dobberstein, M. Sena-Esteves, U. Herrlinger, C.M. Kramm, R.M. Philpot, et al., *New prodrug activation gene therapy for cancer using cytochrome P450 4B1 and 2-aminoanthracene/4-ipomeanol*. Hum Gene Ther, 1998. **9**(9): p. 1261-73.
136. Steffens, S., S. Frank, U. Fischer, C. Heuser, K.L. Meyer, K.U. Dobberstein, et al., *Enhanced green fluorescent protein fusion proteins of herpes simplex virus type 1 thymidine kinase and cytochrome P450 4B1: applications for prodrug-activating gene therapy*. Cancer Gene Ther, 2000. **7**(5): p. 806-12.
137. Frank, S., S. Steffens, U. Fischer, A. Tlolko, N.G. Rainov, and C.M. Kramm, *Differential cytotoxicity and bystander effect of the rabbit cytochrome P450 4B1 enzyme gene by two different prodrugs: implications for pharmacogene therapy*. Cancer Gene Ther, 2002. **9**(2): p. 178-88.
138. Wiek, C., E.M. Schmidt, K. Roellecke, M. Freund, M. Nakano, E.J. Kelly, et al., *Identification of amino acid determinants in CYP4B1 for optimal catalytic processing of 4-ipomeanol*. Biochem J, 2015. **465**(1): p. 103-14.
139. Roellecke, K., E.L. Virts, R. Einholz, K.Z. Edson, B. Altvater, C. Rossig, et al., *Optimized human CYP4B1 in combination with the alkylator prodrug 4-ipomeanol serves as a novel suicide gene system for adoptive T-cell therapies*. Gene Ther, 2016. **23**(7): p. 615-26.
140. Roellecke, K., V.D. Jager, V.H. Gyurov, J.P. Kowalski, S. Mielke, A.E. Rettie, et al., *Ligand characterization of CYP4B1 isoforms modified for high-level expression in Escherichia coli and HepG2 cells*. Protein Eng Des Sel, 2017. **30**(3): p. 205-216.

141. Wilson, B.J., J.E. Garst, R.D. Linnabary, and R.B. Channell, *Perilla ketone: a potent lung toxin from the mint plant, Perilla frutescens Britton*. Science, 1977. **197**(4303): p. 573-4.
142. Garst, J.E., W.C. Wilson, N.C. Kristensen, P.C. Harrison, J.E. Corbin, J. Simon, et al., *Species susceptibility to the pulmonary toxicity of 3-furyl isoamyl ketone (perilla ketone): in vivo support for involvement of the lung monooxygenase system*. J Anim Sci, 1985. **60**(1): p. 248-57.
143. Mochizuki, H., J.P. Schwartz, K. Tanaka, R.O. Brady, and J. Reiser, *High-titer human immunodeficiency virus type 1-based vector systems for gene delivery into nondividing cells*. J Virol, 1998. **72**(11): p. 8873-83.
144. Pietschmann, T., M. Heinkelein, M. Heldmann, H. Zentgraf, A. Rethwilm, and D. Lindemann, *Foamy virus capsids require the cognate envelope protein for particle export*. J Virol, 1999. **73**(4): p. 2613-21.
145. Bukrinsky, M.I., S. Haggerty, M.P. Dempsey, N. Sharova, A. Adzhubel, L. Spitz, et al., *A nuclear localization signal within HIV-1 matrix protein that governs infection of non-dividing cells*. Nature, 1993. **365**(6447): p. 666-9.
146. Naldini, L., *Lentiviruses as gene transfer agents for delivery to non-dividing cells*. Curr Opin Biotechnol, 1998. **9**(5): p. 457-63.
147. Steffy, K. and F. Wong-Staal, *Genetic regulation of human immunodeficiency virus*. Microbiol Rev, 1991. **55**(2): p. 193-205.
148. Parolin, C., T. Dorfman, G. Palu, H. Gottlinger, and J. Sodroski, *Analysis in human immunodeficiency virus type 1 vectors of cis-acting sequences that affect gene transfer into human lymphocytes*. J Virol, 1994. **68**(6): p. 3888-95.
149. Yu, S.F., T. von Ruden, P.W. Kantoff, C. Garber, M. Seiberg, U. Ruther, et al., *Self-inactivating retroviral vectors designed for transfer of whole genes into mammalian cells*. Proc Natl Acad Sci U S A, 1986. **83**(10): p. 3194-8.
150. Iwakuma, T., Y. Cui, and L.J. Chang, *Self-inactivating lentiviral vectors with U3 and U5 modifications*. Virology, 1999. **261**(1): p. 120-32.
151. Zufferey, R., T. Dull, R.J. Mandel, A. Bukovsky, D. Quiroz, L. Naldini, et al., *Self-inactivating lentivirus vector for safe and efficient in vivo gene delivery*. J Virol, 1998. **72**(12): p. 9873-80.
152. Miyoshi, H., U. Blomer, M. Takahashi, F.H. Gage, and I.M. Verma, *Development of a self-inactivating lentivirus vector*. J Virol, 1998. **72**(10): p. 8150-7.
153. DuBridge, R.B., P. Tang, H.C. Hsia, P.M. Leong, J.H. Miller, and M.P. Calos, *Analysis of mutation in human cells by using an Epstein-Barr virus shuttle system*. Mol Cell Biol, 1987. **7**(1): p. 379-87.
154. Pear, W.S., G.P. Nolan, M.L. Scott, and D. Baltimore, *Production of high-titer helper-free retroviruses by transient transfection*. Proc Natl Acad Sci U S A, 1993. **90**(18): p. 8392-6.
155. Aden, D.P., A. Fogel, S. Plotkin, I. Damjanov, and B.B. Knowles, *Controlled synthesis of HBsAg in a differentiated human liver carcinoma-derived cell line*. Nature, 1979. **282**(5739): p. 615-6.
156. Schneider, U., H.U. Schwenk, and G. Bornkamm, *Characterization of EBV-genome negative "null" and "T" cell lines derived from children with acute lymphoblastic leukemia and leukemic transformed non-Hodgkin lymphoma*. Int J Cancer, 1977. **19**(5): p. 621-6.

157. Matsuo, Y. and H.G. Drexler, *Establishment and characterization of human B cell precursor-leukemia cell lines*. Leuk Res, 1998. **22**(7): p. 567-79.
158. Bieber, T., W. Meissner, S. Kostin, A. Niemann, and H.P. Elsasser, *Intracellular route and transcriptional competence of polyethylenimine-DNA complexes*. J Control Release, 2002. **82**(2-3): p. 441-54.
159. Cornetta, K. and W.F. Anderson, *Protamine sulfate as an effective alternative to polybrene in retroviral-mediated gene-transfer: implications for human gene therapy*. J Virol Methods, 1989. **23**(2): p. 187-94.
160. Coelen, R.J., D.G. Jose, and J.T. May, *The effect of hexadimethrine bromide (polybrene) on the infection of the primate retroviruses SSV 1/SSAV 1 and BaEV*. Arch Virol, 1983. **75**(4): p. 307-11.
161. Hanenberg, H., K. Hashino, H. Konishi, R.A. Hock, I. Kato, and D.A. Williams, *Optimization of fibronectin-assisted retroviral gene transfer into human CD34+ hematopoietic cells*. Hum Gene Ther, 1997. **8**(18): p. 2193-206.
162. Ficner, R. and R. Huber, *Refined crystal structure of phycoerythrin from *Porphyridium cruentum* at 0.23-nm resolution and localization of the gamma subunit*. Eur J Biochem, 1993. **218**(1): p. 103-6.
163. Mohr, L., N.G. Rainov, U.G. Mohr, and J.R. Wands, *Rabbit cytochrome P450 4B1: A novel prodrug activating gene for pharmacogene therapy of hepatocellular carcinoma*. Cancer Gene Ther, 2000. **7**(7): p. 1008-14.
164. Matsuura, T., *Natural Furan Derivatives .1. The Synthesis of Perillaketone*. Bulletin of the Chemical Society of Japan, 1957. **30**(4): p. 430-431.
165. Locksley, R.M., N. Killeen, and M.J. Lenardo, *The TNF and TNF receptor superfamilies: integrating mammalian biology*. Cell, 2001. **104**(4): p. 487-501.
166. Valtieri, M., R. Schiro, C. Chelucci, B. Masella, U. Testa, I. Casella, et al., *Efficient transfer of selectable and membrane reporter genes in hematopoietic progenitor and stem cells purified from human peripheral blood*. Cancer Res, 1994. **54**(16): p. 4398-404.
167. Rudoll, T., K. Phillips, S.W. Lee, S. Hull, O. Gaspar, N. Sucgang, et al., *High-efficiency retroviral vector mediated gene transfer into human peripheral blood CD4+ T lymphocytes*. Gene Ther, 1996. **3**(8): p. 695-705.
168. Skeldal, S., D. Matusica, A. Nykjaer, and E.J. Coulson, *Proteolytic processing of the p75 neurotrophin receptor: A prerequisite for signalling?: Neuronal life, growth and death signalling are crucially regulated by intra-membrane proteolysis and trafficking of p75(NTR)*. Bioessays, 2011. **33**(8): p. 614-25.
169. Huss, R., *Isolation of primary and immortalized CD34-hematopoietic and mesenchymal stem cells from various sources*. Stem Cells, 2000. **18**(1): p. 1-9.
170. Sidney, L.E., M.J. Branch, S.E. Dunphy, H.S. Dua, and A. Hopkinson, *Concise review: evidence for CD34 as a common marker for diverse progenitors*. Stem Cells, 2014. **32**(6): p. 1380-9.
171. Krause, D.S., M.J. Fackler, C.I. Civin, and W.S. May, *CD34: structure, biology, and clinical utility*. Blood, 1996. **87**(1): p. 1-13.
172. Sutherland, D.R., A.K. Stewart, and A. Keating, *CD34 antigen: molecular features and potential clinical applications*. Stem Cells, 1993. **11 Suppl 3**: p. 50-7.
173. Fehse, B., A. Richters, K. Putimtseva-Scharf, H. Klump, Z. Li, W. Ostertag, et al., *CD34 splice variant: an attractive marker for selection of gene-modified cells*. Mol Ther, 2000. **1**(5 Pt 1): p. 448-56.

174. Zanger, U.M. and M. Schwab, *Cytochrome P450 enzymes in drug metabolism: regulation of gene expression, enzyme activities, and impact of genetic variation*. *Pharmacol Ther*, 2013. **138**(1): p. 103-41.
175. Adam, M.A., N. Ramesh, A.D. Miller, and W.R. Osborne, *Internal initiation of translation in retroviral vectors carrying picornavirus 5' nontranslated regions*. *J Virol*, 1991. **65**(9): p. 4985-90.
176. Corish, P. and C. Tyler-Smith, *Attenuation of green fluorescent protein half-life in mammalian cells*. *Protein Eng*, 1999. **12**(12): p. 1035-40.
177. Yang, J., M. Liao, M. Shou, M. Jamei, K.R. Yeo, G.T. Tucker, et al., *Cytochrome p450 turnover: regulation of synthesis and degradation, methods for determining rates, and implications for the prediction of drug interactions*. *Curr Drug Metab*, 2008. **9**(5): p. 384-94.
178. Couzin-Frankel, J., *Breakthrough of the year 2013. Cancer immunotherapy*. *Science*, 2013. **342**(6165): p. 1432-3.
179. Postow, M.A., M.K. Callahan, and J.D. Wolchok, *Immune Checkpoint Blockade in Cancer Therapy*. *J Clin Oncol*, 2015. **33**(17): p. 1974-82.
180. Wolchok, J.D., J.S. Weber, M. Maio, B. Neyns, K. Harmankaya, K. Chin, et al., *Four-year survival rates for patients with metastatic melanoma who received ipilimumab in phase II clinical trials*. *Ann Oncol*, 2013. **24**(8): p. 2174-80.
181. Robert, C., A. Ribas, J.D. Wolchok, F.S. Hodi, O. Hamid, R. Kefford, et al., *Anti-programmed-death-receptor-1 treatment with pembrolizumab in ipilimumab-refractory advanced melanoma: a randomised dose-comparison cohort of a phase 1 trial*. *Lancet*, 2014. **384**(9948): p. 1109-17.
182. Administration, F.a.D. *KYMRIAH (tisagenlecleucel)*. 2017 [cited 2017 September 12th]; Available from: <https://www.fda.gov/BiologicsBloodVaccines/CellularGeneTherapyProducts/ApprovedProducts/ucm573706.htm>.
183. Administration, F.a.D. *YESCARTA (axicabtagene ciloleucel)*. 2019 [cited 2019 28th February]; Available from: <https://www.fda.gov/biologicsbloodvaccines/cellulargenetherapyproducts/approvedproducts/ucm581222.htm>.
184. Li, H., H. Wei, Y. Wang, H. Tang, and Y. Wang, *Enhanced green fluorescent protein transgenic expression in vivo is not biologically inert*. *J Proteome Res*, 2013. **12**(8): p. 3801-8.
185. Mavilio, F., G. Ferrari, S. Rossini, N. Nobili, C. Bonini, G. Casorati, et al., *Peripheral blood lymphocytes as target cells of retroviral vector-mediated gene transfer*. *Blood*, 1994. **83**(7): p. 1988-97.
186. Johnson, D., A. Lanahan, C.R. Buck, A. Sehgal, C. Morgan, E. Mercer, et al., *Expression and structure of the human NGF receptor*. *Cell*, 1986. **47**(4): p. 545-54.
187. Li, Z., J. Dullmann, B. Schiedlmeier, M. Schmidt, C. von Kalle, J. Meyer, et al., *Murine leukemia induced by retroviral gene marking*. *Science*, 2002. **296**(5567): p. 497.
188. Bonini, C., M. Grez, C. Traversari, F. Ciceri, S. Marktel, G. Ferrari, et al., *Safety of retroviral gene marking with a truncated NGF receptor*. *Nat Med*, 2003. **9**(4): p. 367-9.
189. Casucci, M., L. Falcone, B. Camisa, M. Norelli, S. Porcellini, A. Stornaiuolo, et al., *Extracellular NGFR Spacers Allow Efficient Tracking and Enrichment of Fully Functional CAR-T Cells Co-Expressing a Suicide Gene*. *Front Immunol*, 2018. **9**: p. 507.

190. Schumm, M., P. Lang, G. Taylor, S. Kuci, T. Klingebiel, H.J. Buhning, et al., *Isolation of highly purified autologous and allogeneic peripheral CD34+ cells using the CliniMACS device*. J Hematother, 1999. **8**(2): p. 209-18.
191. Nielsen, J.S. and K.M. McNagny, *Novel functions of the CD34 family*. J Cell Sci, 2008. **121**(Pt 22): p. 3683-92.
192. Simmons, D.L., A.B. Satterthwaite, D.G. Tenen, and B. Seed, *Molecular cloning of a cDNA encoding CD34, a sialomucin of human hematopoietic stem cells*. J Immunol, 1992. **148**(1): p. 267-71.
193. Satterthwaite, A.B., T.C. Burn, M.M. Le Beau, and D.G. Tenen, *Structure of the gene encoding CD34, a human hematopoietic stem cell antigen*. Genomics, 1992. **12**(4): p. 788-94.
194. Lange, C., Z. Li, L. Fang, C. Baum, and B. Fehse, *CD34 modulates the trafficking behavior of hematopoietic cells in vivo*. Stem Cells Dev, 2007. **16**(2): p. 297-304.
195. Shields, R.L., A.K. Namenuk, K. Hong, Y.G. Meng, J. Rae, J. Briggs, et al., *High resolution mapping of the binding site on human IgG1 for Fc gamma RI, Fc gamma RII, Fc gamma RIII, and FcRn and design of IgG1 variants with improved binding to the Fc gamma R*. J Biol Chem, 2001. **276**(9): p. 6591-604.
196. Armour, K.L., J.G. van de Winkel, L.M. Williamson, and M.R. Clark, *Differential binding to human Fc gamma RIIa and Fc gamma RIIb receptors by human IgG wildtype and mutant antibodies*. Mol Immunol, 2003. **40**(9): p. 585-93.
197. Sadelain, M., R. Brentjens, and I. Riviere, *The basic principles of chimeric antigen receptor design*. Cancer Discov, 2013. **3**(4): p. 388-98.
198. Freeman, S.M., K.A. Whartenby, J.L. Freeman, C.N. Abboud, and A.J. Marrogi, *In situ use of suicide genes for cancer therapy*. Semin Oncol, 1996. **23**(1): p. 31-45.
199. Takahashi, Y., S. Itoh, T. Shimojima, and T. Kamataki, *Characterization of Ah receptor promoter in human liver cell line, HepG2*. Pharmacogenetics, 1994. **4**(4): p. 219-22.
200. Donato, M.T., L. Tolosa, and M.J. Gomez-Lechon, *Culture and Functional Characterization of Human Hepatoma HepG2 Cells*. Methods Mol Biol, 2015. **1250**: p. 77-93.
201. Shimada, T., H. Yamazaki, M. Mimura, Y. Inui, and F.P. Guengerich, *Interindividual variations in human liver cytochrome P-450 enzymes involved in the oxidation of drugs, carcinogens and toxic chemicals: studies with liver microsomes of 30 Japanese and 30 Caucasians*. J Pharmacol Exp Ther, 1994. **270**(1): p. 414-23.
202. Rendic, S. and F.J. Di Carlo, *Human cytochrome P450 enzymes: a status report summarizing their reactions, substrates, inducers, and inhibitors*. Drug Metab Rev, 1997. **29**(1-2): p. 413-580.
203. Schuetz, J.D., D.L. Beach, and P.S. Guzelian, *Selective expression of cytochrome P450 CYP3A mRNAs in embryonic and adult human liver*. Pharmacogenetics, 1994. **4**(1): p. 11-20.
204. Valente, C., L. Alvarez, S.J. Marks, A.M. Lopez-Parra, W. Parson, O. Oosthuizen, et al., *Exploring the relationship between lifestyles, diets and genetic adaptations in humans*. BMC Genet, 2015. **16**: p. 55.
205. Raunio, H., K. Husgafvel-Pursiainen, S. Anttila, E. Hietanen, A. Hirvonen, and O. Pelkonen, *Diagnosis of polymorphisms in carcinogen-activating and inactivating enzymes and cancer susceptibility--a review*. Gene, 1995. **159**(1): p. 113-21.

206. Shimada, T., *Xenobiotic-metabolizing enzymes involved in activation and detoxification of carcinogenic polycyclic aromatic hydrocarbons*. Drug Metab Pharmacokinet, 2006. **21**(4): p. 257-76.
207. Kim, R.B., D. O'Shea, and G.R. Wilkinson, *Relationship in healthy subjects between CYP2E1 genetic polymorphisms and the 6-hydroxylation of chlorzoxazone: a putative measure of CYP2E1 activity*. Pharmacogenetics, 1994. **4**(3): p. 162-5.
208. Bock, K.W., D. Schrenk, A. Forster, E.U. Griese, K. Morike, D. Brockmeier, et al., *The influence of environmental and genetic factors on CYP2D6, CYP1A2 and UDP-glucuronosyltransferases in man using sparteine, caffeine, and paracetamol as probes*. Pharmacogenetics, 1994. **4**(4): p. 209-18.
209. Parkinson, O.T., *Species Differences in the Metabolism and Toxicity of 4-Ipomeanol*, in *Department of Medicinal Chemistry*. 2012, University of Washington: digital.lib.washington.edu.
210. Parkinson, O.T., H.D. Liggitt, A.E. Rettie, and E.J. Kelly, *Generation and characterization of a Cyp4b1 null mouse and the role of CYP4B1 in the activation and toxicity of Ipomeanol*. Toxicol Sci, 2013. **134**(2): p. 243-50.
211. Riddick, D.S., X. Ding, C.R. Wolf, T.D. Porter, A.V. Pandey, Q.Y. Zhang, et al., *NADPH-cytochrome P450 oxidoreductase: roles in physiology, pharmacology, and toxicology*. Drug Metab Dispos, 2013. **41**(1): p. 12-23.
212. Estabrook, R.W., M.R. Franklin, B. Cohen, A. Shigamatzu, and A.G. Hildebrandt, *Biochemical and genetic factors influencing drug metabolism. Influence of hepatic microsomal mixed function oxidation reactions on cellular metabolic control*. Metabolism, 1971. **20**(2): p. 187-99.
213. Miller, W.L., *Minireview: regulation of steroidogenesis by electron transfer*. Endocrinology, 2005. **146**(6): p. 2544-50.
214. Guengerich, F.P., *Rate-limiting steps in cytochrome P450 catalysis*. Biol Chem, 2002. **383**(10): p. 1553-64.
215. Bonini, C. and C. Bordignon, *Potential and limitations of HSV-TK-transduced donor peripheral blood lymphocytes after allo-BMT*. Hematol Cell Ther, 1997. **39**(5): p. 273-4.
216. Traversari, C., S. Markt, Z. Magnani, P. Mangia, V. Russo, F. Ciceri, et al., *The potential immunogenicity of the TK suicide gene does not prevent full clinical benefit associated with the use of TK-transduced donor lymphocytes in HSCT for hematologic malignancies*. Blood, 2007. **109**(11): p. 4708-15.
217. Princen, F., P. Robe, C. Lechanteur, M. Mesnil, J.M. Rigo, J. Gielen, et al., *A cell type-specific and gap junction-independent mechanism for the herpes simplex virus-1 thymidine kinase gene/ganciclovir-mediated bystander effect*. Clin Cancer Res, 1999. **5**(11): p. 3639-44.
218. Zhou, X., A. Di Stasi, S.K. Tey, R.A. Krance, C. Martinez, K.S. Leung, et al., *Long-term outcome after haploidentical stem cell transplant and infusion of T cells expressing the inducible caspase 9 safety transgene*. Blood, 2014. **123**(25): p. 3895-905.
219. Budde, L.E., C. Berger, Y. Lin, J. Wang, X. Lin, S.E. Frayo, et al., *Combining a CD20 chimeric antigen receptor and an inducible caspase 9 suicide switch to improve the efficacy and safety of T cell adoptive immunotherapy for lymphoma*. PLoS One, 2013. **8**(12): p. e82742.
220. Clackson, T., W. Yang, L.W. Rozamus, M. Hatada, J.F. Amara, C.T. Rollins, et al., *Redesigning an FKBP-ligand interface to generate chemical dimerizers with novel specificity*. Proc Natl Acad Sci U S A, 1998. **95**(18): p. 10437-42.

221. Barese, C.N., T.C. Felizardo, S.E. Sellers, K. Keyvanfar, A. Di Stasi, M.E. Metzger, et al., *Regulated apoptosis of genetically modified hematopoietic stem and progenitor cells via an inducible caspase-9 suicide gene in rhesus macaques*. *Stem Cells*, 2015. **33**(1): p. 91-100.
222. Szymczak, A.L., C.J. Workman, Y. Wang, K.M. Vignali, S. Dilioglou, E.F. Vanin, et al., *Correction of multi-gene deficiency in vivo using a single 'self-cleaving' 2A peptide-based retroviral vector*. *Nat Biotechnol*, 2004. **22**(5): p. 589-94.
223. Hanenberg, H.R.L., K.; Wiek, C.; Ibach, T.; Rössig, C., *Patent No. EP 3 293 199 A1*. Date of filing: 08.09.2016 Date of publication: 14.03.2018 (Bulletin 2018/11): Germany. p. 31 Pages.
224. Kenderian, S.S., M. Ruella, O. Shestova, M. Klichinsky, V. Aikawa, J.J. Morrissette, et al., *CD33-specific chimeric antigen receptor T cells exhibit potent preclinical activity against human acute myeloid leukemia*. *Leukemia*, 2015. **29**(8): p. 1637-47.
225. Gill, S., S.K. Tasian, M. Ruella, O. Shestova, Y. Li, D.L. Porter, et al., *Preclinical targeting of human acute myeloid leukemia and myeloablation using chimeric antigen receptor-modified T cells*. *Blood*, 2014. **123**(15): p. 2343-54.
226. Matsuda, T., M. Nomi, M. Ikeya, S. Kani, I. Oishi, T. Terashima, et al., *Expression of the receptor tyrosine kinase genes, Ror1 and Ror2, during mouse development*. *Mech Dev*, 2001. **105**(1-2): p. 153-6.
227. Hudecek, M., T.M. Schmitt, S. Baskar, M.T. Lupo-Stanghellini, T. Nishida, T.N. Yamamoto, et al., *The B-cell tumor-associated antigen ROR1 can be targeted with T cells modified to express a ROR1-specific chimeric antigen receptor*. *Blood*, 2010. **116**(22): p. 4532-41.
228. Yamaguchi, T., K. Yanagisawa, R. Sugiyama, Y. Hosono, Y. Shimada, C. Arima, et al., *NKX2-1/TITF1/TTF-1-Induced ROR1 is required to sustain EGFR survival signaling in lung adenocarcinoma*. *Cancer Cell*, 2012. **21**(3): p. 348-61.
229. Bicocca, V.T., B.H. Chang, B.K. Masouleh, M. Muschen, M.M. Loriaux, B.J. Druker, et al., *Crosstalk between ROR1 and the Pre-B cell receptor promotes survival of t(1;19) acute lymphoblastic leukemia*. *Cancer Cell*, 2012. **22**(5): p. 656-67.
230. Gottschalk, S., C.Y. Ng, M. Perez, C.A. Smith, C. Sample, M.K. Brenner, et al., *An Epstein-Barr virus deletion mutant associated with fatal lymphoproliferative disease unresponsive to therapy with virus-specific CTLs*. *Blood*, 2001. **97**(4): p. 835-43.
231. Janssen, A. and R.H. Medema, *Genetic instability: tipping the balance*. *Oncogene*, 2013. **32**(38): p. 4459-70.
232. Hegde, M., M. Mukherjee, Z. Grada, A. Pignata, D. Landi, S.A. Navai, et al., *Tandem CAR T cells targeting HER2 and IL13Ralpha2 mitigate tumor antigen escape*. *J Clin Invest*, 2016. **126**(8): p. 3036-52.
233. Hegde, M., A. Corder, K.K. Chow, M. Mukherjee, A. Ashoori, Y. Kew, et al., *Combinational Targeting Offsets Antigen Escape and Enhances Effector Functions of Adoptively Transferred T Cells in Glioblastoma*. *Mol Ther*, 2013. **21**(11): p. 2087-2101.
234. Zah, E., M.Y. Lin, A. Silva-Benedict, M.C. Jensen, and Y.Y. Chen, *T Cells Expressing CD19/CD20 Bispecific Chimeric Antigen Receptors Prevent Antigen Escape by Malignant B Cells*. *Cancer Immunol Res*, 2016. **4**(6): p. 498-508.
235. Kloss, C.C., M. Condomines, M. Cartellieri, M. Bachmann, and M. Sadelain, *Combinatorial antigen recognition with balanced signaling promotes selective tumor eradication by engineered T cells*. *Nat Biotechnol*, 2013. **31**(1): p. 71-5.

236. Wu, C.Y., K.T. Roybal, E.M. Puchner, J. Onuffer, and W.A. Lim, *Remote control of therapeutic T cells through a small molecule-gated chimeric receptor*. *Science*, 2015. **350**(6258): p. aab4077.
237. Rueckert, S., I. Ruehl, S. Kahlert, G. Konecny, and M. Untch, *A monoclonal antibody as an effective therapeutic agent in breast cancer: trastuzumab*. *Expert Opin Biol Ther*, 2005. **5**(6): p. 853-66.
238. Balduzzi, S., S. Mantarro, V. Guarneri, L. Tagliabue, V. Pistotti, L. Moja, et al., *Trastuzumab-containing regimens for metastatic breast cancer*. *Cochrane Database Syst Rev*, 2014(6): p. CD006242.
239. Grillo-Lopez, A.J., C.A. White, B.K. Dallaire, C.L. Varns, C.D. Shen, A. Wei, et al., *Rituximab: the first monoclonal antibody approved for the treatment of lymphoma*. *Curr Pharm Biotechnol*, 2000. **1**(1): p. 1-9.
240. McLaughlin, P., A.J. Grillo-Lopez, B.K. Link, R. Levy, M.S. Czuczman, M.E. Williams, et al., *Rituximab chimeric anti-CD20 monoclonal antibody therapy for relapsed indolent lymphoma: half of patients respond to a four-dose treatment program*. *J Clin Oncol*, 1998. **16**(8): p. 2825-33.
241. Velasquez, M.P., C.L. Bonifant, and S. Gottschalk, *Redirecting T cells to hematological malignancies with bispecific antibodies*. *Blood*, 2018. **131**(1): p. 30-38.
242. Bargou, R., E. Leo, G. Zugmaier, M. Klinger, M. Goebeler, S. Knop, et al., *Tumor regression in cancer patients by very low doses of a T cell-engaging antibody*. *Science*, 2008. **321**(5891): p. 974-7.
243. Topp, M.S., N. Gokbuget, A.S. Stein, G. Zugmaier, S. O'Brien, R.C. Bargou, et al., *Safety and activity of blinatumomab for adult patients with relapsed or refractory B-precursor acute lymphoblastic leukaemia: a multicentre, single-arm, phase 2 study*. *Lancet Oncol*, 2015. **16**(1): p. 57-66.
244. Kantarjian, H., A. Stein, N. Gokbuget, A.K. Fielding, A.C. Schuh, J.M. Ribera, et al., *Blinatumomab versus Chemotherapy for Advanced Acute Lymphoblastic Leukemia*. *N Engl J Med*, 2017. **376**(9): p. 836-847.
245. Zhang, M., F. Wang, S. Li, Y. Wang, Y. Bai, and X. Xu, *TALE: a tale of genome editing*. *Prog Biophys Mol Biol*, 2014. **114**(1): p. 25-32.
246. Boch, J., *TALEs of genome targeting*. *Nat Biotechnol*, 2011. **29**(2): p. 135-6.
247. Poirot, L., B. Philip, C. Schiffer-Mannioui, D. Le Clerre, I. Chion-Sotinel, S. Derniame, et al., *Multiplex Genome-Edited T-cell Manufacturing Platform for "Off-the-Shelf" Adoptive T-cell Immunotherapies*. *Cancer Res*, 2015. **75**(18): p. 3853-64.
248. Waseem Qasim, O.C., Stuart Adams, Sarah Inglott, Claire Murphy, Christine Rivat et al., *Preliminary Results of UCART19, an Allogeneic Anti-CD19 CAR T-Cell Product in a First-in-Human Trial (PALL) in Pediatric Patients with CD19+ Relapsed/Refractory B-Cell Acute Lymphoblastic Leukemia*. *Bloodjournal* 2017. **130**(Supl 1 1271).
249. Gouble, A., Philip, B., Poirot, L., Schiffer-Mannioui, C., Galetto, R., Derniame, S., Weng-Kit Cheung, G., Arnould, S., Desseaux, C., Pule, M., & Smith, J., *In Vivo Proof of Concept of Activity and Safety of UCART19, an Allogeneic "Off-the-Shelf" Adoptive T-Cell Immunotherapy Against CD19+ B-Cell Leukemias*. *Blood*, 2014. **Blood**, **124**(21), **4689**.
250. Qasim, W., H. Zhan, S. Samarasinghe, S. Adams, P. Amrolia, S. Stafford, et al., *Molecular remission of infant B-ALL after infusion of universal TALEN gene-edited CAR T cells*. *Sci Transl Med*, 2017. **9**(374).

6 APPENDIX

6.1 List of figures

Figure 1 Evolution of CAR-models with growing signaling capacities	3
Figure 2 Antigen representation on B-lineages and associated B-cell malignancies	8
Figure 3 Toxicities associated with CARs	9
Figure 4 Bioactivation of 4-Ipomeanol via CYP4B1	13
Figure 5 Chemical formulas of 4-Ipomeanol (A) and Perilla ketone (B)	14
Figure 6 Ficoll hypaque density gradient centrifugation	25
Figure 7 Schematic representation of FACS analysis	30
Figure 8 The nerve growth factor receptor p75 A. Schematic model of NGFR B. Protein sequence of the extracellular domain of ΔNGFR	34
Figure 9 The human CD34 antigen A. Schematic model of CD34 B. Protein sequence of ΔCD34	35
Figure 10 pMK-RQ_CD19_CAR	36
Figure 11 Scheme of p2CL21EGT2AR.CD19cowo	36
Figure 12 FACS results of Jurkat cells transduced with CD19 CAR constructs with 10 different hinge regions	38
Figure 13 FACS results after MACS cell separation of transduced Jurkat cell lines	40
Figure 14 FACS results after MACS cell separation of transduced T-cell lines	42
Figure 15 Scheme of p2CL21P+12T2AR.CD19#C3/#C6cowo	43
Figure 16 Cell lysis induced in REH-EG cells by #C3 CAR-expressing T-cells	44
Figure 17 Cell lysis induced in REH-EG cells by #C6 CD19 CAR expressing T-cells	45
Figure 18 Cytotoxicity assay of #C3 T-cells expressing hCYP4B1P+12	46
Figure 19 Cytotoxicity assay of #C6 T-cells expressing hCYP4B1P+12	47
Figure 20 Scheme of p2CL21EGI2Pcowo	48
Figure 21 Toxicity assay - Liver enzyme activity	51
Figure 22 A. Western Blot B. MFI of transduced HepG2 cells	53

6.2 List of tables

Table 1 Commercial Kits and Enzymes	16
Table 2 Length and size standards.....	16
Table 3 Oligonucleotides for Sequencing- PCRs of plasmids.....	16
Table 4 Oligonucleotides for PCR-amplification of plasmid fragments	17
Table 5 Helper plasmids	17
Table 6 Inserts in p2CL21EGT2AR.CD19cowo	18
Table 7 Inserts in p2CL21EGI2Pcowo	19
Table 8 Cell lines	19
Table 9 Antibodies	20
Table 10 Buffers and solutions – cell culture	20
Table 11 Buffers and solution – Analysis and Cloning of DNA.....	21
Table 12 Buffers and solution for protein-biochemical methods.....	21
Table 13 PCR reaction mix Table 14 PCR reaction protocol	22
Table 15 Digestion mix of plasmid DNA	23
Table 16 Transfection dilution	26
Table 17 Constructed inserts cut out of NGFR or CD34 and newly created vectors.....	37
Table 18. Vector constructs used to express different CYP-enzymes in HepG2 cells.....	49

6.3 List of abbreviations

°C	Celsius
4-IPO	4-Ipomeanol
ACT	Adoptive cell therapy
ALL	Acute lymphatic leukemia
AML	Acute myeloid leukemia
BsAb	Bispecific antibody
CAR	Chimeric antigen receptor
CD	Cluster of differentiation
cDNA	Complementary DNA
CEA	Carcino-embryonic antigen

CIR	Chimeric immune receptor
CLL	Chronic lymphatic leukemia
CML	Chronic myeloid leukemia
DLBCL	Diffuse large B-cell lymphoma
DNA	Deoxyribonucleic acid
EBV	Eppstein-Barr virus
EGFP	Enhanced green fluorescent protein
FACS	Fluorescent activated cell sorting
FasL	Fas Ligand
Fc	Fragment chrystalizable
FCS	Fetal calf serum
gr	Gram
g	Gamma
GMP	Good manufacturing practice
GvHD	Graft-versus-Host-Disease
h	Hour
H ₂ O	Water
HIV	Human immunodeficiency virus
HLA	Human leucocyte antigen
HSCT	Hematopoietic stem cell transplantation
HSV-tk	Herpes simplex virus – thymidine kinase
Ig	Immunoglobulin
IL	Interleukin
IFN	Interferon
IRES	Internal ribosomal entry site
IVIG	Intravenous immunoglobulin
k	Kilo
LNGFR	Low-affinity nerve growth factor
LTR	Long terminal repeats
LV	Lentivirus
m	Meter

M	Molar
mAb	Monoclonal antibody
MACS	Magnetic-activated cell sorting
MFI	Mean fluorescent intensity
mg	Milligram
MHC	Major histocompatibility complex
min	Minutes
MOI	Multiplicity of infection
MPSV	Myeloproliferative sarcoma virus
mRNA	Messenger RNA
NGFR	Nerve growth factor receptor
NK	Natural killer
PBS	Phosphate buffered saline
PCR	Polymerase chain reaction
PE	R-Phycoerythrin
PI	Propidium Iodide
PK	Perilla ketone
POR	Cytochrome P450 reductase
RNA	Ribonucleic acid
ROR1	Receptor tyrosine kinase like orphan receptor 1
RT	Room temperature
s	Seconds
SIN	Self-inactivating vector
scFv	Single-chain variable fragment
SDS	Sodium dodecyl sulfate
SDS-PAGE	SDS-Polyacrylamide gel electrophoresis
SNP	Single Nucleotide Polymorphism
TAA	Tumor-associated antigen
T2A	Thosea asigna virus 2A
TALEN	Transcription activator-like effector nucleases
TCR	T-cell receptor

TRAIL	Tumor necrosis factor related apoptosis inducing ligand
TRUCK	T -cells redirected for universal cytokine-mediated killing
VSV	Vesicular stomatitis virus
z	Zeta
μ	Micro

Acknowledgement

Ganz herzlich bedanken möchte ich mich bei meinem Doktorvater, Prof. Dr. Helmut Hanenberg, für die Unterstützung beim Verfassen der Arbeit. Insbesondere auch Danke für die andauernde Begeisterung und Bereitschaft, die Ergebnisse zu diskutieren sowie natürlich für die zahlreichen, intensiven Korrekturen.

Dr. Constanze Wiek stand mir vom ersten Moment der Arbeit an kompetent und hilfsbereit zur Seite. Danke für die grosse Geduld dabei, eine Medizinerin in die Welt der Zellkulturen und Cytochrome einzuführen. Ohne unsere regelmässigen Gespräche über das Forschungsthema und weit darüber hinaus sowie deine andauernde moralische Unterstützung und Aufmunterung wäre diese Arbeit nicht zustande gekommen.

Zudem danke ich Dr. Katharina Roellecke für ihre Unterstützung im Labor und den regen Austausch, besonders zum Ende der Experimente hin. Deine positive Einstellung hat mich immer wieder motiviert und ohne den wunderbaren Süssigkeiten-Support hätte die Zeit im Labor und Büro nur halb so viel Spass gemacht.

Herrn Prof. Schipper möchte ich für die Bereitstellung seines Labors danken. Allen Freunden und Kollegen die mir während der Promotion ihr Blut gespendet haben und sich von mir haben stechen lassen, danke ich. Ohne die freiwilligen Spenden wären die Experimente nicht möglich gewesen.

Ein spezielles, riesiges Dankeschön geht an meine Familie und meinen Freund, die mich den Weg der Promotion hindurch begleitet haben und bis zum Ende mit aufmunternden Worten und uneingeschränkter Unterstützung für mich da waren. Ich kann mich immer auf euch verlassen, und ihr habt mir in den richtigen Momenten die entscheidene Motivation gegeben.